Mineralogical and geochemical link between the bog iron ore deposits and preindustrial slags throughout the lowland Drava River area

Brenko, Tomislav

Sveučilište u Zagrebu

Faculty of Mining, Geology and Petroleum Engineering

Tomislav Brenko

MINERALOGICAL AND GEOCHEMICAL LINK BETWEEN THE BOG IRON ORE DEPOSITS AND PREINDUSTRIAL SLAGS THROUGHOUT THE LOWLAND DRAVA RIVER AREA

DOCTORAL THESIS

Zagreb, 2022

Sveučilište u Zagrebu

Faculty of Mining, Geology and Petroleum Engineering

Tomislav Brenko

MINERALOGICAL AND GEOCHEMICAL LINK BETWEEN THE BOG IRON ORE DEPOSITS AND PREINDUSTRIAL SLAGS THROUGHOUT THE LOWLAND DRAVA RIVER AREA

DOCTORAL THESIS

Supervisor:
Prof. Sibila Borojević Šoštarić, PhD

Zagreb, 2022

Sveučilište u Zagrebu

Rudarsko-geološko-naftni fakultet

Tomislav Brenko

MINERALOŠKA I GEOKEMIJSKA POVEZNICA IZMEĐU MOČVARNOG TIPA LEŽIŠTA ŽELJEZNE RUDE I PREDINDUSTRIJSKE ZGURE U NIZINSKOM SLIVU RIJEKE DRAVE

DOKTORSKI RAD

Mentorica:
dr. sc. Sibila Borojević Šoštarić, redovita profesorica

Zagreb, 2022

Information about the mentor:

Prof. Sibila Borojević Šoštarić, PhD

University of Zagreb

Faculty of Mining, Geology and Petroleum Engineering

Department of mineralogy, petrology and mineral resources

Zahvaljujem

... mentorici dr.sc. Sibili Borojević Šoštarić prije svega na iskazanom povjerenju, predloženoj temi istraživanja, korisnim stručnim i prijateljskim savjetima, poticanju u znanstvenoj i nastavnoj afirmaciji, bezbrojnim satima konstruktivne rasprave i diskusije, konstantnoj potpori te sveukupnoj pomoći pri izradi i vođenju ove doktorske disertacije

... dr.sc. Tajani Sekelj Ivančan što mi je omogućila sudjelovanje na znanstvenom projektu TransFER iz kojeg je proizašla ova disertacija. Hvala Vam na svim korisnim savjetima, spremnosti na objašnjavanje i prenošenje arheoloških spoznaja koje su omogućile pisanje ovog rada

... dr.sc. Stanku Ružičiću na prenesenom znanju, brojnim pedološkim i geološkim diskusijama, pomoći u terenskom radu, pisanju znanstvenih radova i općenito spremnosti na pomoć u svakom trenutku

... dr.sc. Marti Mileusnić što je objeručke prihvatila biti član povjerenstva za ocjenu i obranu, na brojnim konstruktivnim i poučnim primjedbama koje su ovaj rad usmjerile u pravom smjeru

... dr.sc. Ivanu Sondi koji je u svakom trenutku brinuo o mom napretku, davao korisne savjete i životne mudrosti, spremno preuzimao zadatke i na sebe kako bi meni dao dovoljno vremena da se uspješno posvetim izradi ovog rada. Hvala Vam još jednom te se iskreno veselim daljnjoj suradnji

... Teni Karavidović, kolegici i suradnici na projektu, s kojom mi je bilo vrlo ugodno surađivati, diskutirati i zajednički pisati nekolicinu znanstvenih radova. Hvala ti na brojnim raspravama, izmjeni ideja, razmišljanja, prijedlozima i kritikama

... Nevenu Tadeju, čovjeku koji me uvukao u svijet mineralogije i pomagao mi s brojnim interpretacijama XRD analiza i mineraloškim savjetima, te druženju na Zavodu, kao i u planinama, na badmintonskom terenu ili brojnim koncertima

... našim tehničarima, Branki Prši, Vinku Baranašiću i Nadi Čegec, na odrađenom ogromnom dijelu laboratorijskog posla u pripremi i analizi uzoraka. Još jednom se ispričavam za ahatnu posudu!

... dr. sc. Michaeli Hrušková Hasan, što je strpljivo odobravala moje želje za brojnim analizama, te svojim znanjem, savjetima i idejama usmjeravala i dodatno poticala moj rad

... dr.sc. Goranu Durn na uvijek lijepim razgovorima i savjetima

... dr.sc. Vesnici Garašić, koja je uvijek bila spremna za pomoć, te svojim znanjem i povremenim ohrabrenjem, kada je to trebalo, pratila ovaj rad

... dr.sc. Dunji Aljinović, jer je uvijek znala uputiti prave riječi i izvući smiješak na lice

...dr.sc. Ani Maričić, što je svojim pravovremenim savjetima pomagala u oblikovanju ovog rada

... Boženi Vlainić, što je strpljivo i uvijek s osmijehom pomagala s papirologijom kroz sve ove godine

... Draženki Krčelić što je svaki moj ranojutarnji dolazak dočekala sa smiješkom i toplim razgovorom

... svojim cimerima, bivšim i sadašnjim: dr.sc. Duji Smirčiću, za sve one trenutke kada si bio tu, uz glazbu, druženje te rješavanje svih problema, dr.sc. Šimi Biliću, što si uvijek bio spreman na pomoć, posebno s geokemijskom problematikom, Ivoru Perkoviću, mag. geol., na tvojoj zainteresiranosti u ovaj rad, raspravama i idejama oko geostatistike i programiranja.

Hvala kolegama s Rudarsko-geološkog fakulteta u Beogradu, dr.sc. Suzani Erić, dr.sc. Kristini Šarić i dr.sc. Aleksandru Pačevskom, što su mi uljepšali boravak na stranom sveučilištu, te svojim znanjem i diskusijama doveli do nekih zaključaka koji se nalaze u ovom radu

Hvala svim kolegicama i kolegama s Fakulteta, na zajedničkim druženjima kroz sve ove godine, što me oblikovalo kao osobu.

Zahvaljujem se Željki Kurelec, Andrei Gmajnički i Andrei Škomrlj iz Ureda za poslijediplomski na pomoći s obrascima.

Hvala svim studentima, bivšim i sadašnjim, nadam se da ste vi od mene naučili samo djelić onoga što sam ja naučio od vas.

... Mojoj obitelji

“For the Quest is achieved, and now all is over. I am glad you are here with me. Here at the end of all things.”

- J.R.R. Tolkien, The Return of the King

ABSTRACT

Long term field examinations in the Podravina region led to discoveries of iron production in the region, resulting in extensive targeted archaeological field surveys during the previous 30 years. Based on the archaeological evidence, iron ore was locally exploited for individual purposes of local smiths and settlements. Previous geological studies in the region failed to recognize iron ore deposits that would enable such iron production. However, archaeological and geological surveys in southeastern Hungary, with similar geological, pedological and hydrogeological conditions as the Podravina region, point to occurrence and usage of bog iron ore, a sedimentary type of iron ore deposit, as the primary raw material.

Detailed soil analyses, including mineralogical, geochemical and textural analysis, were conducted through the region. Significant content of goethite and higher than average Fe_2O_3 contents in such soil types point to bog iron ore formation. Correlation between groundwater depth with Fe accumulation zones indicates groundwater as the main carrier of the Fe enrichment in soils, with the main precipitation zone between 10 and 100 cm. Established formation mechanism is well in line with discoveries of three bog iron types (soil, nodules and fragments) in the region, which represent bog ore development phases. Mineralogical composition determined variable goethite contents, increasing from soils to fragments, while vice-versa was observed for quartz. Geochemical analysis confirmed Fe_2O_3 and SiO_2 as the two main oxides, with varying iron-silicon ratios, increasing from soil to the fragment samples, indicating different phases of the cementation process during formation.

Analysed archaeological samples of roasted iron ore and iron slags point to thermal reactions between 300 and 1000 °C (average 500–650 °C) for roasted iron ore and above 1000 °C for slags, with presence of hematite and magnetite in roasted ore and fayalite and wüstite in slags. Geochemically, roasted ore has higher Fe_2O_3 contents than bog ore, as part of the ore pre-processing. On the other hand, slags have variable contents of Fe_2O_3, SiO_2 and Al_2O_3, which in some cases indicates temporal and spatial variability of the used ore.

Hierarchical clustering analysis of bog iron ore revealed that Fe does not hold any influence on the contents of trace and rare earth elements, therefore, trace and rare earth elements can be used to create and compare geochemical signatures between bog iron ore and archaeological samples of roasted iron ore and iron slags. By comparing these signatures, similar shapes and peaks were observed between ore and archaeological material, confirming the hypothesis that bog iron ore was the primary raw material used for the iron production in the Podravina region during Late Antique and Early Middle Ages.

PROŠIRENI SAŽETAK

Tijekom višegodišnjih terenskih obilazaka područja Podravine prikupljeni su indikativni površinski nalazi komada talioničke zgure, ulomaka keramičkih sapnica i stijenki glinenih peći koji su potaknula ciljana arheološka iskopavanja na više položaja uz rijeku Dravu (**Sekelj Ivančan i Karavidović, 2021; Valent i dr., 2017; Valent, 2021**). Veliki broj manjih nalaza tragova taljenja i proizvodnje željeza ukazuje da je ruda eksploatirana lokalno, za individualne potrebe ljudi koji su naseljavali taj prostor (**Karavidović, 2020**). Međutim, ranija geološka istraživanja nisu ukazala na pojave željezne rude na području Podravine, stoga se postavilo pitanje o podrijetlu i vrsti korištene rude. Arheološka i geološka istraživanja u jugoistočnoj Mađarskoj ukazala su na pojave močvarne željezne rude, sedimentnog tipa ležišta željezne rude, koja se obično javlja u močvarnim područjima (**Gömöri, 2006; Török i dr., 2015**). S obzirom na slične geološke, pedološke i hidrogeološke uvjete između južne Mađarske i područja Podravine, pretpostavilo se da je i na području Podravine formirana i korištena ista vrsta rude.

Ciljevi i hipoteze

Glavni ciljevi ovog rada bili su utvrditi mogućnost formiranja močvarne željezne rude na području Podravine, utvrditi tipove, mineraloške i geokemijske karakteristike močvarne željezne rude, pržene željezne rude i željezne zgure te utvrditi međusobnu korelaciju između močvarne željezne rude, pržene rude i željezne zgure korištenjem dostupnih mineraloških i geokemijskih analiza. Ciljevi su bazirani na tri hipoteze: (i) tijekom kasne antike i ranog srednjeg vijeka močvarna željezna ruda formirana je na području Podravine, (ii) zbog kompleksnog mehanizma formiranja, očekuje se da će močvarna željezna ruda imati varijabilan mineralni i geokemijski sastav i (iii) močvarna željezna ruda korištena je kao glavna mineralna sirovina za taljenje i proizvodnju željeza na području Podravine tijekom kasne antike i ranog srednjeg vijeka.

Znanstveni doprinos

Rezultati ovog istraživanja doprinose razumijevanju eksploatacije i uporabe željezne rude na području Podravine tijekom kasne antike i ranog srednjeg vijeka kroz analizu mineraloških i geokemijskih karakteristika močvarne željezne rude i pripadajućeg arheološkog materijala. Prvi put pružen je uvid u detaljnu analizu različitih razvojnih faza močvarne željezne rude na području istraživanja i u Republici Hrvatskoj općenito. Posebna pozornost posvećena je udjelima elemenata u tragovima i elemenata rijetkih zemalja, te njihovom ponašanju i mobilnosti prilikom različitih termičkih tretmana. Prikupljeni podaci

korišteni su za provenijencijska istraživanja ulomaka željezne zgure, što predstavlja prvi takav tip istraživanja u Republici Hrvatskoj.

Metode i postupci

U svrhu određivanja prisutnosti močvarne željezne rude u tlima Podravine te je li upravo močvarna željezna ruda bila glavna sirovina za taljenje i proizvodnju željeza tijekom kasne antike i ranog srednjeg vijeka, provedene su detaljne mineraloške i geokemijske analize. Rendgenska difrakcija na prahu (XRD) i induktivno spregnuta plazma (ICP-MS/AES) korištene su na uzorcima tala, različitim tipovima močvarne željezne rude te arheološkim uzorcima pržene rude i željezne zgure. Dodatno su na profilima tla određeni granulometrijski sastav, udio karbonata, te pH i električna vodljivost. U svrhu određivanja korelacije između rude i arheoloških uzoraka korišteni su elementi u tragovima i elementi rijetkih zemalja (REE), kako bi se kreirali i usporedili njihovi geokemijski otisci. Za što preciznije povezivanje rude i uzoraka zgure korištene su statističke analize, poput klaster analize (eng. *hierarchical cluster analysis*) i analize primarnih komponenata (eng. *principal component analysis*).

Rezultati i zaključci

Kako bi se utvrdila mogućnost formiranja močvarne željezne rude na području Podravine, uzorkovano je preko 50 profila tla, u blizini lokaliteta gdje je na površini zamijećena pojava zgure, kojima je određena boja te magnetski susceptibilitet. Šest profila je odabrano za daljnja mineraloška, geokemijska i granulometrijska istraživanja obzirom na značajnu prisutnost željezovitih tragova u obliku prevlaka i ispuna crvene i narančaste boje. Mineraloške analize unutar profila tla ukazale su na prisutnost goethita (Fe-oksihidroksida), dok su geokemijske analize pokazale širok raspon udjela Fe_2O_3 i SiO_2. Unutar svih profila, a poglavito u intervalu 50–100 cm dubine, zabilježeni su povišeni udjeli Fe_2O_3, s maksimalnom vrijednošću od 31,52 mas. % u 60–80 cm intervalu tla s lokaliteta Kalinovac-Hrastova Greda. Navedene dubine obogaćenja odgovaraju prosječnoj razini fluktuacije podzemne vode (**Brkić i Briški, 2018**), za koju je već u ranijim istraživanjima (**Kopić i dr., 2016**) utvrđeno obogaćenje s Fe, Mn i As. S obzirom na navedeno, može se utvrditi da je podzemna voda glavni nositelj redoks-osjetljivih kemijskih elemenata poput Fe, Mn i As u tlima Podravine, a čija se mobilnost mijenja s promjenom redoks uvjeta. Navedeni elementi talože se u intervalu između 10 i 100 cm dubine, u oksidacijskim zonama koje potiču oksidaciju iz Fe^{2+} u Fe^{3+}, odnosno iz Mn^{2+} u $Mn^{3+/4+}$, te As^{3+} u As^{5+}. Trovalentno Fe predstavlja imobilni oblik u tlima, čime je omogućeno postupno taloženje i obogaćenje željeza u tlu. Međutim, uslijed poljoprivrednih procesa i melioracijskih zahvata te regulacija vodnih tokova od 19. stoljeća,

snižava se razina podzemne vode, čime se znatno otežava precipitacija močvarne željezne rude u Podravini. Stoga se pretpostavlja da trenutni nalazi predstavljaju inicijalnu fazu razvoja, s obzirom da je daljnji razvoj onemogućen zbog nepovoljnih uvjeta u okolišu.

Terenskim istraživanjima utvrđene su tri razvojne faze močvarne željezne rude (željezovita tla, nodule i željezoviti fragmenti) koji su mineraloški i geokemijski analizirani. Mineraloške analize ukazuju na varijabilne udjele goethita, čiji udio raste od tala prema fragmentima. Uz njega, zabilježeni su i tipični minerali tla poput kvarca, plagioklasa i filosilikata. Geokemijski udjeli Fe_2O_3 i SiO_2 prate mineraloške analize pa su tako u tlima zabilježeni najniži udjeli Fe_2O_3 (13,20–27,93 mas. %) te najviši udjeli SiO_2 (50,75–63,38 mas. %). U nodulama udjeli Fe_2O_3 (22,99–39,54 mas. %) i SiO_2 (27,06–44,10 mas. %) su podjednaki, dok su kod fragmenata udjeli Fe_2O_3 (32,03–70,89 mas. %) veći od udjela SiO_2 (3,59–30,67 mas. %). Takve vrijednosti ukazuju na slab metalurški potencijal prve dvije razvojne faze močvarne željezne rude (tla i nodule), dok samo močvarno željezni fragmenti pokazuju dovoljno visoke udjele Fe_2O_3, kao posljedicu naprednije Fe cementacije.

Analize uzoraka pržene željezne rude ukazuju na prisustvo Fe-oksida koji nastaju na višim temperaturama, poput hematita i magnetita. Sam proces prženja rude radi se s ciljem oplemenjivanja sirovine pa su sukladno tome u prženim rudama zabilježeni prosječno viši udjeli Fe_2O_3 (8,44–84,97 mas. %), te niži udjeli SiO_2 (4,17–62,67 mas. %). U sklopu analize željeznih zgura, analizirani su arheološki uzorci s tri lokaliteta; Hlebine-Velike Hlebine, Virje-Sušine i Virje-Volarski breg. Minerali fayalit (Fe_2SiO_4) i wüstit (FeO) u uzorcima zgure ukazuju na termalne reakcije između Fe i Si na temperaturama preko 1000 °C, tipičnim za temperature u talioničkim pećima. Varijabilni geokemijski udjeli Fe_2O_3 (52,30–66,46 mas. %) i SiO_2 (11,69–37,28 mas. %) ukazuju na moguću vremensku i prostornu varijabilnost u uzorcima zgura s različitih lokaliteta, kao posljedice geokemijskog sastava rude, što se može i uočiti na dijagramu glavnih komponenti (PCA). Povišene vrijednosti Al_2O_3 u uzorcima s lokaliteta Virje-Volarski breg ukazuju da je ruda s tog lokaliteta sadržavala više alumosilikatne komponente.

Kako bi se odredio izvorišni materijal prženih ruda i željeznih zgura napravljene su klaster analize uzoraka prirodne i pržene rude koje ukazuju da se redoks-osjetljivi elementi poput Fe i Mn odjeljuju od elemenata u tragovima i elemenata rijetkih zemalja (REE). To znači da su elementi u tragovima i REE neovisni o udjelu Fe, što ih čini pogodnima za daljnje određivanje provenijencije i geokemijskih korelacija. Udjeli odabranih elemenata u tragovima i REE normalizirani su na hondrit (**Anders i Greevese, 1989**) te gornju kontinentalnu koru (**Taylor i McLennan, 1995**), te naneseni na multielementne dijagrame, formirajući

geokemijske otiske rude i zgure. Tako prikazani uzorci pokazuju karakteristične pikove, poput povišenog fosfora koji se često veže uz močvarnu željeznu rudu. Udjeli REE pokazuju isti geokemijski otisak kod ruda i zgura, čime se nedvojbeno može zaključiti da je močvarna željezna ruda korištena kao glavna sirovina prilikom taljenja i proizvodnje željeza tijekom kasne antike i ranog srednjeg vijeka na području Podravine.

KEYWORDS

Bog iron ore

Roasted iron ore

Iron slags

Geoarchaeology

Hierarchical cluster analysis

Geochemical signature

KLJUČNE RIJEČI

Močvarna željezna ruda

Pržena željezna ruda

Željezna zgura

Geoarheologija

Hijerarhijska klaster analiza

Geokemijski otisak

TABLE OF CONTENTS

LIST OF FIGURES:

LIST OF TABLES:

1. INTRODUCTION

1.1. Review of archaeological iron research in the Podravina region

Long term field examinations in the Podravina region resulted in discovering and collecting multiple surface finds of various smelting slags, ceramic tuyeres and clayey furnace walls fragments. These discoveries resulted in numerous targeted archaeological field campaigns over the last 30 years, which resulted in several archaeological sites being discovered in the lowland Drava River area and dated to several time periods, spanning over 1,500 years (**Sekelj Ivančan, 2014, 2015; Valent et al., 2017**). Most notable among them are numerous samples of Late Antique and Early Middle Age traces of smelting and smiting of iron and iron ores (**Figure 1-1**).

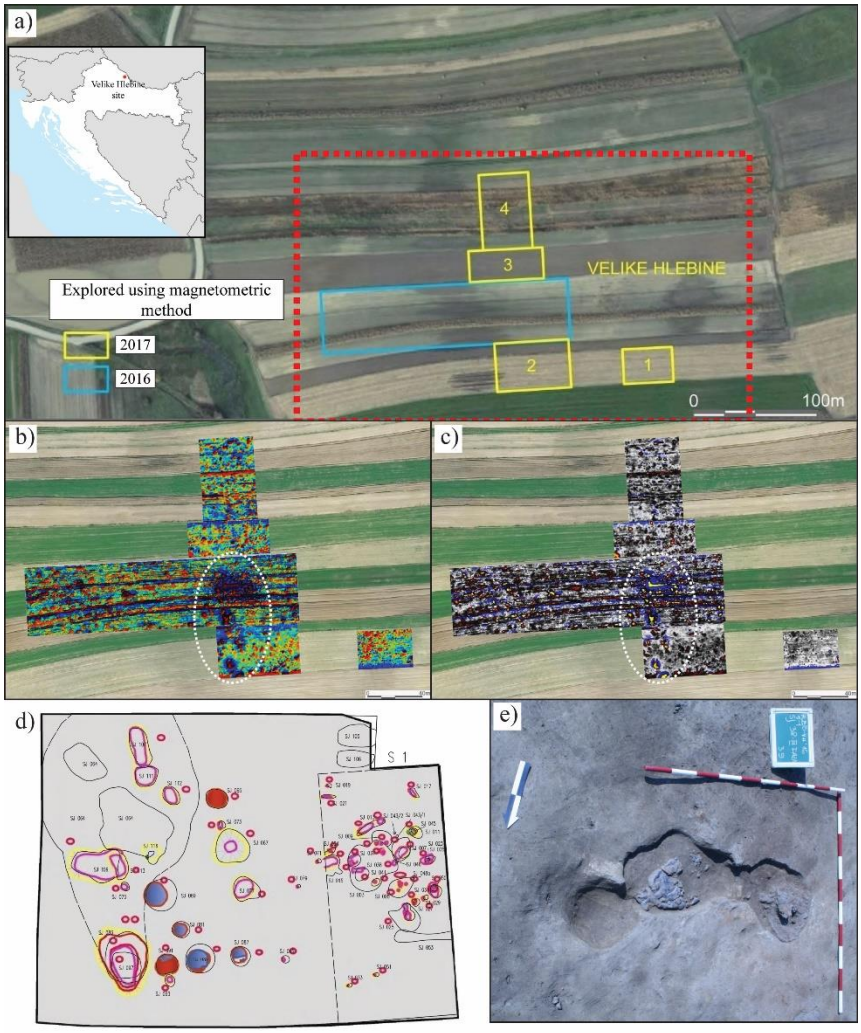

Figure 1-1. Geophysical explorations (a, b and c) that led to archaeological excavations on the Hlebine-Velike Hlebine site (d) and discovery of an *in situ* smelting furnace (e) (modified according to **Mušić and Horn, 2021; Sekelj Ivančan et al., 2021**)

Discovered archaeological sites, such as Virje-Sušine, Virje-Volarski breg and Hlebine-Velike Hlebine, where *in situ* smelting furnace was discovered, point to existence of iron production in the Podravina region (**Sekelj Ivančan and Karavidović, 2021**).

Local and regional settings of the Podravina region have natural prerequisites for the formation of resources necessary for iron production. These include clay and water resources for the production of smelting furnace walls and local wood as an essential fuel component in the process. However, the question of raw ore material remained dubious. Based on several iron smelting workshops found at three locations (**Sekelj Ivančan and Karavidović, 2021**) and on numerous slag and roasted ore findings throughout the Podravina region (**Valent et al., 2017**) it is believed that the ore necessary for the iron production was locally mined in smaller quantities for individual needs of the local smiths (**Karavidović, 2020**). Case studies from several archaeological sites in Southern Hungary (**Gömöri, 2006; Török et al., 2015**), with similar geological, pedological and hydrogeological settings as in Podravina region pointed to the usage of bog iron ore as the primary raw ore material.

1.2. Bog iron ore characteristics and formation mechanisms

Bog iron ore represents sedimentary type of iron deposits (**Ramanaidou and Wells, 2014**), usually occurring in low-lying areas such as swamps, bogs, river valleys and microdepressions where the groundwater table is situated close to the surface (**Kaczorek and Zagórski, 2007**), while drainage is impeded (**Stanton et al., 2007**). This type of terrestrial iron (Fe) accumulations is often developed in hydromorphic, loamy, sandy and clayey alluvium sediments and soils (**De Geyter et al., 1985; Landuydt, 1990**) and is mostly consisted of Fe oxides and oxyhydroxides (**Banning, 2008**). Bog iron ore is widespread in the central and northern Europe, Asia and North America (**Crerar et al., 1979; Breuning-Madsen et al., 2000; Ratajczak and Rzepa, 2011**). It is usually differentiated to three different macromorphological types: (i) a soft, unstable form, often referred to as "soft" bog iron, (ii) randomly distributed concretions, block or nodules in soil and (iii) well-cemented, massive horizons, continuous or discontinuous, often referred as "hard" bog iron (**Thelemann et al., 2017**), which corresponds to development phases, with soft bog iron being the first phase, and hard bog iron being the final phase.

The fundamental process in the bog iron ore formation is the precipitation of the solid phase under the presence of dissolved atmospheric oxygen. Groundwater percolating through regional rocks tends to get enriched with ferrous (Fe^{2+}) iron via dissolution of minerals such as sulphides, silicates and carbonates. These minerals are dissolved through (bio)chemical

weathering, particularly under acidic condition of pH under 7 (**Postawa et al., 2013**). Iron is dissolved as ions or hydroxides into the groundwater, and transported via groundwater flow (**Kaczorek et al., 2004**). Upon reaching zones with higher concentrations of dissolved atmospheric oxygen, oxidation of ferrous to ferric (Fe^{3+}) iron starts to occur. This leads to precipitation of iron in the soil pore space. Pore space is originally occupied by primary soil minerals, such as quartz and clay minerals, that are gradually coated and repressed by the Fe^{3+} oxide/hydroxide matrix. Due to seasonal oscillations of the groundwater table, periods of wetting and drying occur in the soil profile, typically producing an oxidized zone in the upper 50-80 cm interval and an underlying reduced zone in the deeper parts of the soil profile (**Stoops, 1983; Kaczorek and Sommer, 2003**). Changing physico-chemical conditions and redox potential leads to complex mineralogical composition in the bog iron ore. A variety of iron minerals can be found in the bog ore due to oxidation of ferrous iron under acidic conditions that are present in bogs and marshes. Oxidation of ferrous solution typically results in the formation of poorly crystallized iron oxyhydroxides such as ferrihydrite. Ferrihydrite is thermodynamically unstable and as such, acts as the precursor for goethite (**Pinney et al., 2009**) or hematite (**Vodyanitskii, 2010**). Goethite (α-FeOOH) is the main Fe mineral found in bog iron ore, often exhibiting yellow-brownish colour (**Banning, 2008**). Besides goethite, reddish lepidocrocite (γ-FeOOH) is often found in bog iron ore (**Kaczorek et al., 2004**). Other minerals associated with upper horizon include hematite (Fe_2O_3), magnetite ($FeFe_2O_4$) and maghemite (γ- Fe_2O_3) (**Banning, 2008**). In the lower horizon, Fe carbonate siderite ($FeCO_3$), phosphate vivanite ($Fe_3[PO_4]_2$ x $8H_2O$) and sulphide pyrite (FeS_2) can be present (**Kaczorek et al., 2004**). Other minerals associated with bog iron ore include typical soil minerals, such as quartz, feldspars and clay minerals (**Kaczorek and Sommer, 2003; Thelemann et al., 2017**).

Geochemical composition of bog iron ore is predominantly characterized by variable amounts of Fe_2O_3 and SiO_2. The Fe_2O_3 contents in bog iron ore mostly vary between 30 and 60 mass. % (**Thelemann et al., 2017**), but can occasionally reach up to 90 mass. % (**Charlton et al., 2010**). Besides Fe_2O_3 and SiO_2, phosphorous and manganese can often be found in considerable amounts in bog iron ores, with P_2O_5 reaching values up to 8 mass. % and MnO up to 10 mass. %. (**Landuydt, 1990; Thelemann et al., 2017**). Other major oxides, including calcium (CaO), magnesium (MgO), potassium (K_2O), sodium (Na_2O), barium (BaO) and titanium (TiO_2) are often present in minor concentrations. **Table 1-1** presents a summary of Fe_2O_3, SiO_2 and MnO contents and mineralogical composition (where available) of several bog iron ore deposits located in the central Europe.

Composition of the ore largely depends on the composition and characteristics of the parent material in which the ore forms. Secondly, hydrogeological conditions and the chemical composition of the groundwater play a significant role to the overall composition of the ore, mostly on the contents of iron, manganese and phosphorous (**Kaczorek et al., 2004**). Bog iron ore can also act as a sink for heavy metals and potentially toxic metals (metalloids) (**Church et al., 1997**). This is clearly reflected in As contents, that, depending on the geogenic background contents, are often increased in bog iron ore (**Banning et al., 2013**).

Table 1-1. Chemical and mineralogical comparison of several bog iron ores in Europe and North America. Mineral abbreviations: am-Fe – amorphous Fe; Cal – calcite; Fer – ferrihydrite; Gt – goethite; Hem – hematite; Mag – magnetite; Or – orthoclase; Py – pyrite; Qtz – quartz; Sid – siderite; Viv – vivianite.

Source	Country	Location	Nr. of samples	Fe_2O_3	SiO_2	MnO_2	Mineral association
Stoops, 1983	Belgium	Antwerp	/	/	/	/	Gt, Viv, Sid, clays
De Geyter, 1985	Belgium	Antwerp	/	19.30–71.68	/	/	Gt, Viv, Sid, clays
Breuning-Madsen et al., 2000	Denmark	Jutland	?	69.11	10.45	1.39	/
Bricker et al., 2003	USA	Maryland	/	/	/	/	Gt, Mag, Viv, am-Fe
Kaczorek and Sommer, 2003	Poland	Wilanow, Northern Praga, Brwinow	8	57.19–73.49	4.28–27.59	0.36–1.29	Gt, Fer, Qtz, Viv, Sid, am- Fe
Banning, 2008	Germany	western Münsterland	/	8.1–42.18	/	/	Gt, Qtz, am-Fe, Sid
Young, 2010	England	Surrey	2	32.83–48.84	26.22–48.69	1.28–2.09	/
Thelemann et al., 2017	Poland	Silesia	36	1.6– 64.9	10.4–82.3	0.1–4.4	Qtz, Gt, Or, Hem, Mag, Sid, Py, Cal

What separates bog iron ore deposits from other iron deposits is their relatively fast formation and growth. Although there are no empirical studies on the formation time of bog iron ore, some studies (**Bricker et al., 2003**) suggest that smaller deposit can be formed in as short as 25 years, with majority of similar bog iron deposits forming in several hundred or thousand years (**Thelemann et al., 2017**). If the deposit is under constant flux of Fe-enriched

groundwater, economically significant deposit can regrow in a matter of 20 years (**Stanton et al., 2007**).

1.3. Preindustrial iron smelting

The main technique for iron production in the premodern times was the "direct" or bloomery process. Unlike the "indirect" method, bloomery ironmaking involves the reduction of iron oxides to iron metal, while remaining in the solid state (**Pleiner, 2000**). The smelting process occurs inside a smelting furnace that retains the heat, while the combination of fuel and air allows for the chemical interactions, most notably the reduction of iron oxides. Reduced iron oxides form a spongy mass of iron called the bloom (**Charlton et al., 2010**). Main by-product of bloomery smelting is the ferrosilicate slag, formed in the reaction between iron and gangue minerals in the ore. The slag can contain as much as 50 mass. % Fe_2O_3 and has a chemical composition similar to the fayalitic olivine (Fe_2SiO_4). Besides parent material in the ore, other impurities are often incorporated into the slag during smelting process (**Crew, 2000; Velduhijzen, 2005**), such as clay material from furnace wall lining and fuel ash.

Bog iron ore is rarely composed purely of Fe minerals, rather as a combination of Fe minerals and parent material, called the gangue minerals. Smelters are using different chemical and physical methods to separate the metal from the gangue minerals. This pre-processing of ore was also known as the dressing of the ore (**Pleiner, 2000**), and in the Late Antique and Middle Ages most common methods included washing and roasting of the ore. Washing of the ore was conducted to remove clay and soil material from the ore, while roasting was conducted for two reasons. Firstly, heating ore lumps at temperatures between 400 and 800 °C with access to air, enables chemical and mineral transformation from oxyhydroxides and non-oxide iron ores to oxide iron ores, such as hematite, which are more susceptible for smelting. Secondly, roasting has an effect on the physical properties of the ore, making it more porous due to release of gases and vapours when exposed to high temperatures, making ore more amenable to the reduction process (**Pleiner, 2000**).

The bloomery furnace is a cylindrical-shaped feature in which the process of reduction occurs. Different variations regarding shapes and sizes were recognized and described, but the same thermochemical reactions are happening in all of them (**Haubner et al., 2014; Humpris et al., 2018; Madera et al., 2018; Robion-Brunner, 2020**). Burning of fuel inside enclosed furnace leads to incomplete combustion of charcoal, which then produces high quantities of carbon monoxide (CO). This gas travels up the furnace shaft, reacting with the ore and reducing it. Reduction process starts as soon as ore is moving down the furnace shaft, reacting

with carbon monoxide. Iron oxide reacts with the CO, forming carbon dioxide (CO_2) and elemental iron (bloom) (**Pleiner, 2000**), while gangue material reacts with part of the iron forming slag material. Iron formation reaction can be expressed with the following chemical equations:

$$3Fe_2O_3 + CO \rightleftharpoons 2Fe^{2+}Fe^{3+}{}_2O_4 + CO_2$$

$$Fe^{2+}Fe^{3+}{}_2O_4 + 2CO \rightleftharpoons 3FeO + CO_2$$

$$3FeO + 3CO \rightleftharpoons 3Fe + 3CO_2$$

However, inside the furnace, ore, bloom and slag can undergo between reduction, reoxidation, carburization and decarburization.

Several slag types with different morphologies can be produced during iron smelting, based on the used raw materials, furnace design and smelting parameters (**Blakelock et al., 2009**), with different slag types forming inside the same smelt. These slag types include furnace bottom slag, furnace slag, tap slag, ceramic-rich slag and glassy slag (**Veldhuijzen and Rehren, 2007**). Commonly, slags are composed of fayalite (Fe_2SiO_4), wüstite (FeO) and quartz, while additional minerals can point to ore mineralogy or smelting recipe. Geochemically, slag is mostly consisted of Fe_2O_3 and SiO_2, with most smelting slags having similar, almost repetitive pattern with regards to slag composition (**Blakelock et al., 2009**). However, some variations in the chemistry are expected in the final composition due to the human factor, furnace design, used raw materials and smelting parameters and conditions (**Rehren et al., 2007**).

1.4. Provenance studies in iron archaeology

The concept of provenance in archaeology is more than 160 years old and is used to indicate the source of the raw material or the location where the object was manufactured, such as in a workshop (**Wilson and Pollard, 2001**). Different chemical methods and techniques were developed accordingly for provenance of most historically used metals (**Stos-Gale and Gale, 2009; Ling et al., 2013; 2014**). However, numerous studies and efforts were conducted to determine the provenance of iron objects (**Schwab et al., 2006 and references therein**). **Charlton et al.** (**2015**) explained three main reasons for the absence of a universally accepted iron provenance methodology. Firstly, iron can be found in a variety of deposits and geological settings that are evenly distributed, as opposed to other metals used by preindustrial societies that are usually occurring in the form of rare patchy deposits. Iron was often used as a currency in the form of semi-products (“currency bars”) that were exchanged in various quantities on local and regional scale. Secondly, due to constraints of precise

radiocarbon dating, it is difficult to precisely date many early iron production sites (**Killick, 2004**), making provenance studies more difficult to conduct. Finally, questions regarding the type of produced alloy in a particular site and region, and whether these would be recognizable is also raised (**Rehren, 2001; Charlton et al., 2010**).

Most recent provenance studies are focused on studying the chemical composition and analysis of trace elements in ores, slags and slag inclusions (**Desai, 2018**). As the ore plays a key role in the production of iron, it is essential to determine characteristics of ore used in smelting process (**Serneels and Crew, 1997**). First studies were focused on the phase identification, major oxide composition and establishing a link using their mutual ratios (**Hedges and Salter, 1979; Buchwald and Wivel, 1998; Buchwald, 2005; Paynter, 2006**). More recent studies showed a potential for following chemical signature from iron ores to iron slags and iron objects by using trace elements (**Coustures et al., 2003; Schwab et al., 2006; Desaulty et al., 2009; Navasaitis et al., 2010**). Some studies suggested comparing major oxide ratios between ore and slag. However, total slag composition is also under the effect of clayey furnace walls and fuel ash (**Crew, 2000**), therefore, comparing ratios of major oxides to distinguish between different ore sources is only possible as a first discriminant. On the other hand, trace elements during smelting process behave in a certain pattern with regards to their mobility and differentiation, much like the trace elements in rocks during petrological processes. Trace elements that are retained within iron bloom are termed compatible as they can be incorporated into the crystal structure of minerals formed inside the bloom. Trace elements that are more likely to differentiate into the liquid slag are termed incompatible, as they are incompatible in the crystal structure and will try to leave at first available opportunity, i.e. during smelting when high temperature is introduced into the system (**Rollinson, 1993**).

Common methods involve analyses of mineralogical and chemical composition of slag inclusions inside iron object using XRD, (LA-)ICP-MS, SEM-EDS or EMPA (**Gordon and van der Merwe, 1984; Coustures et al., 2003, 2006; Buchwald, 2005; Blakelock et al., 2009; Desaulty et al., 2009; Leroy et al., 2011, Charlton et al., 2012**) and comparing their characteristics to the potential ore body or ironmaking region. Slag inclusions are commonly found in bloomery and wrought iron (**Starley, 1999**). After the bloom is formed and removed from the furnace, it undergoes several stages of processing (primary and secondary smiting) where entrapped slag is removed. A part of slag remains trapped inside the bloom even after smiting processes. The chemical composition of the trapped slag should be equivalent to the one of the smelting slag and the iron ore from which it was derived. Studies using slag

inclusions imply that if enough iron objects were discovered and analysed in the study area, it would make the provenance analysis statistically reliable. However, in the case of the Podravina region where only handful of iron objects were discovered, with majority of them being exhibited as a part of museum collections, slag inclusions could not be analysed. Therefore, clean slates of smelting slag samples were used for provenance studies and XRD, ICP-MS and ICP-AES analyses were conducted. In order to define their chemical signature, special attention was given to incompatible group of elements (rare earth elements-REE, Sc, Y, Th, U, Zr, Hf, Ti, Nb and Ta). By carefully analysing ratios of selected pairs of incompatible elements and plotting them on appropriate diagrams, it was possible to compare the chemical signatures of iron slags to proposed raw material and define the provenance and ore material for iron slags and roasted iron ore in the Podravina region.

1.5. Objectives and hypotheses of research

Main objectives of this research were: (1) to determine the possibility of bog iron ore formation in the study area, (2) to determine the types, mineralogical and geochemical characteristics of bog iron ore, roasted iron ore and iron slags and (3) to determine connection between bog iron ore and iron slags using mineralogical and geochemical methods. These objective were based on three main hypothesis: (i) during Late Antique and Early Middle Ages bog iron ore was formed in the low-land Drava River area, (ii) due to complex formation mechanism in soils of different size texture and mineralogical composition, and influenced by the groundwater with variable chemical composition and Eh/pH, complex and variable geochemical composition of bog iron ore is to be expected and (iii) bog iron ore was used as the primary raw material for the iron production during Late Antique and Early Middle Ages in the Podravina region.

1.6. Scientific contribution

The result of this research leads to better understanding of exploitation and usage of raw iron ore during Late Antique and Early Middle Ages by analysing mineralogical and geochemical characteristics of bog iron ore and accompanying archaeological material. For the first time in Croatia, detailed analysis of several phases of bog iron ore from the study area is presented. Special attention is given to the contents of trace and REE and their behaviour and mobility while undergoing different heat treatments (roasting and smelting). Furthermore, obtained results are used for the provenance studies of iron material in the Podravina region.

2. ORIGINAL SCIENTIFIC PAPERS

Paper 1: Brenko, T., Borojević Šoštarić, S., Ružičić, S. & Sekelj Ivančan, T. (2020) Evidence for the formation of bog iron ore in soils of the Podravina region, NE Croatia: Geochemical and mineralogical study. Quaternary International, 536, 13–29.

Quaternary International 536 (2020) 13–29

Contents lists available at ScienceDirect

Quaternary International

journal homepage: www.elsevier.com/locate/quaint

Evidence for the formation of bog iron ore in soils of the Podravina region, NE Croatia: Geochemical and mineralogical study

T. Brenko[a,*], S. Borojević Šoštarić[a], S. Ružičić[a], T. Sekelj Ivančan[b]

[a] Department of Mineralogy, Petrology and Mineral Resources, Faculty of Mining, Geology and Petroleum Engineering, University of Zagreb, Pierottijeva 6, 10 000, Zagreb, Croatia

[b] The Institute of Archaeology, Ljudevita Gaja 32, 10 000, Zagreb, Croatia

ARTICLE INFO

Keywords:
Bog iron ore
Geochemistry
Soils
Drava river
Podravina region

ABSTRACT

This study brings evidence for possible bog iron ore formation in soils of the Podravina region, NE Croatia. During decades of archaeological investigations in the region, numerous sites with iron smelting workshops, furnaces and iron slag materials were found in the region. As archaeological evidence indicates the presence of near-by bog iron excavation sites, a total of 44 soil profiles were drilled in the vicinity of the archaeological sites. Six soil profiles, consisting of five Gleysols and one Fluvisol, were selected for further mineralogical, geochemical and textural analyses due to their visible redoximorphic features. The X-ray diffraction (XRD) analyses confirmed goethite, quartz, clay minerals, plagioclase, feldspars and dolomite. Chemical analyses indicate Fe content above median values for the Podravina region. The Kalinovac-Hrastova Greda profile showed the highest content of Fe_2O_3, (31.52 wt. %) at 60–80 cm depth, while the other investigated profiles show Fe_2O_3 contents between 3.97 and 10.90 wt. %. Contents of As (1.8–563.6 ppm) and P (484–4513 ppm) indicate high accumulations of these elements in the soils. Textural analyses indicate a high amount of silt and, sporadically, sand in all profiles, while showing a relatively small amount of clay. The enrichment factor of Fe_2O_3 shows significant enrichment in the Kalinovac-Hrastova Greda profile, indicating a possible ore formation. Based on the microelement distribution of Ce, Cs, Hf, La, P and Zr, all soils show a common parent material, but significant differences in contents of Fe and other major oxides indicate different formation processes. This is attributed to differences in the soil texture of the selected soil profiles, oscillations of the groundwater table and changes between oxidative and reductive conditions. The results of this study indicate that the Podravina region is a suitable area for the formation of bog iron ore, although recent conditions inhibit the formation of bog iron ore due to changes in agriculture and melioration which are altering groundwater levels.

1. Introduction

Bog iron ores are sedimentary iron deposits (Ramanaidou and Wells, 2014), typically occurring in low-lying areas such as swamps, bogs, meadows or river valleys and micro-depressions with a groundwater table close to the surface (Kaczorek and Zagórski, 2007). Bog iron ores are terrestrial accumulations of iron (Fe) minerals, especially Fe oxides and hydroxides (Banning, 2008) developed in hydromorphic, loamy, sandy and clayey alluvium and soil (De Geyter et al., 1985; Landuydt, 1990), the occurrence of which has been reported in central and northern Europe, Asia and North America (Crerar et al., 1979; Breuning-Madsen et al., 2000; Ratajczak and Rzepa, 2011). The Fe_2O_3 content in bog iron ore varies between 30 and 50 wt. %, but can reach up to 95 wt. % (Joosten et al., 1998; Sitschick et al., 2005; Charlton et al., 2010).

Due to seasonal oscillations of groundwater, periods of wetting and drying occur in the soil profile, typically producing an oxidized zone in the upper 50–80 cm interval and an underlying reduced zone in the deeper parts of the soil profile (Stoops, 1983; Kaczorek and Sommer, 2003). Pedogenetically, bog iron ores are bound to gleys and gley podzols with varying redox potentials and a constant flux of iron-containing water (Graupner, 1982; Kaczorek et al., 2004). According to Kaczorek et al. (2004) and Thelemann et al. (2017) bog iron ores are often distinguished into three different types based on their macromorphological characteristics and development stage: (i) a soft, unstable form, often referred to as “soft” bog iron, (ii) randomly distributed concretions, block or nodules in soil and (iii) well-cemented, massive horizons, continuous or discontinuous, often referred as “hard”

* Corresponding author. Department of Mineralogy, Petrology and Mineral Resources, Faculty of Mining, Geology and Petroleum Engineering, University of Zagreb, Croatia.

E-mail addresses: tbrenko@rgn.hr (T. Brenko), sborosos@rgn.hr (S. Borojević Šoštarić), sruzicic@rgn.hr (S. Ružičić), tsivancan@iarh.hr (T. Sekelj Ivančan).

https://doi.org/10.1016/j.quaint.2019.11.033
Received 9 September 2019; Received in revised form 11 November 2019; Accepted 16 November 2019
Available online 22 November 2019

bog iron. The composition of the bog iron ore largely depends on the chemical composition of the parent material, which is influenced by both the geological and hydrological factors of the study area, as well as material fluxes due to groundwater fluctuation. The mineralogy of the bog iron ores is complex due to changing physico-chemical conditions and redox potential. Bog iron ore primarily consists of amorphous and crystalline Fe oxyhydroxides (mainly goethite), formed under oxidizing conditions, and Fe carbonate (siderite) and phosphate (vivianite), formed under reducing conditions (Stoops, 1983).

Based on several iron smelting workshops found at three locations in the Podravina region (Sekelj Ivančan and Marković, 2017) and numerous slag and roasted ore findings throughout the Podravina region (Valent et al., 2017), and similar case studies in various archaeological sites in southern Hungary (Gömöri, 2006; Török et al., 2015), it is believed that this type of ore was used for iron production from late Antiquity up until the Middle Ages in the Podravina region of Croatia. The natural setting of the bog iron ore in the Podravina region was probably recognised by local farmers and smiths. It is generally easy to spot areas that potentially contain bog iron by the surface discolouration of soils and stagnant water providing a visual marker for the dissolved iron in the water and precipitated iron in the soil (Weronska, 2009). Aside from soil discoloration, withered grass, a wet environment and hygrophilous grass vegetation could also indicate potential areas for bog iron accumulation (Koschke, 2002). Compared to recent mining and exploitation of iron ore, bog iron extraction and smelting are two relatively simple processes (Bowles et al., 2011).

This paper deals with the following research questions regarding the study area of the Drava River: (i) was the Podravina region favourable for the formation of bog iron ore based on geological, pedological and hydrological characteristics, (ii) what are the mineralogical and geochemical characteristics of soil and potential bog iron horizons and (iii) what was the formation mechanism of iron and other elements in the soil? In order to answer these questions, 44 soil profiles were sampled throughout the Podravina region. Six soil profiles were chosen due to their Fe accumulations for further analysis of their mineral composition, geochemical composition of major oxides, minor and trace elements and their particle size distribution in order to identify potential bog iron horizons and define their formation mechanism.

2. Study area

2.1. Drava river development and sedimentology

Geomorphologically, the study area is situated in the central part of the Drava River Valley, belonging to the Croatian part of the Pannonian Basin, which is a mostly low-lying area with an average altitude of 120 m above sea level (m.a.s.l.). The Pannonian Basin is a back-arc basin, underlain by highly thinned continental lithosphere that formed during the Miocene due to rapid rollback of a slab attached to the European continent (Matenco and Radivojević, 2012). It is surrounded by the Southern and Eastern Alps in the west, the West Carpathians in the north, the Eastern Carpathians in the east and the Dinarides in the south (Fig. 1). Several major rivers flow throughout the Pannonian Basin, transporting and depositing material, mostly from the Alps, filling the basin with Neogene and Quaternary sediments.

The study area covers over 500 km^2 of Drava River catchment area, located in the Podravina region in northeast Croatia (inserted frame at Fig. 1a; Fig. 1b). To the north and northeast, the study area is bound by the Croatian-Hungarian state border and to the south and southwest by the Bilogora hills. The average elevation is between 110 and 140 m.a.s.l., with the relief slightly dipping towards the east. Different lithologies and pedological features, as well as agricultural land use characterise the study area. Recent geomorphological features stem from significant climate changes at the end of the Pleistocene and the beginning of the Holocene. A period of climate warming around 11,700 years b2k (Head, 2019) initiated snow melting in the Alps, followed by large torrent flows resulting in the fluvial erosion noticeable in younger gravel deposits overlying older clay and loess sediments. The accumulation of sand and gravel, and the later forming of the humus layer have shaped the present day geography of the Podravina area (Feletar and Feletar, 2008). The large alluvial plain with the meandering Drava River and its tributaries, mainly formed during the Late Pleistocene and Early Holocene, dominates the area (Fig. 1). The emphasised lateral erosion has caused the formation of terraces, shoals, beaches and river islets, which have been destroyed and re-created over time. Alluvial plain consists of three river terraces with adjoining material. The third river terrace is the oldest, was formed at the end of the Late Pleistocene and is characterised by loess clay-sandy silts. At the time of the terrace's formation, alternating dry and cold weather conditions were common, with a noticeable accumulation of aeolian material, sands and loess, originating from the Drava River. The terrace was occasionally flooded during warmer periods, allowing the formation of fluvial accumulations. The second Drava terrace is of erosion-accumulation character and was formed during the second Würm interglacial (Prelogović and Velić, 1988). It spans between the third and first terrace, discordantly overlying the third terrace sediments. This terrace went through all stages of formation, from coarse-grained gravelly sand at its base to the fine-grained silts at the top. Based on the mineral composition (Mutić, 1975), it can be assumed that this material originated in the Eastern Alps. The first terrace, located between the second terrace and the Drava River channel, is the youngest and was formed during the third Würm interglacial. It is highly altered due to the current flow and meanders of the river. The formation of the first Drava River terrace only included several phases of the floodplain formation and, therefore, its surface is uneven and is frequently flooded during high waters. The main sedimentary materials in this terrace are sands, gravelly sands and sandy gravels (Šimunić et al., 1990).

Flooding sediments were created by deposition of fine-grained material after large floods and torrents, and while the river was returning back into the river channel. Dominant materials are sandy clays and clayey silts with transition to fine-grained material, mostly silty clays. Flooding sediments are often covered with soil horizon features formed by the decomposition of organic materials (Hećimović, 1987).

Since the Drava is a meandering river, there are several abandoned riverbeds, some of them still containing water, forming still waters and pond areas. Abandoned riverbeds are formed as a result of the river finding new flow paths, and simultaneously cutting off existing riverbeds. Abandoned riverbeds are often found on first and second river terrace with fluvial deposition of fine-grained material such as silty sand and silt. According to the literature, swamp, marsh and bog sediments are very often associated with abandoned riverbeds. They consist of silty clays, clayey-sandy silts and clay with organic components. Peat deposits are sometimes found below clays (Bognar, 2008).

Aeolian sand deposits are an important part of the lithology covering the third river terrace. These deposits were part of the Drava fluvial sediments that were transported to the southwest of the river due to strong winds, where they are found today. The thickness of the sand is variable, with up to 2 m on hilly relief, and up to 10 m in flat areas (Pavelić et al., 2016; Galović, 2016).

2.2. Pedology

The most common soil types in the study area are Fluvisols and Gleysols located on the Pleistocene and Holocene sediments, with Stagnosols and Regosols sporadically appearing in some parts. As seen in Fig. 2, most of the pedological profiles are located in bog areas dominated by Gleysols, which occur due to the specific combination of pedogenetic factors in micro-depressions with relatively shallow groundwater. Gleyed (waterlogged) soils are generally characterised by highly localised patterns of redoximorphic features, mainly Fe oxyhydroxides, as a result of concentration and depletion due to complex and variable redox conditions (Husnjak, 2014). Gleysols predominantly

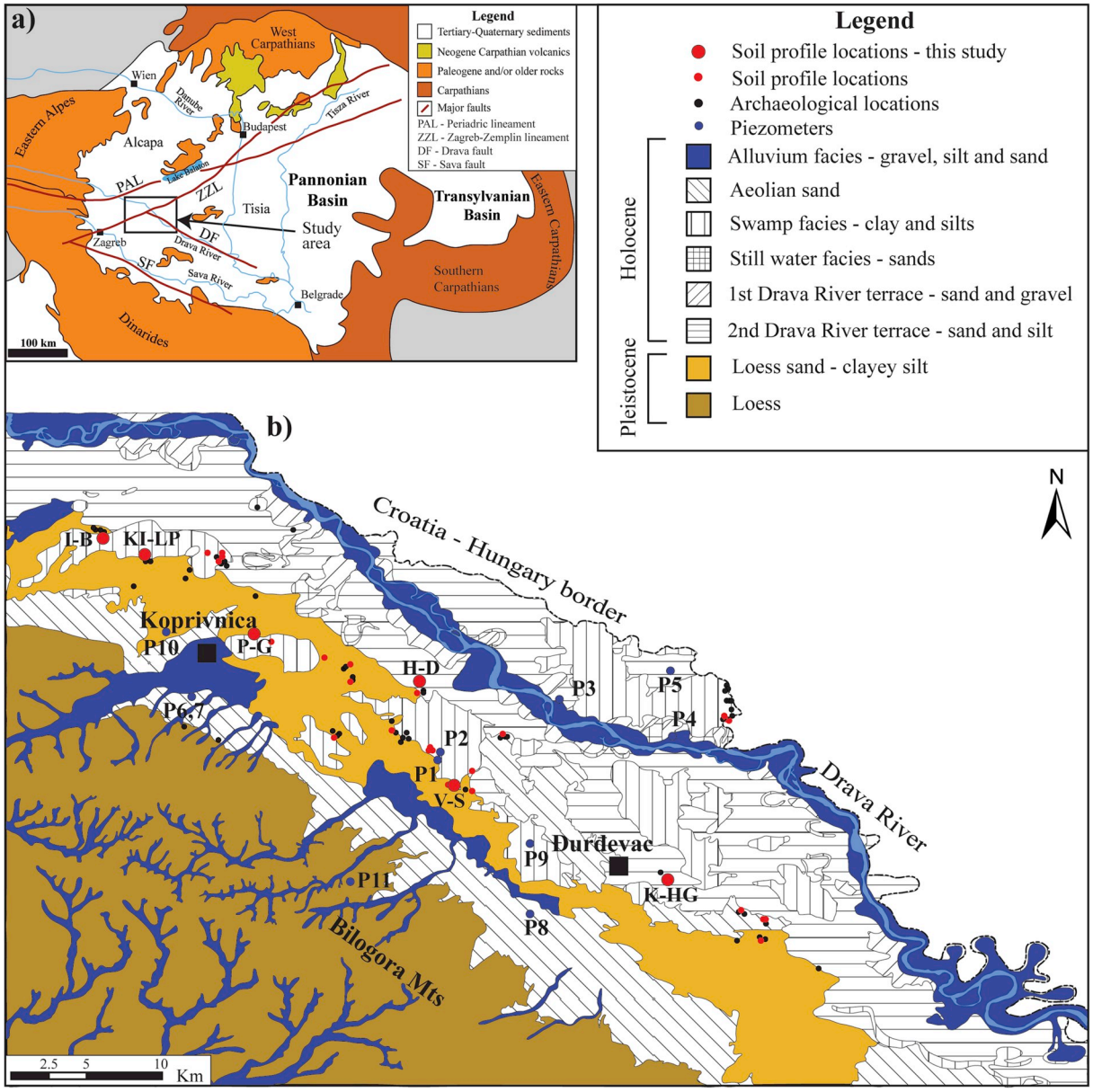

Fig. 1. Simplified geological map of a) the Pannonian Basin, modified according to Seghedi et al. (2004); Schmid et al. (2008) and b) Podravina geological map with inserted sampling locations, archaeological sites and piezometer locations, modified according to Galović and Marković (1979); Korolija and Crnko (1985); Hećimović (1986); Hećimović (1995). Archaeological locations and findings according to Sekelj Ivančan and Marković (2017) and Valent et al. (2017). Piezometer locations according to Nakić et al. (2018).

occur on older, fluvial accumulations with good horizontal and vertical permeability. Lower parts of the soil profiles are mostly below groundwater level (Fig. 3). Because of that, lower parts of the soil profile are usually greyish or bluish in colour, indicating an anaerobic and reducing environment.

According to the Food and Agriculture Organisation (FAO, 2015), Fluvisols are found on alluvial plains with periodical flooding. Soil horizons are weakly developed, with only the initial humus horizon (A) developed, especially in the flooded areas. Fluvisols are characterised by specific formation mechanisms of fluvial sediments. Frequent flooding and transport of suspended particles aggravates pedogenetic processes and the formation of soil horizons. In this type of soil, groundwater is commonly found in the first meter of soil. In the zone of groundwater stagnation, a gley horizon (G) can form (Husnjak, 2014). Physical and chemical characteristics of Gleysols are heterogeneous, both vertically and laterally.

2.3. Drava River aquifer system

The Drava River is a typical glacial river with the highest water levels in late spring and summer (May, June, and July) and lowest water levels during the winter period (January and February). This type of hydrological regime sometimes leads to flooding of the surrounding river terraces. Hydrogeological characteristics have been changing over time as a result of human activities, mostly due to construction works carried out at different times throughout history (Tadić and Brleković, 2018). In recent years, declining linear trends of water levels were noted. Organised flood protections and construction of smaller channels began in the 19th century. Nowadays, floods rarely appear because the natural hydrological characteristics have been altered (Kiss and Andrási, 2017).

The hydrogeological characteristics of the Drava River aquifer are products of tectonic activity and a fluvial depositional environment within the river valley. The aquifer is confined in some part of the study

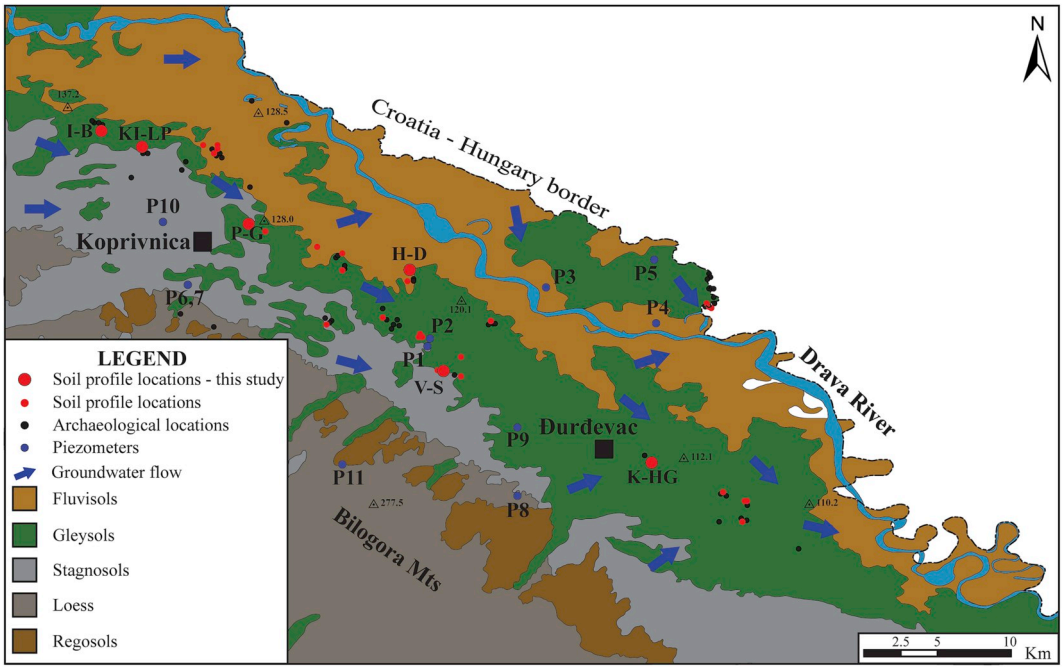

Fig. 2. Pedological map of the study area (map modified according to envi.azo.hr). Archaeological locations and findings according to Sekelj Ivančan and Marković (2017) and Valent et al. (2017). Piezometers locations according to Nakić et al. (2018).

area, while in others it is unconfined, due to heterogeneity of overlying clastic materials. Groundwater is interconnected with the water level in the Drava River and there is a dominant groundwater drainage into the Drava River (Brkić et al., 2010). Brkić and Briški (2018) recognised that groundwater flows from the valley margins in the southwest towards the Drava River in the northeast (Fig. 2), with precipitation being the main source of groundwater recharge. Groundwater levels are several meters below the surface but can also reach the surface (Fig. 3). Values of pH for the observed groundwater range from 6.60 to 7.90, meaning that the groundwater is very slightly acidic, up to neutral and slight alkaline. Redox conditions are very irregular within the aquifer, varying from −73.2 mV in one piezometer up to 319 mV in another piezometer (Table 1). Only 15% of groundwater is saturated with oxygen, while the remaining 85% are depleted with oxygen. The aquifer system is enriched with iron, arsenic and manganese, which can occasionally exceed the maximum allowable concentration for drinking water (Kopić et al., 2016). As seen in Table 1, Figs. 1 and 2, concentrations of Fe and Mn are especially increased in the central part of the study region, with concentrations of Fe exceeding maximum allowed concentrations up to several times. This enrichments can be equally found on both the left and the right floodplains of the Drava River. Naturally increased arsenic values are typical for the aquifer system and groundwater of the Pannonian Basin (Rowland et al., 2011).

3. Materials and methods

3.1. Sampling and sample preparation

During the summer and autumn of 2017, several field campaigns were conducted, and 44 soil profiles were sampled up to a depth of 250 cm using an Eijkelkamp auger set for soils. The profile locations were chosen based on previous archaeological excavation campaigns around discoveries of iron smelting workshops dating back to Late antiquity and the Middle Ages in the Podravina region (Fig. 1) (Sekelj Ivančan and Marković, 2017) and on surface iron slag findings (Valent et al., 2017). Each soil profile was described and classified according to the IUSS Working Group WRB (2015). Each soil profile was further divided into intervals based on the visible macro features and field estimation of the soil texture and mineralogical changes along the profile. The samples were stored in separate plastic bags. After they were transported to the laboratory, samples were air-dried. Then a portion of each interval was crushed and sieved through a 2 mm sieve. Six profiles were chosen based on the abundance of iron features (orange and red colour of soil, orange mottles, noticeable iron linings and pore masses) and analysed for their physical, chemical and mineralogical characteristics.

3.2. Laboratory analyses

Soil colour was determined in the laboratory on dry samples using the Munsell colour chart (Munsell, 1994). Soil pH in H_2O and 1M KCl was measured with a glass electrode immersed in a suspension of 1:5 soil volume and H_2O/1M KCl respectively, according to ISO 10390:2005. Electric conductivity was measured in a suspension of 1:5 soil volume and H_2O. Carbonate content was determined using the volumetric method (ISO 10693, 1995).

The mineralogical composition of 34 soil samples was determined using powder X-ray diffraction (XRD) using a Phillips vertical X-ray goniometer (type X'Pert) equipped with Cu tube and graphite crystal monochromator. Scan settings were 3–70° 2θ, 0.02° step size, 1 s count time per step while generator settings were 40 kV and 20 mA. Minerals were identified using PANalytical X'Pert HighScore software with standardised Powder Diffraction Files (PDF) of the International Centre for Diffraction Data (ICDD) (Newton Square, PA, USA). Major oxides alongside multi-element analyses were performed at MS Analytical, Langley, Canada on six previously selected soil profiles (n = 34). Multi-element contents were analysed using inductively coupled plasma-mass spectrometry (ICP-MS), while 4-acid digestion including hydrochloric, nitric, perchloric and hydrofluoric acids was used for near total digestion. Only the most highly resistant minerals (zircon) were not fully dissolved. Based on five standards and blanks, instrumental precision was 3–5% and the detection limits for most analysed elements were in the part per million (ppm) or lower. Major oxides analysis was performed using inductively coupled plasma-atomic emission spectrometry (ICP-AES) with lithium borate fusion. Loss on ignition (LOI) was determined by weight difference after ignition at 1000 °C. Soil profile

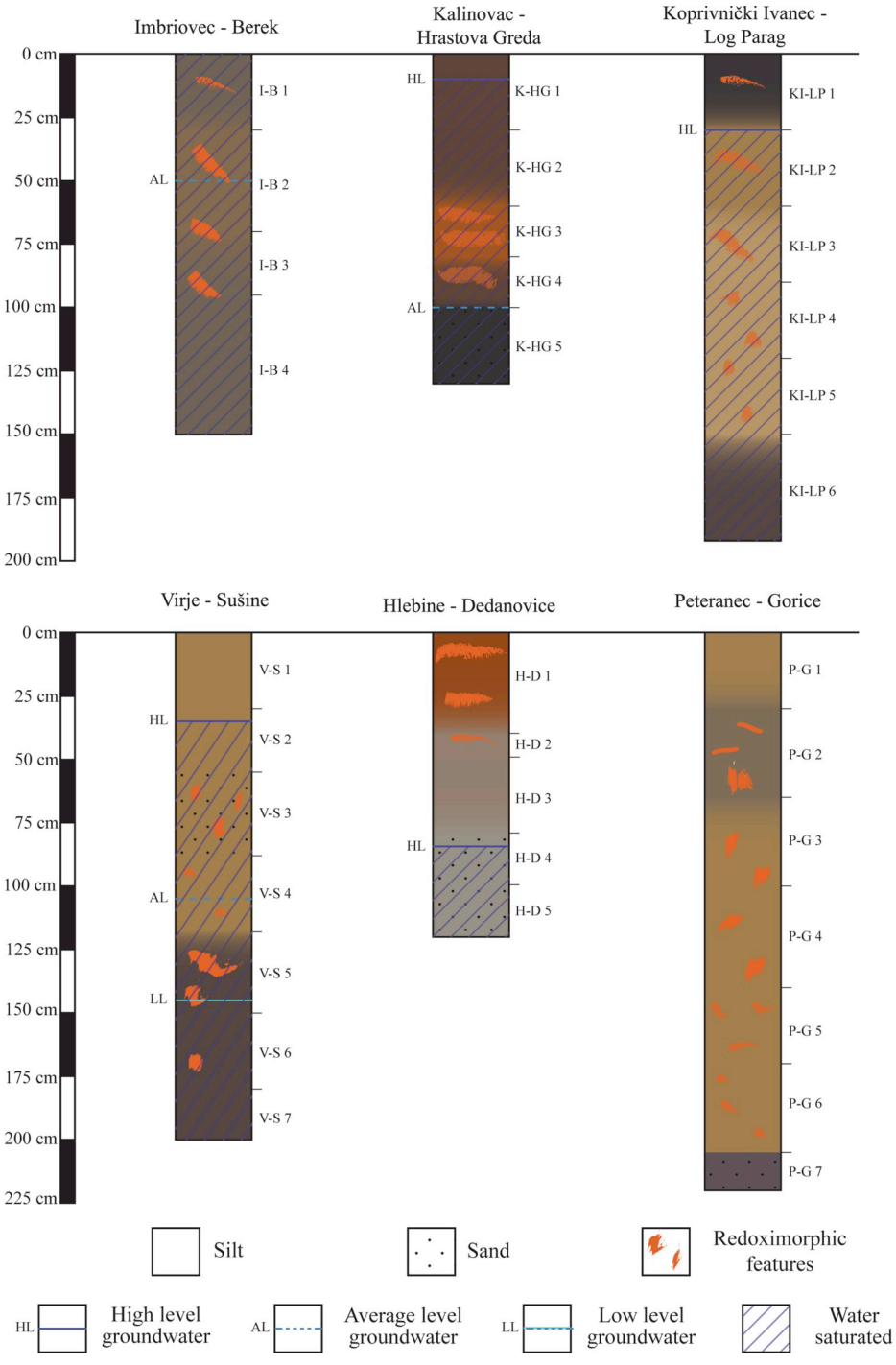

Fig. 3. Schematic drawing of the six selected soil profiles with visible iron redoximorphic features and groundwater depths according to Brkić and Briški (2018). Peteranec-Gorice soil profile is not affected by the groundwater.

texture was characterised using laser diffraction particle size analyser LS 13320 (Beckman Coulter, USA). For this study, the 2000-63-4-μm system was used to determine particle size fractions, and the results are presented in graphs based on the amount of clay, silt and sand (FAO, 2015).

3.3. Enrichment factors

Major oxides and minor elements were compared to the Geochemical Atlas of the Republic of Croatia (Halamić and Miko, 2009). These values represent median values of major oxides and minor elements for topsoils of the Podravina region. Possible enrichment in the soil can be determined with the help of enrichment factors. The enrichment factor (EF) is a relatively simple and easy tool for assessing the enrichment degree of soils due to its universal formula (Benhaddya and Hadjel, 2013). The EF is a normalisation method proposed by Simex and Helz (1981) to assess the regional contents of metals. The index of potential enrichment was calculated using the normalisation of the observed element as a ratio to another reference constituent of soil, defined as:

$$EF = (Metal/RE)_{soil}/(Metal/RE)_{background} \quad (1)$$

Table 1
Geochemical characteristics of the groundwater in the broader Podravina region. Compiled after Hrvatske vode and Nakić et al. (2018)., with the permission of Hrvatske vode.

Piezometers	pH	Eh_{min}	Eh_{max}	$Eh_{average(mV)}$	Fe_{min}	Fe_{max}	$Fe_{average}$ (μg/l)	Mn_{min}	Mn_{max}	$Mn_{average}$ (μg/l)	As_{min}	As_{max}	As $_{average}$ (μg/l)
P1	/	/	/	/	1910	3360	2522	61.9	739	594.68	< 1	6.2	4.12
P2	/	/	/	/	1810	3600	2835.79	467	881	705.95	< 1	4.4	3.26
P3	/	/	/	/	12	63.5	33.26	4.6	28.1	8	< 1	1.5	< 1
P4	/	/	/	/	2860	9040	5180	348	454	399.5	< 1	< 1	< 1
P5	/	/	/	/	2900	4830	3579	463	565	527	< 1	< 1	< 1
P6	7.14	19.5	224	115.36	3.4	2130	488.66	< 1	21.1	11.56	< 1	< 1	< 1
P7	7.26	22	319	145.48	< 1	17.3	7.96	< 1	6.4	1.8	< 1	< 1	< 1
P8	7.34	−73.2	31.2	−10.9	24.6	4230	1047.55	< 2	1010	60.29	< 1	1.5	< 1
P9	7.45	15.2	169.5	78.59	5.6	32.4	16	< 0.5	3.1	< 1	< 1	< 1	< 1
P10	7.18	−43.3	249	73.9	23.1	1210	469.39	6.3	21	16.45	< 1	< 1	< 1
P11	7.48	53.2	114.7	79.85	20.3	39.2	28.9	1.3	7.2	3.85	< 1	< 1	< 1

Table 2
Enrichment categories based on EF index.

Contamination categories based on EF values	
EF < 2	Deficiency to minimal enrichment
2 < EF < 5	Moderate enrichment
5 < EF < 20	Significant enrichment
20 < EF < 40	Very high enrichment
EF > 40	Extremely high enrichment

where RE is the value of the reference element. A reference element is an element particularly stable in the soil, which is characterised by the absence of vertical mobility through the soil profile. In this study, titanium was used as the reference metal (Isakson et al., 1997). The numerical results are indicative of different pollution levels. Values of $0.5 \leq EF \leq 1.5$ suggest that the metal content comes from entirely natural weathering processes. The EF index can be used as an indication for the soil quality based on values falling into different classes (Table 2), ranging from EF < 2 (Deficiency to minimal enrichment) up to EF > 40 (Extremely high enrichment) (Loska and Wiechuła, 2003).

4. Results

4.1. Physico-chemical characteristics of the selected soil profiles

Six chosen soil profiles are presented in Fig. 3 and their soil characteristics are provided in Table 2. The Hlebine-Dedanovice profile is determined as Fluvisol, while the remaining five profiles are classified as Gleysols (Fig. 3; Table 3). Changes in colour through the profiles are gradient, with the bottom interval often being greyish and dark grey, indicating a gley horizon. All six profiles show signs of iron (Fe), mostly as precipitations on soil particles in the form of soft masses or pore linings. This affects the colour of the interval, showing orange and red colours for intervals where Fe is present in significant concentrations, such as in the 60–100 cm interval in the Kalinovac-Hrastova Greda profile (Table 3). The pH range measured in KCl is substantially lower than the pH in H_2O. The profiles are characterised by a slightly acidic to neutral and slightly alkaline pH in H_2O (5.85–7.81), or moderately acidic to neutral pH in KCl (4.36–7.50). In both H_2O and KCl, there is a visible trend of increasing pH with increasing depth of profiles. The Kalinovac-Hrastova Greda profile stands out as being the most acidic, with a pH below 7.0 in both H_2O and KCl. The carbonate content is low, usually below 1 wt. % with only the profile Hlebine-Dedanovice showing carbonate values over 5 wt. %. Silt is the dominant component in most of the Gleysols. The Fluvisols have similar contents of silt and sand as the Gleysols. Silt is the dominant phase, followed by sand, with clay particles being a minor component, rarely exceeding 10%. Sand is the dominant phase in the lower interval of the Kalinovac-Hrastova Greda, Peteranec-Gorice and Virje-Sušine profiles. In profiles Kalinovac-Hrastova Greda and Peteranec-Gorice there is a noticeable coarsening in the middle and lower parts of the profiles. Contents of clay, silt and sand are presented in Table 3 and Fig. 6. Based on the IUSS Working Group WRB (2015) soil texture classification, the majority of samples are classified as silt loam with some intervals being classified as loam, sandy loam and loamy sand.

4.2. Mineralogy

According to XRD analysis, most of the soil profiles have similar mineral assemblages. Quartz is the dominant mineral phase, followed by clay minerals and micas with feldspar and/or plagioclase minerals. Clay minerals mostly consist of 10 and 14 Å minerals such as illite, smectite and, in some cases, chlorite minerals. The Kalinovac-Hrastova Greda profile differs from the other profiles in terms of the dominant mineral phases. In the middle part of the profile, from a depth of 60–100 cm, goethite (iron oxyhydroxide) is the dominant mineral phase alongside quartz (Fig. 4). Weak indication of ferrihydrite is also noticeable in the samples K-HG 3 and K-HG 4 (60–100 cm interval) of the Kalinovac-Hrastova Greda profile due to the slightly increased background values that can be seen between 33 and 36° 2θ although the diffraction lines are partially overlapping by the quartz and goethite diffraction lines. In other profiles, goethite is less present and mainly found in the upper and middle parts of the profiles (Table 4).

4.3. Geochemistry

The soil profiles were analysed for the content of major oxides and trace elements, including arsenic (As) and phosphorus (P) (Table 5). The full list of analysed major, minor and trace elements is presented in the Appendix. Geochemical analysis of Fe was conducted due to known preindustrial iron smelting activity in the surrounding area. The oxide composition of the soil samples is mainly comprised of silicon-dioxide (SiO_2), aluminium (III) oxide (Al_2O_3) and iron (III) oxide (Fe_2O_3). The SiO_2 component varies from 38.90 (middle part of the Kalinovac-Hrastova Greda profile) up to 73.85 wt. % (lower part of the Peteranec-Gorice). The iron oxide content greatly varies between the profiles, with the general trend being a higher content of Fe oxides in upper and middle parts of profiles. The Kalinovac-Hrastova Greda profile shows the highest content of Fe oxide, reaching 31.52 wt. % at the 60–80 cm interval. Contents of As (1.8–563.6 ppm, average 63.4 median 23.6) and P (484–4513, average 1334.8 ppm, median 1033.5 ppm) show elevated values compared to Clark's values for the upper continental crust (Rudnick and Gao, 2003) and topsoil values in Croatia based on the Geochemical Atlas (Halamić and Miko, 2009). Several microelements show elevated contents in the soil profiles (Appendix 1). Cs (2.51–12 ppm), Rb (54–188.3115.16 ppm), Y (15.3–38.5 ppm), Th (7.9–20.8 ppm) and Ce (41.38–108.3 ppm) show slightly elevated values in all profiles except Kalinovac-Hrastova Greda. Heavy metals (Ni, Co, V, Cr and Cu, Zn and Pb) show elevated contents in all profiles, with Ni showing very high values in the lower part of the Peteranec-Gorice

Table 3
Physico-chemical characteristics of selected soil profiles in the Podravina region.

Location	Depth, cm	Soil type	Colour	pH (H_2O)	pH (KCl)	EC, μS/cm (H_2O)	$CaCO_3$, wt. %	Clay, %	Silt, %	Sand, %	Soil texture
Imbriovec - Berek	0–30	Gleysols	5Y 5/2	6.97	5.41	128.43	0.85	8.55	60.96	30.5	Silt loam
	30–70		2.5Y 6/3	7.23	6.50	166.30	0.57	5.44	63.92	30.64	
	70–95		2.5Y 7/2	7.47	7.05	147.00	1.41	7.68	72.2	20.12	
	95–150		2.5Y 7/3	7.60	7.02	120.77	1.55	6.94	70.7	22.37	
Kalinovac - Hrastova Greda	0–30	Gleysols	10 YR 3/4	5.85	4.96	109.93	0.76	6.75	48.23	45.01	Sandy loam
	30–60		10 YR 3/4	6.06	5.10	99.83	1.68	9.45	49.95	40.6	Silt loam
	60–80		7.5 YR 5/8	6.39	5.45	110.43	0.983	11.34	47.98	40.69	Loam
	80–100		7.5 YR 5/6	6.51	5.66	103.37	0.702	15.42	49.86	34.73	Silt loam
	100–130		2.5 Y 2.5/1	6.08	5.23	242.00	0.844	4.16	30.14	65.69	Sandy loam
Koprivnički Ivanec - Log Parag	0–30	Gleysols	2.5Y 4/2	6.68	5.48	96.23	1.05	8.38	64.62	27	Silt loam
	30–60		2.5Y 5/4	6.84	5.79	57.33	0.84	9.25	75.75	15.01	
	60–90		2.5Y 5/4	6.91	6.20	84.13	0.43	8.64	72.83	18.52	
	90–120		2.5Y 5/4	7.05	6.11	62.23	0.42	8.47	74.31	17.22	
	120–150		2.5Y 5/4	6.97	6.10	115.70	0.43	9.16	74.04	16.8	
	150–192		5Y 4/1	6.96	6.10	140.73	0.15	8.67	73.49	17.84	
Virje - Sušine	0–30	Gleysols	2.5Y 5/3	5.93	4.73	94.70	0	7.45	67.61	24.94	Silt loam
	30–55		2.5Y 6/4	6.08	4.87	76.43	0	5.54	60.48	33.99	
	55–88		2.5Y 5/4	6.23	5.07	53.83	0	6.05	35.36	58.59	Sandy loam
	88–118		2.5Y 6/4	6.56	5.21	41.37	0.24	8.06	78.48	13.46	Silt loam
	118–150		5Y 4/1	6.84	5.31	46.23	0.38	17.05	67.13	15.82	
	150–180		5Y 3/1	6.93	5.30	49.93	0.85	15.36	52.54	32.1	
	180–200		5Y 3/1	6.83	5.32	55.73	0.57	10.36	47.68	41.97	Loam
Hlebine - Dedanovice	0–40	Fluvisols	10 YR 6/8	7.46	6.94	219.00	1.28	7.93	63.96	28.1	Silt loam
	40–50		2.5Y 6/2	7.81	7.18	128.20	7.39	7.71	70.53	21.76	
	50–80		2.5Y 6/2	7.80	7.50	148.53	4.86	3.86	38.7	57.44	Sandy silt
	80–100		2.5Y 6/2	7.72	7.50	181.97	5.28	2.93	36.75	60.32	
	100–120		2.5Y 6/2	7.45	7.28	631.67	6.25	4.06	51.35	44.59	Silt loam
Peteranec - Gorice	0–30	Gleysols	2.5Y 5/2	5.94	4.36	139.60	1.14	9.55	62.63	27.83	Silt loam
	30–65		2.5Y 5/2	6.20	5.12	41.60	0.86	10.2	64.52	25.28	
	65–100		2.5Y 5/6	6.60	5.54	46.93	2.01	13.21	62.71	24.08	
	100–140		2.5Y 5/6	6.82	5.69	48.43	1	6.02	63.33	30.66	
	140–170		5Y 6/2	6.84	5.75	81.73	0.86	5.04	68.08	26.88	
	170–205		5Y 6/2	7.08	6.76	97.03	1.57	5.11	49.84	45.05	Sandy loam
	205–220		5Y 5/2	7.28	6.96	63.43	4.15	2.37	17.43	80.2	Loamy sand

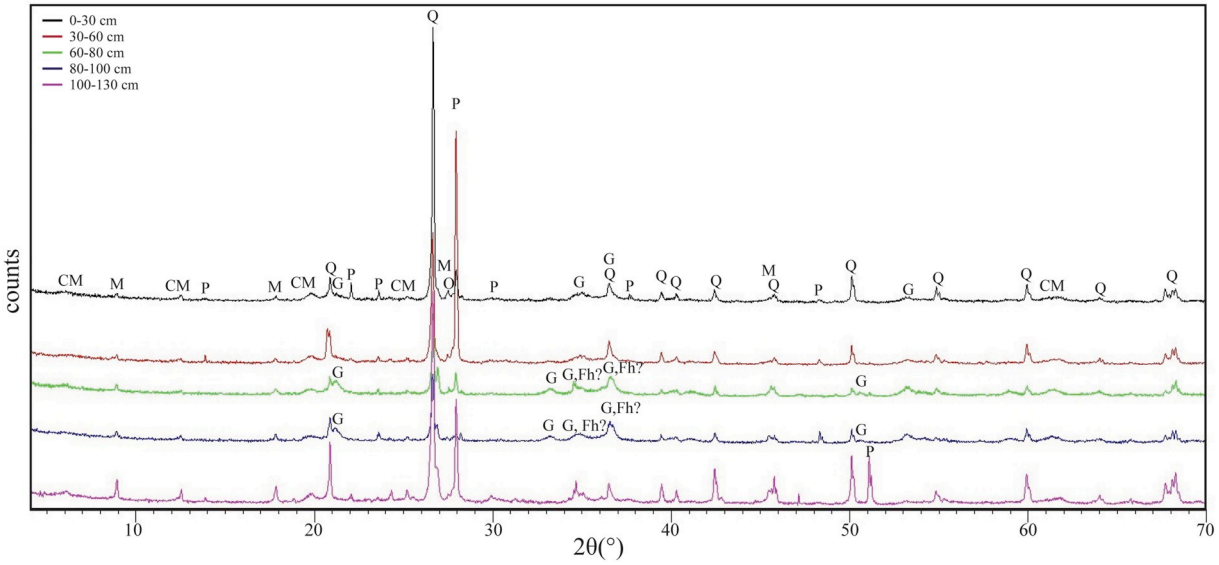

Fig. 4. XRD pattern for the Kalinovac-Hrastova Greda soil profile. Mineral abbreviations: Q –quartz; G - goethite; M - mica; P - plagioclase; O – orthoclase; CM – clay minerals, Dol – dolomite, Fh - ferrihydrite.

Table 4
Results of mineral composition based on the XRD analysis for grain size < 2 mm (Abbreviations: Qtz – quartz, Gt – goethite, Ms – muscovite, Pl – plagioclase, Or – orthoclase, Dol – dolomite, CM – clay minerals, Fh - ferrihydrite). Mineral abbreviations after the International Mineralogical Association (IMA). + = mineral present in the sample, ? = mineral is probably present in the sample but due to the low content and/or overlapping of diffraction peaks cannot be confirmed with certainty, - = mineral not present in the sample.

Location	Sample ID	Depth (cm)	Qtz	Gt	Ms	CM	Pl	Or	Dol	Fh
Imbriovec - Berek	I–B 1	0–30	+ + +	–	+	+	+	+	–	–
	I–B 2	30–70	+ + +	?	+	+	+	?	–	–
	I–B 3	70–95	+ + +	+	+	+	+	?	–	–
	I–B 4	95–150	+ + +	–	+	+	+	?	+	–
Kalinovac - Hrastova Greda	K-HG 1	0–30	+ + +	+	+	+	+	–	–	–
	K-HG 2	30–60	+ +	+	+ +	+	+ +	–	–	–
	K-HG 3	60–80	+ +	+ + +	?	+	+	–	–	?
	K-HG 4	80–100	+ +	+ + +	?	+	+	–	–	?
	K-HG 5	100–130	+ + +	?	?	+	+	–	–	–
Koprivnički Ivanec - Log Parag	KI-LP 1	0–30	+ + +	+	+	+	+	–	–	–
	KI-LP 2	30–60	+ + +	+	+	+	+	+	–	–
	KI-LP 3	60–90	+ + +	–	+	+	+	+	–	–
	KI-LP 4	90–120	+ + +	?	+	+	+	–	–	–
	KI-LP 5	120–150	+ + +	?	+	+	+	+	–	–
	KI-LP 6	150–192	+ + +	–	+		+	+	–	–
Virje - Sušine	V–S 1	0–30	+ + +	–	+	+	+	–	–	–
	V–S 2	30–55	+ + +	+	+	+	+	+	–	–
	V–S 3	55–88	+ + +	+	+	+	+	+	–	–
	V–S 4	88–118	+ + +	?	+	+	+	+	–	–
	V–S 5	118–150	+ + +	+	+	+	+	?	–	–
	V–S 6	150–180	+ + +	+	+	+	?	–	–	–
	V–S 7	180–200	+ + +	–	+	+	+	?	–	–
Hlebine – Dedanovice	H-D 1	0–40	+ + +	+	+ +	+	+	+	?	–
	H-D 2	40–50	+ + +	?	+ +	+	+	?	+	–
	H-D 3	50–80	+ + +	–	+ +	+	+	–	+	–
	H-D 4	80–100	+ + +	+	+ +	+	+	+	+	–
	H-D 5	100–120	+ + +	?	+ +	+	+	–	+	–
Peteranec – Gorice	P-G 1	0–30	+ + +	?	+	+	+	–	–	–
	P-G 2	30–65	+ + +	+	+	+	+ +	+	–	–
	P-G 3	65–100	+ + +	+	+	+	+	–	–	–
	P-G 4	100–140	+ + +	+	+	+	+	+	–	–
	P-G 5	140–170	+ + +	?	+	+	+	+	–	–
	P-G 6	170–205	+ +	–	+	+	+	+	+	–
	P-G 7	205–220	+ + +	–	+	+	+	–	–	–

+ - relative abundance of minerals within horizons based on X-ray diffraction (no quantitative value assigned to +); + + + major component, + + minor component; + traces.

profile (361.9 ppm) (Appendix). Multivariate diagrams were created for all six profiles (Fig. 5), with normalisation to the upper continental crust (Taylor and McLennan, 1985). All profiles are of similar appearance, indicating enrichment of P, especially in upper parts of the profiles. Most of the calculated geochemical diagrams show enrichments of Cs, La and Ti, with depletions of Rb, Sr, Zr and Hf.

4.4. Enrichment factors of major oxides, As and P

The relative enrichments of major oxide compositions and As and P were calculated (Table 6) with Ti as the reference element (Isakson et al., 1997). The Hlebine-Dedanovice profile shows moderate to significant enrichment of Mg and Ca oxides from 10 to 140 cm depth and moderate enrichment of As in the topsoil compared to Halamić and Miko (2009). The Kalinovac-Hrastova Greda profile shows significant enrichment of Fe (EF = 11.07) in the top 100 cm of the profile and moderate enrichment in the lower part, similar to P. Mn values indicate moderate enrichment in upper and middle parts, correlating to Fe enrichment. Values of As indicate very high (EF = 32.53) and extremely high enrichment (EF = 61.39) in upper and middle parts of the profile and a slight significant enrichment below 100 cm in the profile. The profile Koprivnički Ivanec-Log Parag shows moderate enrichment of Mn in the 30–60 cm interval (EF = 4.51. There are no detectable enrichments in profiles Imbriovec-Berek, Peteranec-Gorice and Virje-Sušine.

5. Discussion

5.1. Regional settings of the Podravina region regarding the potential formation of bog iron ore

The dominant feature of the Podravina region is the Drava River, whose influence is undeniable in regard to the geological, pedological and hydrological characteristics of the whole study area. Due to the river flow, constant sediment flux is present in the river valley. It is well documented that the Drava River occasionally flooded throughout the region, forming a several km wide floodplain (Lóczy, 2013). Therefore, the sedimentation has the characteristics of a typical floodplain, with alluvial sediments, such as silty deposits, being the most prominent (Lóczy et al., 2014). Since the Drava is a meandering river, oxbow lakes, swamps and bogs are also a constant feature, spread throughout the region, mostly localised in smaller micro-depressions. The groundwater table, also under the influence of the Drava River (Brkić and Briški, 2018), is close to the surface, providing interchanges of oxidative and reductive conditions and forming Gleysols, which is the most common soil type in the region. All of the above-mentioned characteristics of the

Table 5
Geochemical characteristics of selected soil profiles in the Podravina region. Bolded values represent values higher than Clark's values for upper continental crust (Rudnick and Gao, 2003).

Location	Sample	Depth (cm)	SiO_2	TiO_2	Al_2O_3	Fe_2O_3	MgO	MnO	CaO	K_2O	Na_2O	As	P	LOI
			wt. %									ppm		wt. %
Imbriovec - Berek	I–B 1	0–30	46.88	**0.82**	**18.63**	**6.46**	2.06	0.05	1.43	2.30	0.79	**11.6**	**1078**	20.13
	I–B 2	30–70	56.44	**0.94**	**17.15**	**7.59**	2.31	0.07	1.67	2.65	1.39	**23.9**	**1331**	9.33
	I–B 3	70–95	56.03	**0.93**	**16.50**	**7.18**	**3.03**	0.07	3.33	2.70	1.52	**26.4**	**1025**	9.20
	I–B 4	95–150	60.69	**0.98**	14.82	**6.38**	**2.61**	0.07	2.65	2.38	1.59	**28.6**	**923**	7.66
Kalinovac - Hrastova Greda	K-HG 1	0–30	48.42	0.46	9.15	**17.77**	0.93	**0.21**	1.24	1.02	0.70	**280.0**	**2756**	18.18
	K-HG 2	30–60	44.59	0.47	10.18	**22.71**	1.10	**0.27**	1.39	1.09	0.64	**379.4**	**3225**	17.96
	K-HG 3	60–80	38.90	0.37	7.98	**31.52**	0.93	**0.16**	1.26	0.87	0.52	**563.6**	**4513**	17.48
	K-HG 4	80–100	49.31	0.48	9.54	**20.53**	1.10	0.10	1.38	1.12	0.78	**225.5**	**2629**	16.43
	K-HG 5	100–130	57.68	0.54	9.57	**8.86**	1.07	0.07	1.46	1.22	1.06	**64.6**	**897**	18.97
Koprivnički Ivanec - Log Parag	KI-LP 1	0–30	47.45	**0.85**	**17.42**	**9.11**	1.91	**0.37**	1.43	2.18	0.80	**43.3**	**1377**	19.47
	KI-LP 2	30–60	54.49	**0.96**	15.35	**9.81**	1.61	**0.70**	1.20	2.26	1.19	**55.2**	**1749**	11.42
	KI-LP 3	60–90	61.31	**1.05**	15.30	**8.06**	1.54	**0.24**	1.18	2.32	1.47	**36.9**	**1419**	8.51
	KI-LP 4	90–120	61.40	**1.06**	**15.41**	**7.82**	1.59	**0.11**	1.16	2.41	1.47	**31.6**	**1448**	7.95
	KI-LP 5	120–150	57.21	**1.00**	**16.49**	**7.03**	1.85	0.07	1.22	2.57	1.30	**13.4**	**1042**	11.01
	KI-LP 6	150–192	50.81	**0.83**	**16.86**	**6.89**	2.11	0.07	1.42	2.50	1.03	**11.9**	**990**	18.36
Virje - Sušine	V–S 1	0–30	63.79	**1.08**	12.97	**5.68**	1.31	**0.11**	1.08	1.74	1.34	**15.0**	**850**	9.66
	V–S 2	30–55	**71.26**	**1.54**	11.08	**5.99**	1.12	**0.17**	1.23	1.44	1.44	**9.2**	**810**	4.12
	V–S 3	55–88	**72.78**	**1.86**	9.48	**6.59**	1.01	**0.19**	1.30	1.11	1.25	**8.5**	**859**	2.93
	V–S 4	88–118	**69.53**	**1.19**	11.78	**5.82**	1.24	**0.14**	1.08	1.67	1.25	**13.9**	**957**	5.91
	V–S 5	118–150	52.80	**0.94**	**16.21**	**10.53**	1.71	**0.22**	1.17	1.99	0.72	**39.7**	**2243**	12.99
	V–S 6	150–180	49.04	**0.82**	**20.50**	**8.38**	2.12	0.06	1.26	2.43	0.52	**27.2**	**933**	15.07
	V–S 7	180–200	57.68	**0.77**	**17.35**	**6.23**	1.70	0.06	1.20	2.06	0.86	**12.8**	484	12.01
Hlebine - Dedanovice	H-D 1	0–10	51.17	**0.84**	**15.52**	**10.90**	2.47	**0.17**	3.03	2.47	1.48	**56.4**	**1529**	13.33
	H-D 2	10–40	49.29	**0.84**	**15.47**	**7.00**	**4.11**	0.10	**6.73**	2.57	1.56	**18.0**	**856**	13.24
	H-D 3	40–75	63.50	**0.83**	11.48	4.41	**3.25**	0.08	**5.24**	1.72	1.96	**12.3**	**824**	8.22
	H-D 4	75–105	64.61	**0.84**	10.50	3.97	**3.10**	0.09	**6.07**	1.57	1.86	**8.6**	**783**	9.00
	H-D 5	105–140	53.32	**0.79**	12.21	4.57	**3.85**	**0.11**	**5.85**	2.00	1.66	**15.8**	**731**	17.08
Peteranec - Gorice	P-G 1	0–30	50.11	**0.94**	**17.62**	**8.88**	1.51	**0.14**	0.95	2.28	0.71	**23.2**	**1234**	16.35
	P-G 2	30–65	53.16	**0.92**	**18.33**	**9.53**	1.69	**0.13**	1.18	2.27	0.93	**30.8**	**944**	13.05
	P-G 3	65–100	58.02	**0.95**	**16.42**	**8.82**	1.53	0.10	1.17	2.16	1.15	**31.0**	**935**	9.82
	P-G 4	100–140	66.21	**1.08**	14.33	**7.43**	1.53	0.09	1.37	2.18	1.61	**22.3**	**1115**	5.71
	P-G 5	140–170	64.69	**1.09**	**15.54**	**6.54**	1.70	0.07	1.34	2.43	1.80	**7.8**	**1070**	5.38
	P-G 6	170–205	63.75	**1.04**	14.16	**7.21**	2.25	0.08	2.12	2.27	1.79	**5.0**	**1135**	6.12
	P-G 7	205–220	**73.85**	**0.99**	9.22	4.93	2.03	**0.11**	2.70	1.23	1.33	1.8	**688**	4.15

Podravina region correlate with similar areas in central and northern Europe and North America where bog iron ores are found (Crerar et al., 1979; Kaczorek et al., 2004; Banning, 2008; Thelemann et al., 2017). Some authors believe that bog iron ores are forming today (Bricker et al., 2003; Scott et al., 2011), although to a lesser extent than in the past due to several centuries of agriculture and melioration processes. The combination of these processes and environmental changes not only inhibit the formation of new bog iron ore deposits but also leads to degradation of the remaining deposits (Kaczorek and Sommer, 2003; Puttkammer, 2012). Based on above-mentioned, it is believed that the Podravina area was a suitable region for the formation of bog iron ores.

5.2. Granulometric and geochemical correlations of the selected soil profiles

Based on the macroscopic field determination and on laboratory analyses, there are some noticeable similarities and differences between the analysed five Gleysols and one Fluvisol profiles. Most of them are weakly and moderately acidic to neutral (Table 3) with relatively low carbonate content, apart from the Hlebine-Dedanovice profile. Contents of SiO_2, Al_2O_3 and Fe_2O_3 vary throughout each soil profile (Table 5). Based on Fig. 6, the profiles Hlebine-Dedanovice, Imbriovec-Berek, Koprivnički Ivanec-Log Parag, Peteranec-Gorice and Virje-Sušine show a visible correlation of Fe_2O_3 and Al_2O_3 with clay and silt fractions. Clay and silt fractions often consist of aluminosilicates and hydrated oxides (Hillel, 2008). Although all six profiles show signs of Fe accumulations in the form of orange and red mottles throughout the soil horizons, the profiles are grouped based on the Fe enrichment factor. Selected soil profiles can be classified into two groups: (1) profiles with small enrichments of Fe (Imbriovec-Berek, Koprivnički Ivanec-Log Parag, Virje-Sušine, Hlebine-Dedanovice and Peteranec-Gorice); and (2) the Kalinovac-Hrastova Greda profile with significant Fe accumulation (Table 6). Main formation mechanism for the Fe enrichments in the soil profiles most probably was the precipitation of Fe minerals due to the close to the surface oxidized conditions (Kaczorek et al., 2004). Also, variable clay and silt amounts could also be a reason for some of Fe enrichments in the selected soils due to a higher specific adsorption capacity, where Fe is adsorbed to clay minerals (Akhbarizadeh et al., 2017). Due to high enrichment of Fe, the Kalinovac-Hrastova Greda profile will be considered for further discussion.

The Kalinovac-Hrastova Greda soil profile showed almost no visible soil horizons, indicating that it is weakly to moderately developed, the pH is slightly to strongly acidic, with the tendency of increasing with depth, similar to other Gleysols in the region (Tomašić et al., 2013). The soil is mainly composed of silt and sand, while the clay content is fairly low. This is also indicated by small amounts of phyllosilicates and clay minerals and a larger amount of sand (Fig. 6). The SiO_2 content is in line with quartz, indicating that most of the Si is bound to quartz. A similar correlation is found for Fe_2O_3 and goethite, indicating that this is the main mineral in which most of the Fe is concentrated. The remaining clay minerals represent typical soil and floodplain minerals

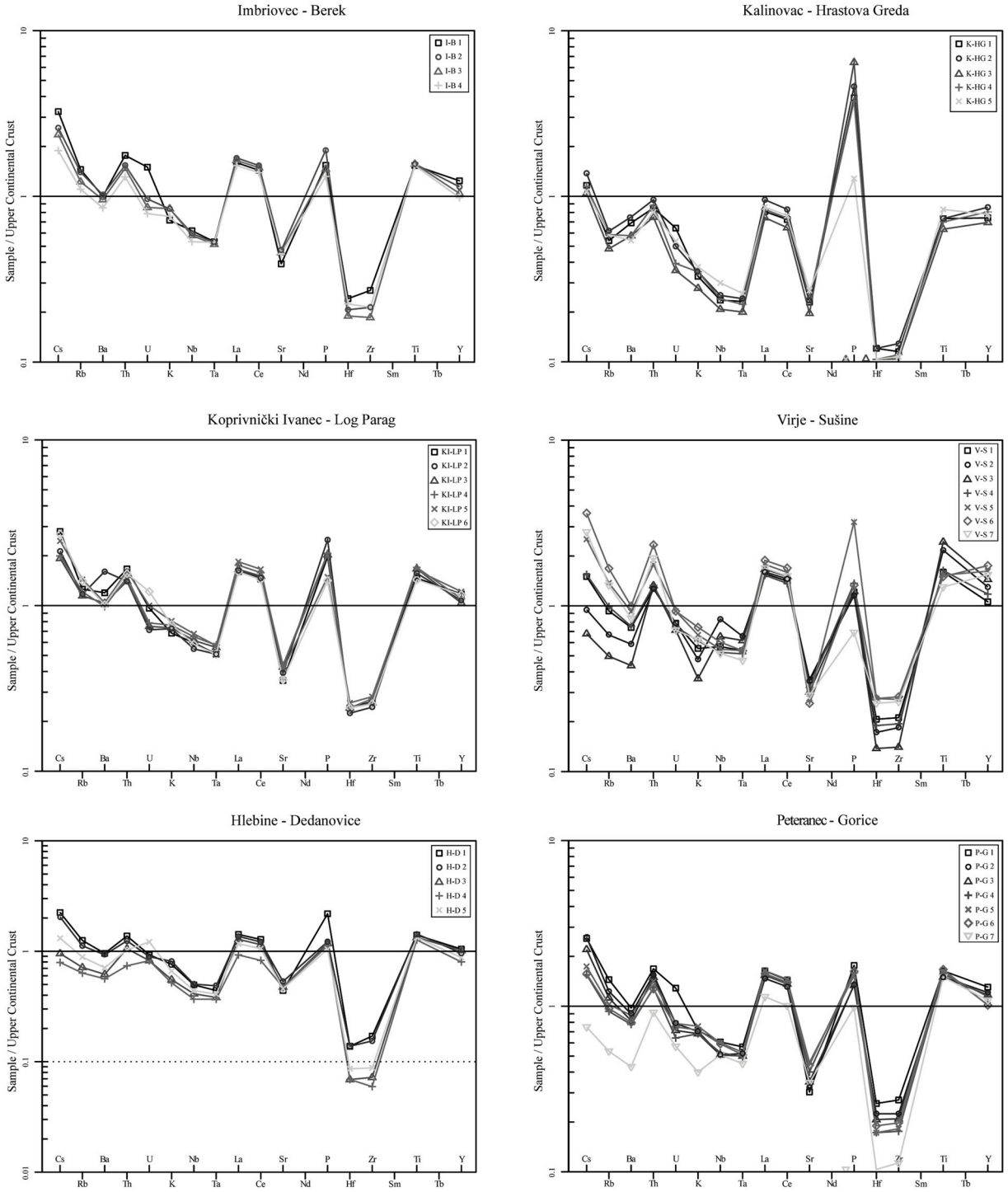

Fig. 5. Multivariate diagrams for the six selected soil profiles (according to Taylor and McLennan, 1985).

(Sokolova et al., 2013; Długosz et al., 2018). The Fe content throughout the whole soil profile is higher than the median values of Fe_2O_3 for the Podravina region (Halamić and Miko, 2009). The middle part of the soil profile has the highest enrichment factors for Fe, As and P (Table 6), with Fe showing significant enrichment. According to Raimandou and Wells (2014), the Fe values are high enough to be considered as an iron ore deposit. A high positive correlation was established between iron and arsenic/phosphorous ($r_{Fe/As}$ = 0.97 and $r_{Fe/P}$ = 0.99) respectively (Fig. 7a), with As contents reaching extremely high values (563.6 ppm). Halamić and Peh (2009) determined that in the Posavina and Podravina regions, As varies from 0.5 to 92 ppm in soils. The same authors noted that the highest content was measured in the proximity of the Molve and Kalinovac area, which is close to the location of the Kalinovac-Hrastova Greda soil profile. Previous studies (Drahota et al., 2009; Borch et al., 2010) have indicated that the redox environment is the main factor controlling As content in groundwater and soils. Banning et al. (2013) showed that pyrite (FeS_2) represents a major As carrier in unaltered soil layers, while Fe oxyhydroxides control As behaviour above the redox boundary. Prevailing pH conditions in the Kalinovac-Hrastova Greda soil profile (slightly to moderately acidic) should prefer the adsorption of As(III) rather than As(V) (Mai et al., 2014). Sorption processes regulate the partitioning of As between solid and aqueous

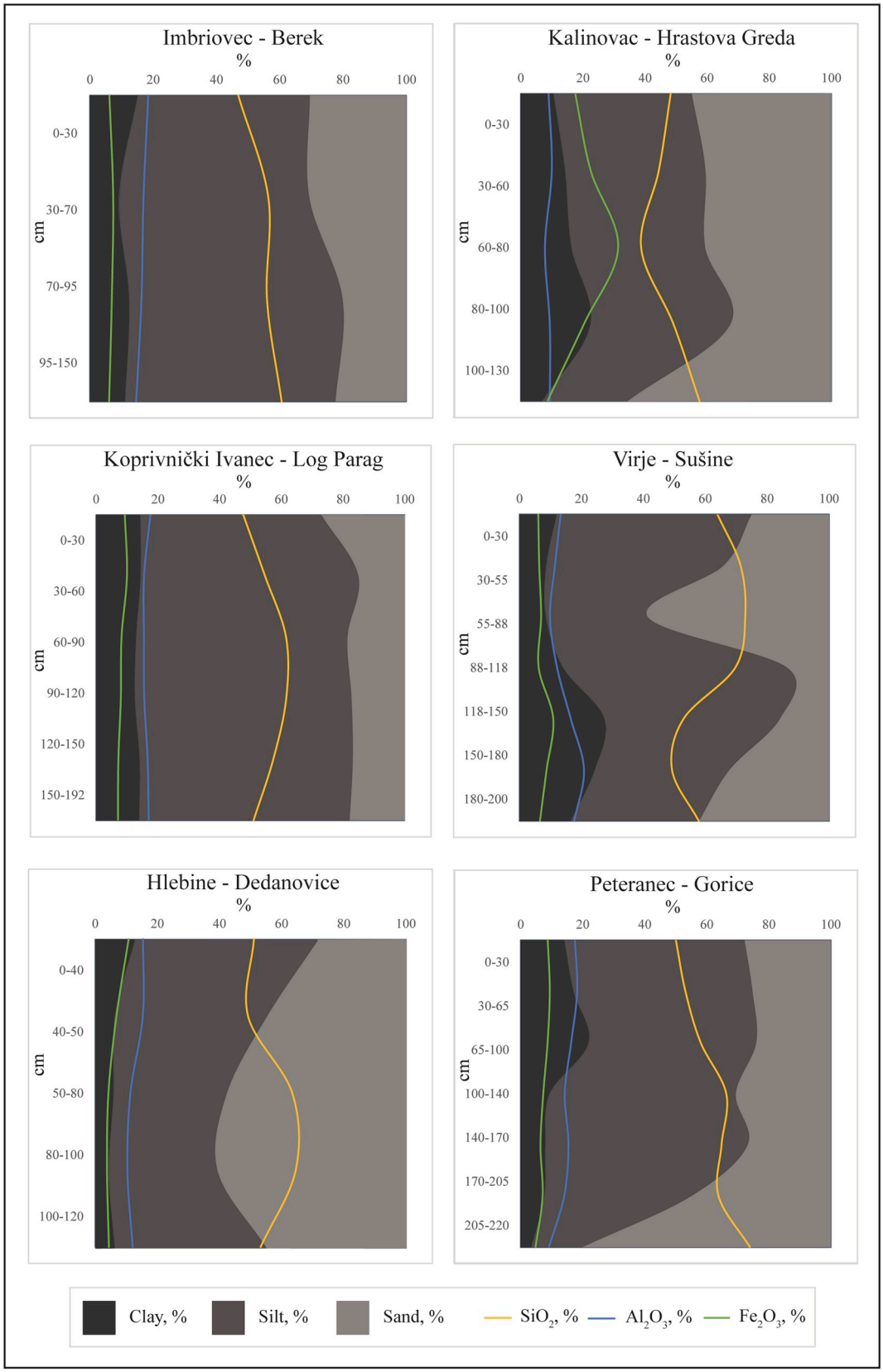

Fig. 6. Soil texture in the selected soil profiles with inserted contents of SiO_2, Al_2O_3 and Fe_2O_3.

phases of the soil. The main sorbents of As species in soils are the iron oxides, oxyhydroxides and hydroxides such as goethite or amorphous iron, whereas As(V) is generally found in oxidizing environments and As(III) is commonly found in reducing environments (Oremland and Stolz, 2005). Several studies indicated that AsO_4^{3-} and AsO_3^{3-} co-ordinate with the surface of iron oxides as stable inner sphere surface complexes (Fendorf et al., 1997; Manning et al., 1998; O'Reilly et al., 2001). Although both forms show a strong geochemical association

Table 6
Enrichment factors for the selected soil profiles with Ti as reference element (Isakson et al., 1997). Bolded values show moderate or higher enrichment.

Location	Sample	Depth, cm	Al_2O_3	Fe_2O_3	MgO	MnO	CaO	K_2O	Na_2O	As	P
Imbriovec - Berek	I–B 1	0–30	1.50	1.02	1.19	0.38	0.81	0.66	0.33	0.57	0.58
	I–B 2	30–70	1.21	1.05	1.17	0.46	0.82	0.66	0.50	1.02	0.63
	I–B 3	70–95	1.17	1.00	1.54	0.47	1.66	0.68	0.55	1.14	0.49
	I–B 4	95–150	1.00	0.85	1.26	0.44	1.25	0.57	0.55	1.18	0.42
Kalinovac - Hrastova Greda	K-HG 1	0–30	1.32	**5.02**	0.96	**2.83**	1.25	0.52	0.51	**24.53**	**2.65**
	K-HG 2	30–60	1.43	**6.28**	1.11	**3.56**	1.37	0.55	0.46	**32.53**	**3.04**
	K-HG 3	60–80	1.43	**11.07**	1.19	**2.68**	1.58	0.55	0.48	**61.39**	**5.40**
	K-HG 4	80–100	1.31	**5.56**	1.09	1.29	1.33	0.55	0.55	**18.93**	**2.43**
	K-HG 5	100–130	1.17	**2.13**	0.94	0.80	1.25	0.53	0.66	**4.82**	0.74
Koprivnički Ivanec - Log Parag	KI-LP 1	0–30	1.36	1.39	1.07	**2.69**	0.78	0.60	0.32	**2.05**	0.72
	KI-LP 2	30–60	1.06	1.33	0.80	**4.51**	0.58	0.55	0.42	**2.32**	0.81
	KI-LP 3	60–90	0.96	1.00	0.70	1.41	0.52	0.52	0.47	1.42	0.60
	KI-LP 4	90–120	0.96	0.96	0.71	0.64	0.51	0.54	0.47	1.20	0.60
	KI-LP 5	120–150	1.09	0.91	0.88	0.43	0.57	0.61	0.44	0.54	0.46
	KI-LP 6	150–192	1.34	1.08	1.21	0.52	0.79	0.71	0.42	0.58	0.53
Virje - Sušine	V–S 1	0–30	0.79	0.68	0.58	0.63	0.46	0.38	0.42	0.56	0.35
	V–S 2	30–55	0.48	0.51	0.34	0.68	0.37	0.22	0.32	0.24	0.23
	V–S 3	55–88	0.34	0.46	0.26	0.63	0.32	0.14	0.23	0.18	0.20
	V–S 4	88–118	0.65	0.64	0.49	0.73	0.42	0.33	0.36	0.47	0.36
	V–S 5	118–150	1.14	1.46	0.86	1.45	0.58	0.50	0.26	1.70	1.06
	V–S 6	150–180	1.65	1.33	1.23	0.45	0.71	0.70	0.21	1.34	0.50
	V–S 7	180–200	1.49	1.05	1.05	0.48	0.72	0.63	0.38	0.67	0.28
Hlebine - Dedanovice	H-D 1	0–10	1.22	1.69	1.39	1.25	1.67	0.69	0.60	**2.71**	0.81
	H-D 2	10–40	1.22	1.08	**2.32**	0.74	**3.71**	0.72	0.63	0.86	0.45
	H-D 3	40–75	0.91	0.69	1.86	0.60	**2.92**	0.49	0.80	0.60	0.44
	H-D 4	75–105	0.83	0.61	1.75	0.66	**3.35**	0.44	0.75	0.41	0.41
	H-D 5	105–140	1.02	0.75	**2.31**	0.86	**3.43**	0.60	0.71	0.81	0.41
Peteranec - Gorice	P-G 1	0–30	1.24	1.23	0.76	0.92	0.47	0.57	0.26	0.99	0.58
	P-G 2	30–65	1.32	1.35	0.87	0.87	0.59	0.58	0.34	1.35	0.45
	P-G 3	65–100	1.14	1.21	0.76	0.65	0.57	0.54	0.41	1.32	0.44
	P-G 4	100–140	0.88	0.89	0.67	0.52	0.59	0.48	0.50	0.83	0.46
	P-G 5	140–170	0.94	0.78	0.74	0.40	0.57	0.53	0.56	0.29	0.43
	P-G 6	170–205	0.90	0.90	1.03	0.48	0.94	0.51	0.58	0.19	0.48
	P-G 7	205–220	0.62	0.65	0.97	0.69	1.26	0.29	0.45	0.07	0.31

with Fe, it is thought that in the environments with pH lower than 8 the oxidized, As(V) species is more strongly bound to the goethite (von der Heyden and Roychoudhury, 2015). Contents of As in the Kalinovac-Hrastova Greda soil profile show a correlation with the Fe content throughout the soil profile, with the highest enrichment of As in the same soil interval as the highest content of Fe in the form of goethite. It is commonly thought that As in the Pannonian basin originates from the dissolution of As bearing Fe-oxides, controlled by microbial processes, desorption of As from Fe-oxides and/or clay minerals as well as competition for the sorption sites with organic matter and PO_3^- (Rowland et al., 2011). On the other hand, phosphate anion is an important plant nutrient, often found as an ingredient in fertilisers. However, in higher contents, P can act as an agricultural pollutant. Phosphate ions binds strongly to Fe oxyhydroxides (Nowack and Stone, 2006). The role of goethite as a P sorbent has been studied by several authors (Ognalaga et al., 1994; Frossard et al., 1995), and it was well established that most clay minerals sorb less P than goethite and other Fe oxyhydroxides (Addiscott and Thomas, 2000). Since Kalinovac-Hrastova Greda, and all the other soil profiles are found in close proximity to agricultural land and comparing to the data for phosphorous from the Geochemical atlas of Republic of Croatia (Halamić and Miko, 2009) that are between 230 and 4120 ppm with median of 910 ppm and where the highest concentrations have been found in agricultural areas, it is safe to assume that P predominantly has an agricultural origin. It is believed that excess P was washed down and transported through the soil and was then bound to the Fe oxyhydroxides where it formed inner sphere complexes, similar to As (Weng et al., 2012). Since P shows similar geochemical behaviour to As regarding adsorption onto Fe oxyhydroxides, the highest P enrichment is also found in the same profile interval where the highest enrichment of Fe is found in the form of goethite. Similar correlations were found for remaining five soil profiles (Fig. 7b), where remaining profiles except for Imbriovec-Berek and Peteranec-Gorice showed similarly high correlations, indicating that soil profiles found in similar groundwater fluctuation zone have similar behaviour between these elements (see Chapter 5.4.).

5.3. Minor and trace elements distribution

The abundance of microelements of corresponding soils was normalised to the upper continental crust (UCC), as suggested by Taylor and McLennan (1985). Microelements, especially rare earth elements (REE), vary according to their parent material, weathering of the soil, and content of organic matter and clay minerals. Therefore, the contents in the soil could vary considerably (Tyler, 2004). Based on the similarities of the multivariate diagrams (Fig. 5), it can be determined that all six soils, located within an area of about 500 km^2, have a common source material, which is probably flooding material from the Alps transported by the Drava River (Halamić et al., 2003). The measured values of some microelements (Ni, Pb and Zn) in the soil profiles are higher than the median values in the topsoil of the Podravina region (Halamić and Miko, 2009). Reasons for these high contents are the consequence of long-standing mining activities of Pb–Zn ore in Slovenia (e.g. Mežica) and Austria (e.g. Bleiberg) where the Drava River drains areas that are naturally rich in Pb–Zn ore and mineralisation. High contents of Zn in soils of the Drava River could also be the consequence of anthropogenic input of Zn in the form of fertilisers that are leached in

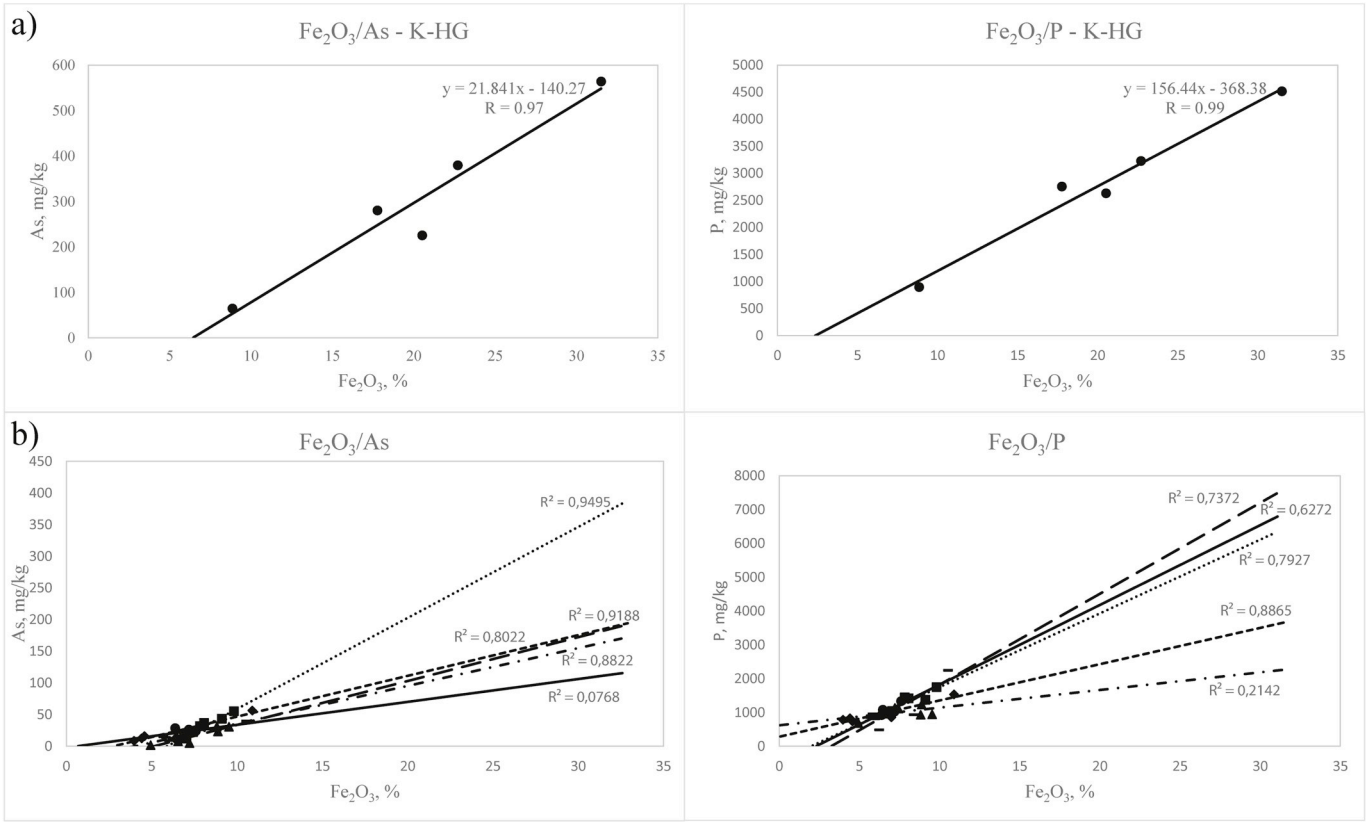

Fig. 7. Correlation of Fe with As and P in the a) Kalinovac-Hrastova Greda soil profil and b) remaining profiles.

the aquatic system (Mortvedt and GIlkes, 1993). Microelements in the selected six soil profiles generally follow a similar trend as established by Halamić et al. (2003), where the content of heavy metals decreases up to 80 cm depth, and then slowly increases in the lower part. On the other hand, some microelements such as Zr, U and Hf show depletions in the soil profiles. This could be due to partial dissolution of resistant minerals during preparation for ICP-MS. Since most of the Zr and Hf are bound in zircon (Wang et al., 2010), which is a highly resistant mineral, it is possible that the samples weren't fully dissolved, thus leaving zircon grains whole and intact. Large ion lithophile elements, such as Rb and Ba, are depleted in the soils compared to UCC, due to their similar geochemical behaviour and solubility as a result of chemical weathering (Jahn et al., 2001), while other such as Cs are enriched in soils due to their substitution with potassium in mica minerals, such as muscovite (Négrel et al., 2018).

5.4. Groundwater as main source of iron and accompanying elements

Based on the hydrological map of Podravina (Brkić and Briški, 2018), the soil profiles are subject to different influences of groundwater. All soil profiles except Peteranec-Gorice showed signs of groundwater influence (Fig. 3) during field work. As previously determined, all six soil profiles have a common parent material but show significant variations in Fe content. This is due to different fluctuation depths of the groundwater table in the selected soil profiles (Fig. 8). Profile Imbriovec-Berek is fully saturated with groundwater during most of the year. As a result of wet conditions, the diffusion of oxygen into the soil profile is impaired and this is probably causing reductive conditions throughout the profile and thus making Fe and other elements mobile (Mansfeldt et al., 2012). Profiles Koprivnički Ivanec-Log Parag, Virje-Sušine and Hlebine-Dedanovice are only briefly saturated with groundwater, which is probably not enough time to enable higher precipitation of Fe and other elements, or the fluctuations of groundwater are too deep in the soil profile where reductive conditions prevent the precipitation of Fe and other elements. The Kalinovac-Hrastova Greda soil profile shows the highest enrichment factors of Fe, As and P and moderate enrichment of Mn (Fig. 8; Table 6). Groundwater can be enriched with Fe, As, Mn and P while exposed to reductive conditions (Welch et al., 2000; Nicolli et al., 2010). Once oxidative conditions are reached due to seasonal fluctuations of the groundwater table, Fe is the first element to precipitate in the form of Fe^{3+} due to Eh/pH differentiation, forming ferrihydrite and/or goethite (Yee et al., 2006). The average groundwater level depth at the Kalinovac-Hrastova Greda soil profile is around 100 cm, with groundwater reaching a maximum depth of 10 cm below the surface during high-water periods (Fig. 3). Contents of As, Mn and P were able to be correlated with the fluctuations of groundwater (Fig. 8). Both As and P show the highest contents at the 60–80 cm interval, similar to Fe, while Mn shows the highest content at the 30–60 cm depth interval. This difference in precipitation depth of Fe and Mn is due to the different behaviour of these two elements and the interchanges of redox conditions, as present in the Podravina region (Table 1). Fe and Mn often occur together in groundwater, with Mn usually present in much lower concentrations (Nádaská et al., 2012). In systems where oxides are the dominant phases, as is the case with this soil profile where Fe oxides are the most abundant phase, Mn precipitation and solubility are highly affected by slight changes in both Eh and pH (Hem, 1963). In the presence of different complexes, such as bicarbonates and sulphates, Fe is less soluble than Mn if the pH is less than 4.8 and the Eh is greater than 880 mV (Collins and Buol, 1970). There is an even greater difference in the solubility of Fe and Mn in conditions where the pH ranges from 6 to 8 and the Eh ranges from 400 to 600 mV. This pH range correlates with the measured pH of the soil profile (Table 3). Eh is proposedly higher in the topsoil horizon due to a larger amount of oxygen, allowing the precipitation of Mn only in the upper parts of the profile as Mn^{4+}, and making it a mobile element in lower parts (Atta et al., 1996). Since Fe

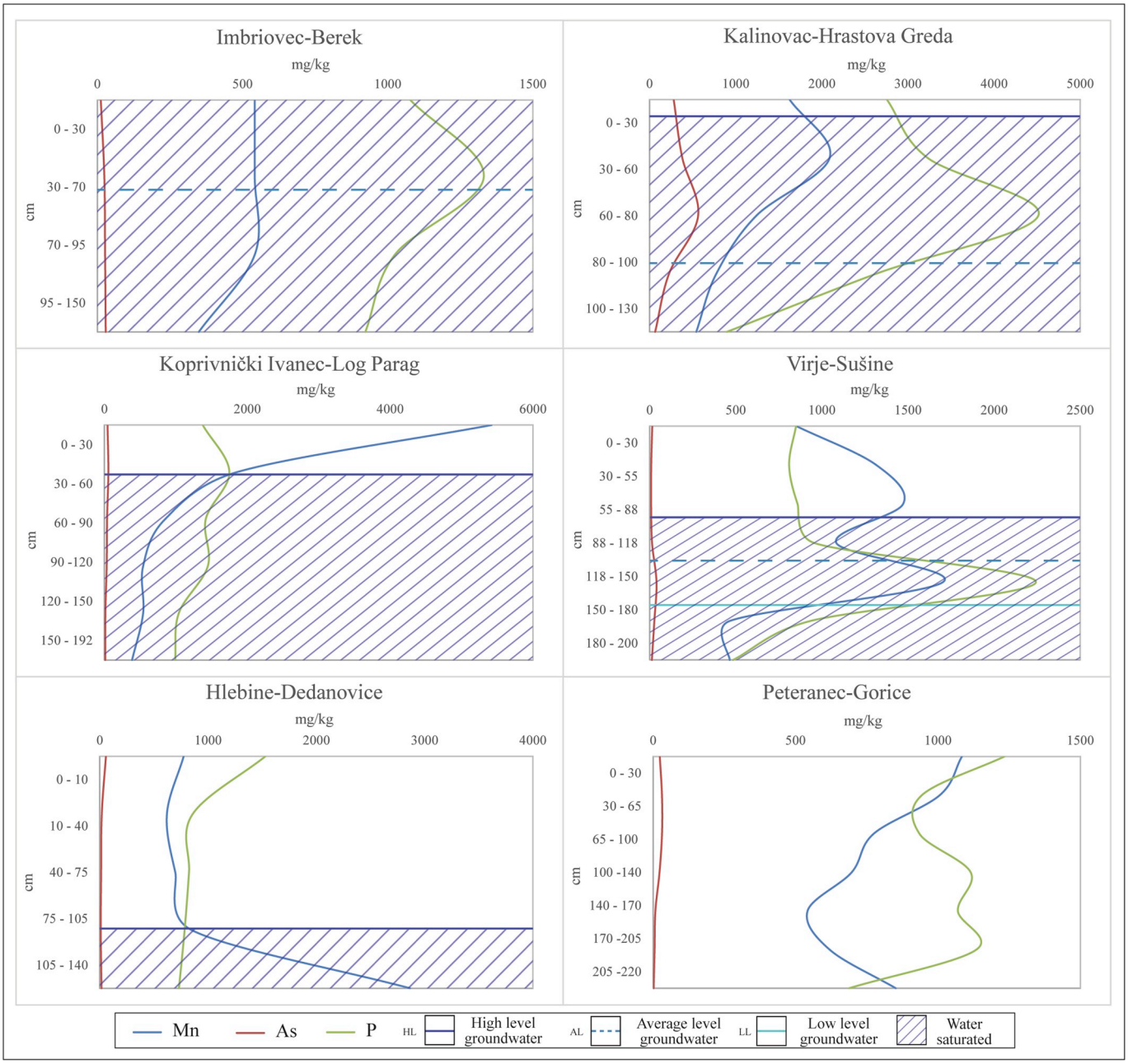

Fig. 8. Correlation of groundwater depth to Mn, As and P contents in the soil profiles.

tends to precipitate at lower pH/Eh, it is often found in deeper parts of soil profiles, such as in the case of the Kalinovac-Hrastova Greda profile, where the highest content of Fe is found in the 60–80 cm interval.

Elevated As in groundwater has been identified in many parts of the world. In the 1940s, As contamination was detected in well waters of the Pannonian Basin in both Romania and Hungary (Mukherjee et al., 2006; Gurzau and Pop, 2012) and in the eastern part of Croatia (Ujević et al., 2010; Ujević Bošnjak et al., 2013). Similar occurrences were recognised in other European countries such as England, Germany, Greece and Spain (Nordstrom, 2002). Currently, reported concentrations of As are above standards in more than 70 countries worldwide (Ravenscroft et al., 2009). For most known instances of extensive As contamination in groundwater, the sources of the As have been shown to be geogenic (Smedley and Kinniburgh, 2002). In the Pannonian Basin of Hungary and Romania, Quaternary sediments of fluvial and aeolian origin have contributed As to the groundwater. These sediments are composed of sands and loess. Quartz, feldspar, carbonates (calcite and dolomite), muscovite, chlorite and clay minerals are reported alongside fine particles of Fe hydroxides (Varsányi and Kovács, 2006). Other Fe-bearing minerals, from which As may be released, are reported to include goethite, lepidocrocite, pyrite, and siderite (Rowland et al., 2011). Since both As and P have a high affinity for Fe compounds (Kaczorek et al., 2009; Weng et al., 2012; Watts et al., 2014), they could be adsorbed on the surface of goethite in the same interval, forming this enriched interval.

5.5. *Kalinovac-Hrastova Greda – potential bog iron ore?*

Bog iron ore is a sedimentary type of iron deposit, mostly occurring in lowland areas where the groundwater table is close to the surface and the drainage is slow or completely impeded (Stanton, 1972; Stoops, 1983; Ramanaidou and Wells, 2014). The main iron minerals in bog iron are goethite and ferrihydrite (Kaczorek and Sommer, 2003), with a variable Fe content between 30 and 50 wt. %. Bog iron ore is often

found in Gleysols associated with alluvial sands (Kaczorek and Zagórski, 2007). The middle part of the soil profile at Kalinovac-Hrastova Greda between 60 and 80 cm depth shows similarity to the first macro-morphological type of bog iron ore ("soft bog iron") (Kaczorek and Sommer, 2003; Banning, 2008). As previously stated, this interval stands out from the rest of the profile due to its colour, indicating high enrichment of Fe oxides. Based on geochemical and mineralogical data, there are several similarities to bog iron ores of central Europe (Thelemann et al., 2017). Goethite is the dominant Fe mineral phase, while ferrihydrite is found at the 60–100 cm depth and the total Fe_2O_3 content is above 30 wt. %. The enrichment factor of Fe in this middle part is 11.07, indicating significant accumulation of Fe in one location. A high negative correlation could be established between Fe and Si, representing the typical pattern for bog iron ores of different qualities (Thelemann et al., 2017). This relationship between Fe and Si represents different stages in the formation and evolution of bog iron ore. Further development and compaction of bog iron is indicated by an increase in the Fe content and a decrease in the Si content. Bog iron ores often show elevated contents of Mn and P (Graupner, 1982). The contents of Mn are low with values between 0.07 and 0.27 wt. %, while the P values of between 897 and 4513 ppm are typical for bog iron ores (Appendix 1). Fe originates from the groundwater and is subject to seasonal fluctuations of the water table, which gives rise to periods of wetting and drying, thus producing an overlying oxidized zone with a high Fe content and orange colour, and an underlying reduced zone with noticeably lower Fe content and dark colour (De Geyter et al., 1985). During one field investigation, smaller (5–25 mm) nodules were found on the surface of the soil, perhaps representing a second type of bog iron ore, but as these nodules weren't part of this study they weren't investigated further. Several locations with higher concentrations of smelting slag were found around a small hill located a couple hundred meters from the soil profile at Kalinovac-Hrastova Greda (Valent et al., 2017). This high concentration of slag at one location also indicates that during the Middle Ages local people knew that the bog iron ore was in close proximity, and they decided to settle close to it (Bowles et al., 2011). All this indicates that in the past, probably in the Middle Ages, bog iron ore formed at the Kalinovac-Hrastova Greda site. It is also believed that this probably wasn't the only location where bog iron ore formed but is perhaps one of the few that has been preserved until today, while many no longer exist due to agriculture and melioration of the Podravina region. Since bog iron ore is found on the northern floodplain of the Drava River, in Inner Somogy, Hungary (Gömöri, 2006; Török et al., 2015), it is believed that the bog iron also formed on the southern floodplain, in the Podravina region.

6. Conclusions

Previous archaeological excavations and findings of iron slags and smelting material indicate the locations that could be favourable for the formation of bog iron. A total of 44 soil profiles was sampled and one Fluvisol and five Gleysol profiles were chosen for detailed mineralogical, geochemical and textural analyses. The selected soil profiles are located on the 2nd Drava River terrace, where sand and silt are the dominant lithological units. Based on the correlation of minor and trace elements all soil profiles share a similar parent material, probably originating from the Alps and derived from the sediments of the Drava floodplains. Five of the analysed soil profiles showed similar characteristics regarding the content of major oxides, while the Kalinovac-Hrastova Greda profile stands out due to high enrichment factors of Fe (EF = 11.07), As (EF = 61.39) and P (EF = 5.40), and shows moderate enrichment of Mn (EF = 3.56). Following the Fe, high content of As and P is noticed in almost all profiles. All six profiles show signs of goethite, quartz, clay minerals, feldspars and, sporadically, dolomite and in one case, ferrihydrite. According to textural analyses, all soil profiles are mostly comprised of silt and sand, with small quantities of clay material, typical for floodplains. Groundwater in general is enriched with Fe and occasionally with Mn, while the prevailing redox conditions are always changing from reductive to oxidative. Correlations of groundwater fluctuation depths indicate that the Imbriovec-Berek profile is constantly saturated with groundwater, forming almost permanent reductive conditions and preventing Fe accumulations. On the other hand, profiles Koprivnički Ivanec-Log Parag, Virje-Sušine, Hlebine-Dedanovice and Peteranec-Gorice are too briefly saturated with groundwater to enable significant Fe accumulations. Fluctuation of groundwater at Kalinovac-Hrastova Greda enables the saturation of groundwater higher up in the profiles, where, due to oxidative conditions, Fe is starting to precipitate in the form of Fe oxyhydroxides and accumulate at significant contents. Based on that, the Kalinovac-Hrastova Greda profile shows ideal conditions for the formation of bog iron ore and similarities to the first formation phase ("soft" bog iron). In summary, several indicators suggest the occurrences of bog iron ore in the Podravina region. Based on its geological, pedological and hydrological characteristics, the Podravina region is a favourable area for bog iron ore formation. Previous archaeological excavations found a large number of possible smelting workshops and slag sites in the study area. This, however, is in contrast to the number of occurrences of bog iron ore. Possible reasons for this are land use throughout history, mining, agricultural activities and landscape changes due to deforestation. The current climate, characterised by dry and cool conditions, differs compared to that of the period in which bog iron was mostly formed.

Declaration of competing interest

None.

Acknowledgements

This work has been fully supported by the Croatian Science Foundation under the project TransFER (Grant No. 5047). We would like to thank Ivan Valent and Ivan Zvijerac for their help during extensive field work in 2017 and 2018. Publication process is supported by the Development Fund of the Faculty of Mining, Geology and Petroleum Engineering, University of Zagreb.

Appendix A. Supplementary data

Supplementary data to this article can be found online at https://doi.org/10.1016/j.quaint.2019.11.033.

References

Addiscott, T.M., Thomas, D., 2000. Tillage, mineralization and leaching: phosphate. Soil Tillage Res. 53, 255–273.
Akhbarizadeh, R., Moore, F., Keshavarzi, B., Moeinpour, A., 2017. Microplastics and potentially toxic elements in coastal sediments of Iran's main oil terminal (Khark Island). Environ. Pollut. 220 (A), 720–731.
Atta, S.K., Mohammed, S.A., Van Cleemput, O., Zayed, A., 1996. Transformations of iron and manganese under controlled Eh, Eh-pH conditions and addition of organic matter. Soil Technol. 9 (4), 223–237.
Banning, A., 2008. Bog iron ores and their potential role in arsenic dynamics: an overview and a „paleo example". Eng. Life Sci. 8/6, 641–649.
Banning, A., Rüde, T.R., Dölling, B., 2013. Crossing redox boundaries – aquifer redox history and effects on iron mineralogy and arsenic availability. J. Hazard Mater. 15, 905–914.
Benhaddya, M.L., Hadjel, M., 2013. Spatial distribution and contamination assessment of heavy metals in surface soils of Hassi Messaoud, Algeria. Environ. Earth Sci. 71 (3), 1473–1486.
Bognar, A., 2008. Geomorfološka obilježja korita rijeke drave i njenog poloja u širem području naselja Križnica (*eng.* Geomorphologic characteristics of the Drava River bed and its floodplain in wider area of the Settlement Križnica). Hrvat. Geogr. Glas. 70/2, 49–71.
Borch, T., Kretzschmar, R., Kappler, A., van Cappelen, P., Ginder-Vogel, M., Voegelin, A., Campbell, K., 2010. Biogeochemical redox processes and their impact on contaminant dynamics. Environ. Sci. Technol. 44 (1), 15–23.
Bowles, G., Bowker, R., Samsonoff, N., 2011. Viking expansion and the search for bog iron. Platforum 12, 25–37.
Breuning-Madsen, H., Rønsbo, J., Holst, M.K., 2000. Comparison of the composition of iron pans in Danish burial mounds with bog iron and spodic material. Catena 39, 1–9.

Bricker, O.P., Newell, W.L., Simon, N.S., 2003. Bog iron formation in the Nassawango watershed, Maryland. Gordon Conf. Catchment Sci.: Interact. Hydrol., Biol. Geochem. 7.
Brkić, Ž., Briški, M., 2018. Hydrogeology of the western part of the Drava Basin in Croatia. J. Maps 14 (2), 173–177.
Brkić, Ž., Larva, O., Urumović, K., 2010. The quantitative status of the groundwater in alluvial aquifers in northern Croatia. Geol. Croat. 63/3, 283–298.
Charlton, M., Crew, P., Rehren, T., Shennan, S., 2010. Explaining the evolution of ironmaking recipies – an example from northwest Wales. J. Anthropol. Archaeol. 29, 352–367.
Collins, J.F., Buol, S.W., 1970. Effects of fluctuations in the Eh-pH environment on iron and manganese equilibria. Soil Sci. 110 (2), 111–118.
Crerar, D.A., Knox, G.W., Means, J.L., 1979. Biogeochemistry of bog iron of the New Jersey Pine barrens. Chem. Geol. 24, 111–135.
De Geyter, G., Vandengerghe, R.E., Verdonck, L., Stoops, G., 1985. Mineralogy of holocene bog-iron ore in northern Belgium. Neues Jahrbuch fuer Mineralogie 153, 1–17.
Drahota, P., Rohovec, J., Filippi, M., Mihaljevič, M., Rychlovský, P., Červený, V., Pertold, Z., 2009. Mineralogical and geochemical controls of arsenic speciation and mobility under different redox conditions in soil, sediment and water at the Mokrsko-Wesr gold deposit, Czech Republic. Sci. Total Environ. 407, 3372–3384.
Długosz, J., Kalisz, B., Łachacz, A., 2018. Mineral matter composition of drained floodplain soils in north-eastern Poland. Soil Sci. Ann. 69 (3), 184–193.
enviazohr – Croatian Agency for the Environment and Nature – Pedological Map of Croatia.
Feletar, D., Feletar, P., 2008. The Natural Basis as a Factor of the Inhabitation of the Upper Croatian Podravina Region. pp. 167–212 Podravina vol. II.
Fendorf, S., Eick, M.J., Grossl, P., Sparks, D.L., 1997. Arsenate and chromate retention on goethite: I. Surface structure. Environ. Sci. Technol. 31, 315–320.
Frossard, E., Brossard, M., Hedley, M.J., Methrell, A., 1995. Reactions controlling the cycling of P in soils. In: Tiessen, H. (Ed.), Phosphorous Cycling in Terrestrial and Aquatic Ecosystems. John Wiley, New York, pp. 107–137.
Galović, L., 2016. Sedimentological and mineralogical characteristics of the Pleistocene loess/paleosol sections in the Eastern Croatia. Aeolian Res. 20, 7–23.
Galović, L., Marković, S., 1979. Basic Geological Map of Yugoslavia, M 1:100 000, Sheet Virovitica. Geological Survey Zagreb. Federal Geological Institute Beograd published by.
Gömöri, J., 2006. The bloomery museum at Somogyfajsz (Hungary) and some archaeometallurgical sites in pannonia from the Avar- and early Hungarian period. J. Metall. Assoc. Metall. Eng. Serbia 183–196.
Graupner, A., 1982. Raseneisenstein in Niedersachsen. Entstehung, Vorkommen, Zusammensetzung und Verwendung. Forschungen zur niedersächsischen Landeskunde 118. Kommissionsverlag Göttinger Tageblatt GmbH & Co. KG, Göttingen (in German).
Gurzau, A.E., Pop, C., 2012. A new public health issue: contamination with arsenic of private water sources. In: Proceedings of the AERAPA Conference, Available from. aerapa.conference.ubbcluj.ro/2012/Gurzau.htm, Accessed date: 25 March 2019.
Halamić, J., Galović, L., Šparica Miko, M., 2003. Heavy Metal (As, Cd, Cu, Hg, Pb and Zn) Distribution in Topsoil Developed on Alluvial Sediments of the Drava and Sava Rivers in NW Croatia. Geologia Croatica 56 (2), 215–232.
Halamić, J., Miko, S. (Eds.), 2009. Geochemical atlas of the republic of Croatia. Croatian Geological Survey, Zagreb, pp. 87.
Halamić, J., Peh, Z., 2009. Geochemical Atlas of the Republic Croatia. Regional Spatial Distribution of Arsenic. Croatian Geological Survey, Zagreb, pp. 34–35.
Head J., M., 2019. Formal subdivision of the Quaternary System/Period: Present status and future directions. Quaternary International 500, 32–51. https://doi.org/10.1016/j.quaint.2019.05.018.
Hećimović, I., 1986. Basic Geological Map of Yugoslavia, M 1:100 000, Sheet Đurđevac. Geological Survey Zagreb, Zagreb.
Hećimović, I., 1987. Explanatory Notes for Geological Map 1 : 100 000, Sheet Đurđevac (In Croatian). Federal Geological Institute Belgrade, pp. 1–39.
Hećimović, I., 1995. Tektonski Odnosi Šireg Područja Kalnika. PhD Thesis. Faculty of Mining, Geology and Petroleum Engineering, University of Zagreb, Zagreb, pp. 152 in Croatian.
Hem, J.D., 1963. Chemical equilibria affecting the behavior of manganese in natural water. Hydrol. Sci. J. 8 (3), 30–37.
Hillel, D., 2008. Soil Physical Attributes. Chapter 5 in: Soil in the Environment. pp. 55–77.
Husnjak, S., 2014. Sistematika Tala Hrvatske (*Eng.* Soil Systematics of Croatia). Hrvatska sveučilišna naklada, Zagreb, pp. 373 in Croatian.
Isakson, J., Oblad, M., Selin Lindgren, E., Djupstrom Fridell, M., Pacyna, J.M., Mäkinen, M., 1997. Perturbation of background aerosol at rural sites in the Nordic countries. Atmos. Environ. 31, 3077–3086.
ISO 10693, 1995. Soil Quality–Determination of Carbonate Content–Volumetric Method. International Organisation for Standardisation, Switzerland.
IUSS Working Group WRB, 2015. World reference base for soil resources, update 2015. In: International Soil Classification System for Naming Soils and Creating Legends for Soil Maps. World Soil Resources Reports, vol. 106 FAO, Rome.
Jahn, B., Gallet, S., Han, J., 2001. Geochemistry of the Xining, Xinfeng and Jixian sections, Loess Plateau of China: eolian dust provenance and paleosol evolution during last 140ka. Chem. Geol. 178 (1–4), 71–94.
Joosten, I., Jansen, B., Kars, H., 1998. Geochemistry and the past: estimation of the output of a Germanic iron production site in The Netherlands. J. Geochem. Explor. 62, 129–137.
Kaczorek, D., Sommer, M., 2003. Micromorphology, chemistry and mineralogy of bog iron ores from Poland. Catena 54, 393–402.
Kaczorek, D., Zagórski, Z., 2007. Micromorphological characteristics of the bsm horizon in soils with bog iron ore. Pol. J. Soil Sci. 40, 81–87.
Kaczorek, D., Sommer, M., Andruschkewitsch, I., Oktaba, L., Czerwinski, Z., Stahr, K., 2004. A comparative micromorphological and chemical study of „Rasseneisenstein "(bog iron ore) and „Ortstein". Geoderma 121, 83–94.
Kaczorek, D., Brümmer, G.W., Sommer, M., 2009. Content and binding forms of heavy metals, aluminum and phosphoruis in bog iron ores from Poland. J. Environ. Qual. 38, 1109–1119.
Kiss, T., Andrási, G., 2017. Hydro-morphological responses of the Drava River on various engineering works. Ekonomska i Ekohistorija 13 (13), 14–24.
Kopić, J., Loborec, J., Nakić, Z., 2016. Hydrogeological and hydrogeochemical characteristics of a wider are of the regional well field Eastern Slavonia – Sikirevci. Mining-Geol.-Pet. Eng. Bull. 31 (3), 47–66.
Korolija, B., Crnko, J., 1985. Basic Geological Map of Yugoslavia, M 1:100 000, Sheet Bjelovar. Geological Survey Zagreb, Zagreb.
Koschke, W., 2002. Raseneisenerz und Eisenhüttenindustrie in der nördlichen Oberlausitz, 18. Freundeskreis Stadt- und Parkmuseum, Bad Muskau. in German.
Landuydt, C.J., 1990. Micromoprhology of iron minerals from bog ores of the Belgian Campine area. Soil Micro-Morphol.: Basic Appl. Sci. 289–294.
Lóczy, D., 2013. Hydrogeomorphological-geoecological Foundations of Floodplain Rehabilitation: Case Study from Hungary. Lambrecht Academic Publishing, Saarbrücken, pp. 382.
Lóczy, D., Dezső, J., Czigány, S., Gyenizse, P., Pirkhoffer, E., Halász, A., 2014. Rehabilitation potential of the Drava River floodplain in Hungary. In: Conference Paper.
Loska, K., Wiechula, D., 2003. Application of principal component analysis for the estimation of source of heavy metal contamination in surface sediments from rybnik reservoir. Chemosphere 51, 723–733.
Mai, N.T.H., Postma, D., Trang, P.T.K., Jessen, S., Viet, P.H., Larsen, F., 2014. Adsorption and desorption of arsenic to aquifer sediment on the red river floodplain at Nam du, Vietnam. Geochem. Cosmochim. Acta 142 (1), 587–600.
Manning, B., Fendorf, S., Goldberg, S., 1998. Surface Structures and Stability of arsenic (III) on goethite: Spectroscopic evidence for inner-sphere complexes. Environ. Sci. Technol. 32 (16), 2383–2388.
Mansfeldt, T., Schuth, S., Häusler, W., Wagner, F.E., Kaufold, S., 2012. Iron oxide mineralogy and stable iron isotope composition in a Gleysol with petrogleyic properties. J. Soils Sediments 12 (1), 97–114.
Matenco, L., Radivojević, D., 2012. On the formation and evolution of the Pannonian Basin: constraints derived from the structure of the junction area between the Carpathians and Dinarides. Tectonics 31 (6), 1–31.
Mortvedt, J.J., GIlkes, R.J., 1993. Zinc fertilizers. Chapter 3 in: zinc in soils and plants. Dev. Plant Soil Sci. 55, 33–44.
Mukherjee, A., Sengupta, M.K., Hossain, M.A., Ahamed, S., Das, B., Nayak, B., Lodh, D., Rahman, M.M., Chakraborti, D., 2006. Arsenic contamination in groundwater: a global perspective with emphasis on the Asian scenario. J. Health Popul. Nutr. 24, 142–163.
Munsell, A.H., 1994. Soil Colour Charts, revisedth ed. Macbeth Division of Kollmorgan Instruments Corporation, Baltimore.
Mutić, R., 1975. Pijesak rijeke Drava u naslagama bušotine B-12 nedaleko Podravske Slatine (*eng.* Drava river sand in deposits from B-12 well near Podravska Slatina area). Geološki vjesnik 28, 243–268.
Nádaská, G., Lesnỳ, J., Michalík, I., 2012. Environmental Aspect of Manganese Chemistry. http://heja.szif.hu/ENV/ENV-100702-A/env100702a.pdf, Accessed date: 25 March 2019.
Nakić, Z., Parlov, J., Perković, D., Kovač, Z., Buškulić, P., Špoljarić, D., Ugrina, I., Stanek, D., 2018. Case Study: Definiranje Kriterija Za Određivanje Pozadinskih Koncentracija I Graničnih Vrijednosti Onečišćujućih Tvari U Tijelima Podzemne Vode U Panonskom Dijelu Hrvatske. Hrvatske Vode. (in Croatian).
Négrel, P., ladenberger, A., Reinmann, C., Birke, M., Sadeghi, M., the GEMAS project Team, 2018. Distribution of Rb, Ga and Cs in agricultural land soils at European continental scale (GEMAS): implications for weathering conditions and provenance. Chem. Geol. 479, 188–203.
Nicolli, H.B., Bundschuh, J., García, J.W., Falcón, C.M., Jean, J.S., 2010. Sources and controls for the mobility of arsenic in oxidizing groundwater from loess type sediments in arid/semi arid dry climates – evidence from the Chaco-Pampean plain (Argentina). Water Res. 44 (19), 5589–5604.
Nordstrom, D.K., 2002. Worldwide occurrences of arsenic in ground water. Science 296, 2143–2145.
Nowack, B., Stone, A., 2006. Competitive adsorption of phosphate and phosphonates onto goethite. Water Res. 40 (11), 2201–2209.
O'Reilly, E.O., Strawn, D.G., Sparks, D.L., 2001. Residence time effects on arsenate adsorption/desorption mechanisms on goethite. Soil Sci. Soc. Am. J. 65 (1), 67–77.
Ognalaga, M., Frossard, E., Thomas, F., 1994. Glucose-1-phosphate and myo-insitol hexaphosphate adsorption mechanisms on goethite. Soil Sci. Soc. Am. J. 58 (2), 332–337.
Oremland, R.S., Stolz, J.F., 2005. Arsenic, microbes and contaminated aquifers. Trends Microbiol. 13 (2), 45–49.
Pavelić, D., Kovačić, M., Banak, A., Jiménez-Moreno, G., Marković, F., Pikelj, K., Vranjković, A., Premužak, L., Tibljaš, D., Belak, M., 2016. Early Miocene European loess: a new record of aridity in southern Europe. Geol. Soc. Am. Bull. 128 (1–2), 110–121.
Prelogović, E., Velić, I., 1988. Kvartarna tektonska aktivnost zapadnog dijela Dravske depresije (*eng.* Quaternary tectonic activity of western part of the Drava basin). Geološki vjesnik 42, 287–299 in Croatian.
Puttkammer, T., 2012. Auf den Spuren der Germanen. Begleitband zur Wanderausstellung. Museum der Westlausitz, Kamenz. in German.
Ramanaidou, E., Wells, M.A., 2014. Sedimentary hosted iron ores. Treatise Geochem. 13, 313–355.

Ratajczak, T., Rzepa, G., 2011. Lokalne Kopaliny mineralne mineralne A możliwości ich wykorzystania W ochronie srodowiska (Na przykładzie mazurskich rud darniowych). Inżynieria Ekologiczna 27, 161–169 in Polish.
Ravenscroft, P., Brammer, H., Richards, K., 2009. Arsenic Pollution: A Global Synthesis. Wiley-Blackwell, pp. 588.
Rowland, H., Omoregie, E., Millot, R., Jimenez, C., Mertens, J., Baciu, C., Hug, S.J., Berg, M., 2011. Geochemistry and arsenic mobilization to groundwaters of the Pannonian Basin (Hungary and Romania). Appl. Geochem. 26, 1–17.
Rudnick, R.L., Gao, S., 2003. Composition of the continental crust. Treatise Geochem. 3, 1–51.
Schmid, S., Bernoulli, D., Fügenschuh, B., Matenco, L., Schefer, S., Schuster, R., Tischler, M., Ustaszewski, K., 2008. The Alpine-Carpathian-Dinaridic orogenic system: correlation and evolution of tectonic units. Swiss J. Geosci. 101, 139–183.
Scott, P.W., Ealey, P.J., Rollinson, G.K., 2011. Bog iron ore from lowland point, St Keverne, lizard, cornwall. Geoscience in South-West England 12, 260–268.
Seghedi, I., Downes, H., Szakács, A., Mason, P., Thirwall, M.F., Roşu, E., Pécskay, Z., Márton, E., Panaiotu, C., 2004. Neogene-Quaternary magmatism and geodynamics in the Carpathian-Pannonian region: a synthesis. Lithos 72, 117–146.
Sekelj Ivančan, T., Marković, T., 2017. The primary processing of iron in the Drava River basin during the late Antiquity and the early Middle Ages – the source of raw materials. In: Archaeological Studies: Raw Material Exploitation from Prehistory to the Middle Ages, 143-161. Belgrade, Serbia.
Simex, S.A., Helz, G.R., 1981. Regional geochemistry of trace element in Chesapeake Bay. Environ. Geol. 3, 315–323.
Šimunić, A., Hećimović, I., Avanić, R., 1990. Basic Geological Map of the Republic of Croatia, M 1:100 000, Sheet Koprivnica (L33-70). Croatian Geological Survey.
Sitschick, H., Ludwig, F., Wetzel, E., Luckert, J., Höding, T., 2005. Raseneisenerz –auch in Brandenburg ein mineralischer Rohstoff mit bedeutender wirtschaftlicher Vergangenheit. Brand. Geowiss. Beitrage 12, 119–128 in German.
Smedley, P.L., Kinniburgh, D.G., 2002. A review of the source, behaviour and distribution of arsenic in natural waters. Appl. Geochem. 17, 517–568.
Sokolova, T.A., Tolpeshta, I.I., Rusakova, E.S., Maksimova, Y.G., 2013. Clay minerals in the Stream floodplain soils in the undisturbed landscapes of the southern taiga (with the soil of the state central forest nature and biosphere reserve as an example. Mosc. Univ. Soil Sci. Bull. 68 (4), 154–163.
Stanton, M.R., Yager, D.B., Fey, D.L., Wright, W.G., 1972. formation and geochemical significance of iron bog deposits. In: Integrated Investigations of Environmental Effects of Historical Mining in the Animas River Watershed, San Juan County, Colorado.
Stoops, G., 1983. SEM and light microscopic observations of minerals in bog-ores of the Belgian Campine. Geoderma 30, 179–186.
Tadić, L., Brleković, T., 2018. Hydrological characteristics of the Drava River in Croatia. In: Lóczy, D. (Ed.), The Drava River. Springer Geography, pp. 79–90.
Taylor, S.R., McLennan, S.M., 1985. The Continental Crust: its Composition and Evolution. Blackwell Scientific Publication, Carlton, pp. 312.
Thelemann, M., Bebermeier, W., Hoelzmann, P., Lehnhardt, E., 2017. Bog iron ore as a resource for prehistoric iron production in Central Europe – a case study of the Widawa catchment area in eastern Silesia, Poland. Catena 149 (1), 474–490.
Tomašić, M., Zgorelec, Ž., Jurišić, A., Kisić, I., 2013. Cation exchange capacity of dominant soil types in the republic of Croatia. J. Cent. Eur. Agric. 14 (3), 937–951.
Török, B., Kovács, Á., Gallina, Z., 2015. Iron metallurgy of the Pannonin Avars of the 7-9th century based on excavations and material examinations. Der Anscnhitt, Beiheft 26, 229–237.
Tyler, G., 2004. Rare earth elements in soil and plant systems – a review. Plant Soil 267, 191–206.
Ujević Bošnjak, M., Casiot, C., Duić, Ž., Fazinić, S., Halamić, J., Sipos, L., Santo, V., Dadić, Ž., 2013. Sediment characterization and its implications for arsenic mobilization in the deep aquifers of eastern Croatia. J. Geochem. Explor. 126–127, 55–66.
Ujević, M., Duić, Ž., Casiot, C., Sipos, L., Sano, V., Dadić, Ž., Halamić, J., 2010. Occurrence and geochemistry of arsenic in the groundwater of Eastern Croatia. Appl. Geochem. 25, 1017–1029.
Valent, I., Zvijerac, I., Sekelj Ivančan, T., 2017. Topografija arheoloških lokaliteta s talioničkom djelatnošću na prostoru Podravine (*eng.* Topography of Archaeological localities with smelting plants in the area of Podravina). Podravina 16 (32), 5–25 in Croatian.
Varsányi, I., Kovács, L.Ó., 2006. Arsenic, iron, and organic matter in sediments and groundwater in the Pannonian Basin, Hungary. Appl. Geochem. 21, 949–963.
von der Heyden, B.P., Rorychoudhury, A.N., 2015. Application, chemical interaction and fate of iron minerals in polluted sediment and soils. Curr. Pollut. Reports 1, 265–279.
Wang, X., Griffin, W.L., Chen, J., 2010. Hf contents and Zr/Hf ratios in granitic zircons. Geochem. J. 44, 65–72.
Watts, H.D., Tribe, L., Kubicki, J.D., 2014. Arsenic adsorption onto minerals: connecting experimental observations with density functional theory calculations. Miner. Basel 4 (2), 208–240.
Welch, A.H., Westjohn, D.B., Helsel, D.R., Wanty, R.B., 2000. Arsenic in ground water of the United States: occurrence and geochemistry. Gr. Water 38 (4), 589–604.
Weng, L., Van Riemsdijk, W.H., Hiemstra, T., 2012. Factors controlling phosphate interactions with iron oxides. J. Environ. Qual. 41 (3), 628–635.
Weronska, A., 2009. Influnece of environmental conditions on holocene iron ores accumulation. Gospod. Surowcami Miner. 25 (2), 23–36.
Yee, N., Shaw, S., Benning, L.G., Hien Nguyen, T., 2006. The rate of ferrihydrite transformation to goethite via the Fe(II) pathway. Am. Mineral. 91, 92–96.

Paper 2: Brenko, T., Borojević Šoštarić, S., Karavidović, T., Ružičić, S. & Sekelj Ivančan, T. (2021) Geochemical and mineralogical correlations between the bog iron ores and roasted iron ores of the Podravina region, Croatia. Catena, 105353.

Catena 204 (2021) 105353

Contents lists available at ScienceDirect

Catena

journal homepage: www.elsevier.com/locate/catena

Geochemical and mineralogical correlations between the bog iron ores and roasted iron ores of the Podravina region, Croatia

T. Brenko [a,*], S. Borojević Šoštarić [a], T. Karavidović [b], S. Ružičić [a], T. Sekelj Ivančan [b]

[a] University of Zagreb, Faculty of Mining, Geology and Petroleum Engineering, Department of Mineralogy, Petrology and Mineral Resources, Pierottijeva 6, 10 000 Zagreb, Croatia
[b] The Institute of Archaeology, Ljudevita Gaja 32, 10 000 Zagreb, Croatia

ARTICLE INFO

Keywords:
Geochemical fingerprinting
Hierarchical clustering
Rare earth elements
Experimental roasting
Geoarchaeology

ABSTRACT

Throughout the Podravina region, NE Croatia, over one hundred locations with signs of iron production, dating to the late Antique period and the Middle Ages, have been discovered in the last 30 years. Recently, signs of various bog iron ore types and formations were discovered throughout the area. This study investigates the mineralogical and geochemical characteristics of local bog iron and roasted iron ores. Furthermore, statistical clustering of different geochemical components in the ores is presented, while the abundance and distribution of macro-, micro- and rare earth elements (REE) and how they correlate within the bog iron ores and roasted iron ores is considered. A total of 15 samples acquired from geological investigations and 13 samples found during archaeological excavations were analysed using geochemical and mineralogical methods. In bog iron ores, X-ray diffraction (XRD) confirmed goethite and quartz as the primary mineral phases, while roasted iron ores contained several Fe minerals and had variable quartz and clay mineral contents. Chemical analyses confirmed high Fe contents in both bog iron ores (up to 70.89 mass. %) and roasted iron ores (up to 84.97 mass. %), with a distinct differentiation of Fe and Si between the different bog iron ore types. Scanning electron microscopy with attached EDS detector (SEM-EDS) showed features of laminar Fe and Mn mineralization, confirming the theory that bog iron ore forms as seasonal precipitation from groundwater. Using the hierarchical clustering analysis, a geochemical correlation of the iron component in bog iron ores and roasted iron ores was compared to other major oxides, micro- and REEs. It was established that the iron component has very little influence on REE and microelements behaviour. Therefore, microelements and REEs were used as a tracer for establishing a geographical connection between the bog iron ores and roasted iron ores in the Podravina region.

1. Introduction

Numerous sites connected to bloomery iron production were identified during decades of extensive archaeological field surveys in the Podravina region (Valent et al., 2017). Over the last decade, several sites with clear indicators of bloomery iron production and contemporary settlement features were excavated. The sites have been radiocarbon (C^{14}) dated to the late Antiquity and early Middle Ages (Sekelj Ivančan 2017a, 2017b). Samples of roasted and unroasted iron ore were found among the iron production debris and other archaeological finds. As the Podravina region is a lowland area of the Drava River valley, with the natural prerequisites for the formation of bog iron ore, it has been assumed that local bog iron ore was exploited and used for iron production during the late Antiquity and early Middle Ages (Sekelj Ivančan and Marković, 2017; Brenko et al., 2020). Bog iron ores are sedimentary accumulations of iron and accompanying elements (Ramanaidou and Wells, 2014), often found in wet lowland environments, such as clayey and alluvial soils, with a groundwater table close to the surface (Kaczorek and Zagórski, 2007). Bog iron ores are usually differentiated into three macromorphological types: (i) bog iron soils; (ii) bog iron nodules and concretions; and (iii) bog iron fragments and continuous, cemented horizons (Thelemann et al., 2017). These authors concluded that these ore types often represented development phases, with bog iron soils being the first type (phase), and bog iron fragments being the very last. Variable contents of Fe_2O_3 and SiO_2 are to be expected in different types depending on the bog iron formation mechanism.

Numerous efforts were made to determine the provenance of iron objects, starting as early as the middle of the 19th century (Schwab et al., 2006 and references therein). Even today, very little or no consensus has been reached among scientists regarding the appropriate analytical

* Corresponding author.

https://doi.org/10.1016/j.catena.2021.105353
Received 17 July 2020; Received in revised form 29 March 2021; Accepted 2 April 2021

methods, data sets and statistical methods for proving the origins of iron ores and roasted iron ores (Charlton et al., 2012). Researchers commonly use heavy metals and other trace elements such as Al, P, V, Cr, Mn, Co, Ni, Cu and As to determine the link between the iron ores and iron objects (Devos et al., 2000), or in case of slag material, using slag inclusions to compare the chemical composition with potential ore formations (Blakelock et al., 2009; Leroy et al., 2012). However, no one has previously investigated the changes in the geochemical composition of elements and the mineralogical characteristics resulting from different ore pre-treatment processes in such detail. Pre-treatment processes, such as the washing of iron ores and their roasting in an open fire, could lead to the differentiation of several chemical elements. Tracking these changes from natural, untreated ores through to roasted ores could provide evidence of geochemical behaviour of elements during the smelting process. Analysing these changes could provide a more precise correlation between the bog iron ores and iron slags.

To provide geochemical evidence for the origin of bog iron ore and roasted iron ore, macro-, micro- and rare earth elements were analysed. Due to their specific mobility and behaviour, the REEs have found an application in fingerprinting geological and anthropogenic sources and in investigating geochemical processes that lead to the fractionation of this group of elements in various environments (Migaszewski et al., 2016). It is well known that REE in the surface environment are strongly influenced by genetic processes that can led to varying vertical distribution of REE in the soil profile (Mihajlović et al., 2019). Slight variability in microelements and REEs was also noticed in the soils of the Podravina region (Brenko et al., 2020). However, due to the bog iron ore fast formation and regeneration mechanism (Bricker et al., 2003), it is believed that geochemical fractionation is not occurring at such level. Therefore, REE and microelements are used as tracers to provide the geochemical connection between the bog iron ores and the roasted iron ores in the Podravina region.

This study addresses the following research questions: (i) what are the geochemical and mineralogical characteristics of different bog iron types and roasted iron ores in the Podravina region?; (ii) what geochemical changes occur during bog iron ore roasting?; and (iii) is it possible to correlate the bog iron ores and the roasted bog iron ores based on their respective macro-, micro- and REE contents? In order to answer these questions, three samples of bog iron soils, three samples of bog iron nodules, nine samples of bog iron fragments and thirteen samples of roasted iron ores from different locations were analysed using geochemical and mineralogical methods (ICP-MS, ICP-AES, SEM-EDS, XRD). From each bog iron type, at least one sample was roasted in laboratory conditions to determine changes in REE and micro-elemental contents. Based on experimental data and using statistical methods, the formation mechanisms and geochemical correlation between the bog iron ores and roasted bog iron ores was explored.

2. Study area

The study area is situated in the central part of the Podravina region, NE Croatia, bound by the Croatian-Hungarian state border to the north and northeast, and by the Bilogora hills to the south and southwest. Due to the low-lying terrain, a central feature of the area is the meandering Drava River, along with many smaller tributaries, bogs and swamps. Surrounding the Drava River is a wide alluvial plain with three river terraces, that formed during the Holocene climatic warming period (Head, 2019). Due to constant floods in the past (Lóczy et al., 2014), the main lithological units in the area are flooding sediments, such as sands, silts, clays and, occasionally, gravels. The most common soil types in the study area are Fluvisols and Gleysols located on the Pleistocene and Holocene sediments, with Stagnosols and Regosols sporadically appearing in some parts of the region (Bašić, 2013). The groundwater table is relatively close to the surface (Brkić and Briški, 2018), and is connected with the Drava River (Brkić et al., 2010), while the aquifer system is generally enriched with iron, arsenic and manganese (Kopić et al., 2016; Brenko et al., 2020). For more detailed information on the geological, pedological and hydrological characteristics of the Podravina region, the reader is referred to Brenko et al. (2020) and references therein. The focus of this study are locations where samples of different bog iron formation phases were collected, and locations of archaeological sites where both bog iron ores and roasted iron ores were found (Fig. 1).

Samples from the Virje–Volarski breg site were found in features within the settlement dated by the analysis of ceramic material to the middle or second half of the 8th century (Sekelj Ivančan, 2017a). The site is temporally and spatially (distance of 200 m) connected to a bloomery smelting workshop, which has been radiocarbon dated to the end of the 8th or beginning of the 9th century. The Virje–Sušine site was inhabited several times throughout history, from early and late Iron Age, throughout late Antiquity and the early Middle Ages and even during the 16th century. Traces of bloomery smelting activities during late Antiquity and the early Middle Ages have been identified at the site. The analysed roasted ore samples (V-S 1, 5, 6) originate from a layer of smelting debris that was radiocarbon dated to the 4th – 5th century (Sekelj Ivančan, 2014) and from the surface soil layer (V-S 3) of the same trench. Other samples (V-S 2, 4) from the Virje–Sušine site are attributed to features from within the settlement grounds dated to the 8th century (Sekelj Ivančan, 2017b; Sekelj Ivančan and Tkalčec, 2018). Two other sites, the Hlebine–Velike Hlebine and Hlebine–Dedanovice, have both been radiocarbon dated to around the middle of the 7th century (Sekelj Ivančan and Valent 2020). Samples from Hlebine–Velike Hlebine were found within a bloomery smelting workshop (Sekelj Ivančan and Valent, 2017) while samples from the contemporary Hlebine–Dedanovice site were found in features that were probably located at the edge of the settlement (Sekelj Ivančan, 2019).

3. Materials and methods

A total of 15 samples of different bog iron ore types and 13 samples of roasted iron ores from archaeological sites were selected (Tables 1 and 3). Samples were found on the surface of agricultural fields processed by deep ploughing and divided into three different types: bog iron soils, nodules, and fragments. Bog iron soils are found close to the surface and due to their reddish-orange colour (5YR 5/8) can be distinguished from surrounding soils (10YR 3/4). Bog iron nodules and ore fragments most likely originate from subsurface layers. They stand out from the soils due to their hardness and morphology, having spherical shapes with a diameter of up to 1 cm, while fragments are comprised of nodules bound together as a conglomeration, with sizes of up to 20 cm. They tend to be orange-brownish in colour (7.5YR 4/6, 7.5YR 5/8), with some samples being dark brown (10YR 3/2) and black (10YR 2/1). Analysed archaeological samples originate from several sites in the region, dated to late Antiquity and the early Middle Ages.

All samples were air-dried prior to the mineralogical and geochemical analyses. A part of each sample was homogenized in an agate grinding set to produce the powder fraction. The mineralogical composition of each sample was determined by X-ray powder diffraction (XRD) using a Phillips vertical X-ray goniometer (type X'Pert) equipped with Cu tube and graphite crystal monochromator. Scan settings were 3–70° 2θ, 0.02° step size, 1 s count time per step while generator settings were 40 kV and 35 mA. Minerals were identified using PANalytical X'Pert HighScore software with standardised Powder Diffraction Files (PDF) of the International Centre for Diffraction Data (ICDD) (Newton Square, PA, USA). The geochemical composition, including the main oxides, major-, micro- and REEs was determined in MSALabs (Langley, Canada). Multielement contents of micro and REEs were analysed using inductively coupled plasma-mass spectrometry (ICP-MS), while 4-acid digestion including hydrochloric, nitric, perchloric and hydrofluoric acids was used for near total digestion. Only the most highly resistant minerals (zircon) were not fully dissolved. Based on two internal standards and several blanks, instrumental precision was between 3 and 5%

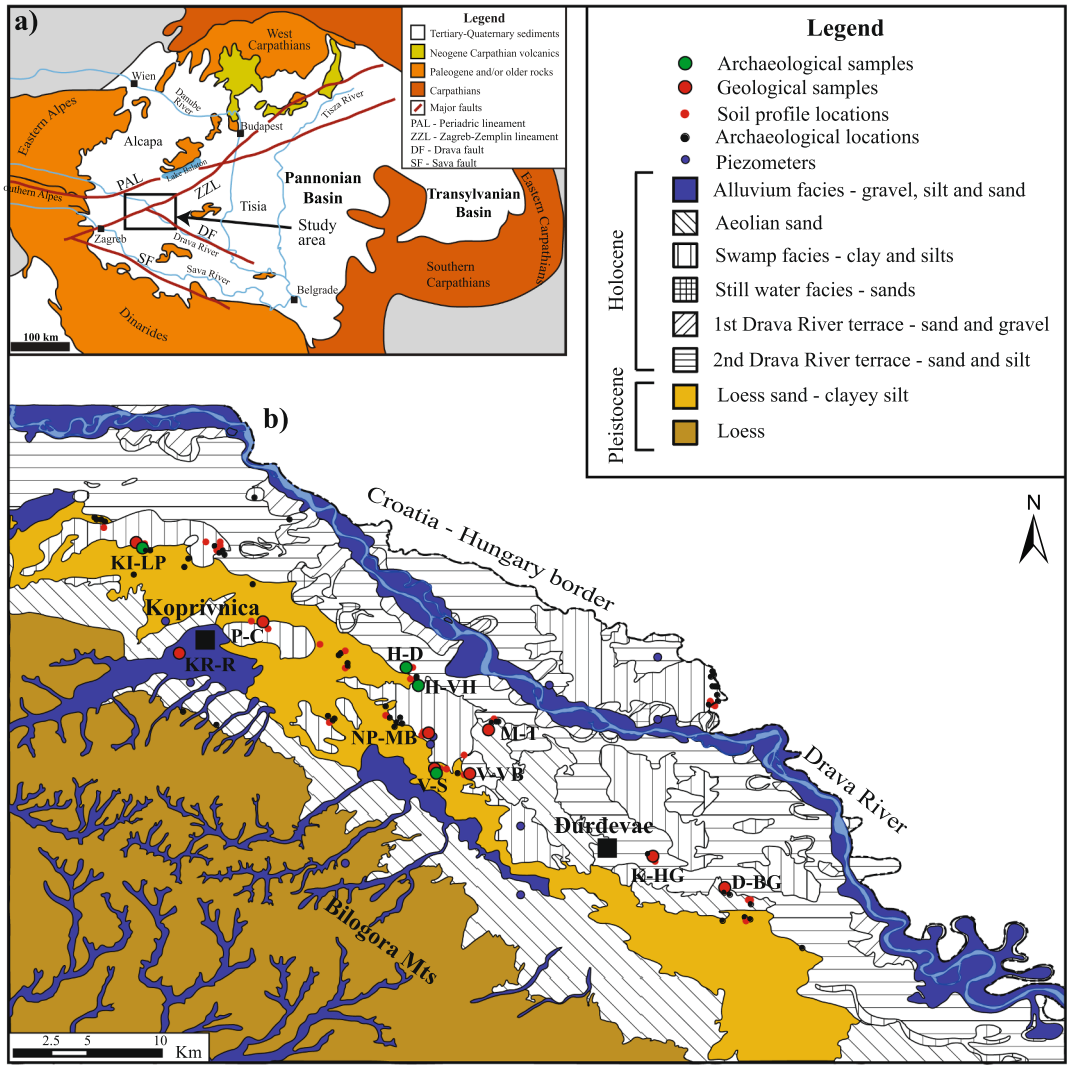

Fig. 1. Geological map of the study area with positions where bog iron ores and roasted iron ores were discovered. Modified according to Brenko et al. (2020) and references therein.

Table 1
Mineral composition of different bog iron ore types and experimentally roasted iron ores from geological and archaeological surveys. Mineral abbreviations: AM – amorphous matter; Cal – calcite; CM – clay minerals; Gth – goethite; Hem – hematite; Or – orthoclase; Pl – plagioclase; Pyr – pyrolusite; Qz – quartz.

Sample	Location	Bog iron ore type	Qz	Gth	Pl	Or	Pyr	Cal	CM	AM	Hem
K-HG 1	Kalinovac–Hrastova greda	Nodules	+++	+	+	+			+		
K-HG 2		Soil	+++	+	+				+		
K-HG 2 R		Roasted soil	+++						+		+++
K-HG 3		Soil	++	++	+				?		
NP-MB 16	Novigrad Podravski–Milakov Berek	Fragments	+	+++	+		+	+		++	
NP-MB 16R		Roasted fragments	+					+			+++
NP-MB 17		Fragments	++	++	+		+		+	+	
NP-MB 18		Fragments	+	+++			?			++	
NP-MB 18R		Roasted fragments	+								+++
D-BG	Draganci–Bokčev grob	Nodules	+++	+	+	+			+		
P-C	Peteranec–Ciglene	Nodules	+++	+	+				++		
P-C R		Roasted nodules	+++		+				+		++
M-T	Molve–Topolovo	Soil	+++	+	+	+			++		
V-VB 1	Virje–Volarski Breg	Fragments	++	++	+				+/++	?	
V-VB 2		Fragments	++	++	+				+	?	
V-VB 3		Fragments	++	++					+	?	
V-S 1	Virje–Sušine	Fragments	+	+++	+						
KI-LP 1	Koprivnički Ivanec–Log Parag	Fragments	++	++	+				+	+	
KR-R	Koprivnička Reka–Rudina	Fragments	++	++							

+ - relative abundance of minerals within horizons based on X-ray diffraction (no quantitative value assigned to +); +++ major component, ++ minor component; + traces; ? – not enough diffraction peaks to fully confirm

Table 2
Geochemical composition of bog iron ore samples in the Podravina region. All values given in mass. %.

Sample	Location	Bog iron ore type	SiO_2	TiO_2	Al_2O_3	Fe_2O_3	MgO	MnO	CaO	K_2O	Na_2O	P_2O_5	BaO	SrO	LOI	TIC	TOC	**Total**
K-HG 1	Kalinovac–Hrastova greda	Nodules	38.46	0.32	5.67	36.02	0.47	2.89	0.72	0.72	0.69	0.54	0.30	0.01	11.49	0.03	0.61	98.30
K-HG 2		Soil	63.38	0.44	7.34	14.43	0.67	0.10	0.83	0.92	0.97	0.38	0.03	<0.01	9.03	0.04	0.64	98.52
K-HG 3		Soil	50.75	0.38	6.82	27.93	0.68	0.31	0.83	0.85	0.90	0.31	0.04	<0.01	9.27	0.04	0.66	99.07
NP-MB 16	Novigrad Podravski–Milakov Berek	Fragment	8.69	0.06	2.50	32.03	0.70	21.04	5.67	0.42	0.44	0.62	0.76	0.15	21.39	0.81	0.51	94.47
NP-MB 17		Fragment	10.98	0.07	3.25	45.35	0.48	14.85	1.18	0.45	0.36	0.70	0.74	0.09	15.95	0.03	0.43	94.45
NP-MB 18		Fragment	3.59	0.01	0.57	68.41	0.16	5.68	0.62	0.12	0.08	1.00	0.12	0.02	15.14	0.03	0.41	95.52
D-BG	Draganci–Bokčev grob	Nodules	27.06	0.39	7.29	39.54	0.76	4.32	1.04	0.94	0.74	1.86	0.24	0.01	15.31	0.03	1.62	99.50
P-C	Peteranec–Ciglene	Nodules	44.10	0.76	12.24	22.99	0.95	0.57	0.78	1.76	0.96	1.87	0.08	0.01	11.29	0.05	1.02	98.36
M-T	Molve–Topolovo	Soil	57.92	0.68	12.35	13.20	1.18	0.10	1.14	1.33	1.04	0.28	0.04	0.01	9.52	0.05	1.24	98.79
V-VB 1	Virje–Volarski Breg	Fragment	24.16	0.30	8.72	37.28	0.59	5.25	0.97	0.86	0.34	0.24	0.15	<0.01	15.45	0.04	0.46	94.31
V-VB 2		Fragment	30.67	0.37	8.58	38.94	0.59	1.59	0.72	0.90	0.46	0.66	0.07	<0.01	13.29	0.04	0.43	96.84
V-VB 3		Fragment	25.92	0.29	7.52	46.86	0.48	1.69	0.60	0.80	0.34	0.45	0.06	<0.01	13.43	0.03	0.42	98.44
V-S 1	Virje–Sušine	Fragment	10.12	0.03	1.90	70.89	0.14	0.98	0.34	0.30	0.13	0.49	0.09	<0.01	11.91	0.04	0.6	97.32
KI-LP 1	Koprivnički Ivanec–Log Parag	Fragment	16.67	0.12	4.53	49.45	0.65	3.13	1.27	0.79	0.42	1.90	0.19	0.01	16.02	0.02	0.48	95.15
KR-R	Koprivnička Reka–Rudina	Fragment	29.09	0.45	5.99	45.82	0.83	0.04	1.28	1.07	0.27	0.28	0.02	<0.01	10.57	*	*	95.71

* Sample volume too small to conduct all analyses.

and the detection limits for most analysed elements were in the part per million (ppm) or lower. Major oxides contents were determined using inductively coupled plasma-atomic emission spectrometry (ICP-AES) with lithium borate fusion. Loss on ignition (LOI) was determined by weight difference after ignition at 1000 °C. In collaboration with the Faculty of Mining and Geology, University of Belgrade, a JEOL JSM-6610 scanning electron microscopy with attached energy dispersive X-ray spectroscopy (SEM-EDS) was used to define the micro-morphological characteristics of the bog iron ore types, their formation mechanisms and to determine structural similarities and differences between bog iron ores and roasted ores. To correlate bog iron ores with roasted ores from the same region, microelements and REEs were analysed using the GCD Toolkit in R language (Janoušek et al., 2006). To supress the Oddo-Harkins effect and characterize the geochemical signature of bog iron types and roasted ores, the REE and microelements were normalized to chondrite (Anders and Grevesse, 1989) and to Upper Continental Crust (Taylor and McLennan, 1995) and then plotted on the appropriate diagrams. Alongside collected samples, one sample of bog iron soil (K-HG 2R), one sample of bog iron nodules (P-C R) and two samples of bog iron fragments (NP-MB 16R and NP-MB 18R) were roasted under laboratory conditions at temperature between 750 and 800 °C. This temperature was chosen based on several previous archaeological experiments on bog iron roasting and based on complete transformation of Fe-oxyhydroxides to hematite (Rzepa et al., 2016). Experimental roasting was done in order to determine the behaviour of REE and other selected microelements in bog iron ores during the roasting process.

The basic descriptive statistics, including minimum, maximum, mean value and standard deviation were reported for all bog iron types and roasted ores. Hierarchical clustering method using tree diagrams was conducted to better distinguish the geochemical correlation of data among samples. As geochemical data does not follow normal data distribution, the data sets were log-transformed. Following log-transformation, the data was standardized to ensure that each variable is weighted equally. The data standardization resulted in new values Z (z-score or z-value) with a mean of zero that are measured in units of standard deviation. The Z-values were obtained by subtracting the mean value of the distribution of each variable and dividing the resulting value by the standard deviation of each variable. Hierarchical plotting of data was conducted in Statistica 12 (StatSoft Inc., 2012) software and presented in the form of joint tree diagrams where the correlation of 39 variables is plotted. For this study, the Euclidean distance was chosen as the main distance measure (similarity measurement) between the geochemical variables. The variables that show the largest similarity are grouped first. Groups of samples are connected with a linkage rule. The grouping and linkage processes are repeated until all variables are connected. Ward's method was used as the linkage rule, giving more homogenous and geochemically similar clusters.

4. Results

4.1. Geochemical and mineralogical characteristics of different bog iron ore types

Three different bog iron types were analysed in this study: bog iron soils, bog iron nodules and bog iron fragments. Mineral composition varies both between the bog iron types, as well as between same types from different sampling sites (Table 1). Generally, all bog iron types consist of quartz (SiO_2) and goethite (α-FeOOH). Bog iron soils have the lowest content of goethite and the highest content of quartz, often appearing with plagioclase, orthoclase and clay minerals. Bog iron nodules show higher contents of goethite, and proportionally to that, lower contents of quartz, while plagioclase, orthoclase and clay minerals frequently occur in trace amounts. Bog iron fragments mainly consist of goethite and quartz and often show variable amounts of amorphous matter. The mineral composition of fragments varies between locations.

Table 3
Mineralogical composition of roasted iron ores from archaeological sites in the Podravina region. Mineral abbreviations: CM – clay minerals; Gth – goethite; Lpc – lepidocrocite; Hem – hematite; Mag – magnetite; Mgh – maghemite; Pl – plagioclase; Qz – quartz.

Sample	Location	Qz	Gth	Lpc	Hem	Mag	Mgh	Pl	CM
H-D 1	Hlebine–Dedanovice	+			+++				
H-D 2		+			+++		+		
H-D 3		++			+++		++		
H-D 4		+			+++		++		
H-VH 1	Hlebine–Velike Hlebine	++	++			++			+
H-VH 2		++	+	+	+	++	+	+	
H-VH 3		+	++	+	+	++	+	?	?
V-S 2	Virje–Sušine	+++			+				+
V-S 3		+++			+			+	+
V-S 4		+++			+			+	+
V-S 5		+++			++		+		+
V-S 6		+	++	+		++	+	?	
KI – LP 2	Koprivnički Ivanec–Log Parag	+++			+			+	+

+ - relative abundance of minerals within horizons based on X-ray diffraction (no quantitative value assigned to +); +++ major component, ++ minor component; + traces; ? – not enough diffraction peaks to fully confirm.

The biggest difference is in the appearance of pyrolusite (MnO_2) in the fragments from Novigrad Podravski–Milakov Berek location. Plagioclase and clay minerals occur in traces in some of the samples, while calcite was detected in sample NP-MB 16.

Several samples of bog iron nodules (K-HG 1, P-C) and fragments (NP-MB 16, NP-MB 18, KI-LP 1) were selected for SEM-EDS analysis based on their archaeometallurgical potential and, in some cases, due to extremely high contents of Mn. The SEM back-scattered images show interlamination of Fe-rich layers (grey to dark grey reflectivity) and Mn-rich layers (light grey to white), especially in the bog iron fragments (Fig. 2). In both nodules and fragments, detrital grains are mainly composed of quartz and feldspars that often appear dispersed in the micro-crystalline goethite, Mn oxides and phyllosilicate matrix (Fig. 2A, 2B, 2E). Nodules from P-C have slightly concentric structure as can be seen in Fig. 2C. Fe oxides are usually present in the outer rims, while Mn oxides are often found in the central parts of the nodules. In the bog iron fragment from the KI-LP location, a 70 μm Fe-Mn nodule was found embedded in a matrix composed of Fe-enriched and detrital minerals zone (Fig. 2D). Bog iron fragments from Novigrad Podravski–Milakov Berek show a highly laminated micro-structure (Fig. 2F; H), where Mn oxides show two types of morphology; well laminated micro-crystalline structures (Fig. 2F, 2H), often with varying lamina sizes, but with no recognizable mineral grains and well-developed, tabular crystals, usually elongated and several μm in size (Fig. 2G). The main difference in the chemical composition of the two Mn phases is the barium (Ba) content, which is mostly concentrated in the laminated parts while being almost entirely absent from the well-crystallized parts. Occurrence of calcite in the form of veins was noticed inside the fragment from Novigrad Podravski location (Fig. 2F).

The oxide composition of all bog iron types is mostly comprised of silicon-dioxide (SiO_2) and iron (III) oxide (Fe_2O_3), whereby the content varies greatly between the different types (Table 2). Bog iron soils show the highest amounts of SiO_2, which varies between 50.75 and 63.38 mass. %, while the Fe content varies between 13.20 and 27.93 mass. %. Bog iron nodules contain moderate amounts of SiO_2 (27.06 – 44.10 mass. %) and Fe_2O_3 (22.99 – 39.54 mass. %), while bog iron fragments have the highest Fe_2O_3 content (32.03 – 70.89 mass. %) with a lower SiO_2 content (3.59 – 30.67 mass. %). The MnO content in the bog iron fragments varies from trace amounts up to extremely high contents in the fragments from the Novigrad Podravski–Milakov Berek site (14.85 and 21.04 mass. % in NP-MB 16 and NP-MB 17), with values generally exceeding 1 mass. % in all fragments (Table 2). Except for Al_2O_3, with contents varying from 0.57 to 12.35 mass. %, other oxides are present in bog iron ores in trace amounts. Loss on ignition (LOI) is relatively high, with values between 9.03 and 21.39 (χ = 13.27 mass. %), while the contents of total organic (TOC) and total inorganic carbon (TIC) are low.

Geochemical contents of major oxides and microelements (Appendix A) in all three bog iron types were classified using the hierarchical cluster analysis (HCA). The classification of samples and variables is based on visual observation of constructed dendrograms. The HCA resulted in three dendrograms of bog iron soils, nodules, and fragments with similar clustering of some major oxides and elements (Fig. 3). Even without using the phenon line to distinguish the clusters, a clear distinction into two geochemically different clusters can be observed in all three bog iron types. Generally, Fe_2O_3 and MnO oxides are grouped in one cluster together with As, BaO and P_2O_5. Other observed microelements are usually clustered with SiO_2, Al_2O_3 and other major oxides. A closer inspection of the dendrograms reveals a further dissimilarity between the clusters where clusters containing Fe_2O_3, MnO and related variables are linked to the other clusters at an elevated distance, proving that these variables are geochemically distinct from the others.

4.2. *Geochemical and mineralogical characteristics of roasted iron ore in the Podravina region*

Roasted iron ores differ from the collected bog iron ores mostly in their visual appearance, being reddish in colour. Mineralogically, roasted ores mainly consist of quartz and one or several iron minerals, with hematite (Fe_2O_3) being the most common mineral phase. Magnetite ($FeFe_2O_4$) and maghemite (γ-Fe_2O_3) mostly occur as minor and trace components, with plagioclase also occurring as a trace component (Table 3). Virje–Sušine samples differ from other sites due to the presence of clay minerals.

Two samples of roasted iron ore from the Hlebine–Dedanovice site were analysed using SEM-EDS based on their archaeometallurgical potential. Unlike the bog iron samples, roasted iron ore show greater homogeneity in their micro-structure (Fig. 4A). Both samples are composed of a hematite micro-crystalline matrix surrounding detrital mineral grains. Compared to the bog iron samples, the significant difference is the higher volume of pores in roasted ore (Fig. 4B; D) and a lack of any sort of lamination in the observed samples. Occasionally, detrital mineral zones with feldspar, plagioclase and phyllosilicates can be found in some parts of the samples (Fig. 4C). Regarding the geochemical composition, Fe and O are the dominant chemical phases, while Mn is rarely observed.

The geochemical composition of the sampled roasted iron ores mainly consists of Fe_2O_3 (8.44 – 84.97 mass. %, χ = 52.29 mass. %) and SiO_2 (4.17 – 62.67 mass. %, χ = 27.49 mass. %) (Table 4). A differentiation in the iron concentrations is noticeable between the archaeological sites. The iron content of roasted ores from the Hlebine–Dedanovice site shows the highest concentrations of Fe_2O_3 (χ = 84.00, n = 4). The samples from Hlebine–Velike Hlebine have a bit more variability of Fe_2O_3 (χ = 70.31, n = 3). On the other hand, samples from the Virje–Sušine site have the highest variability and the lowest

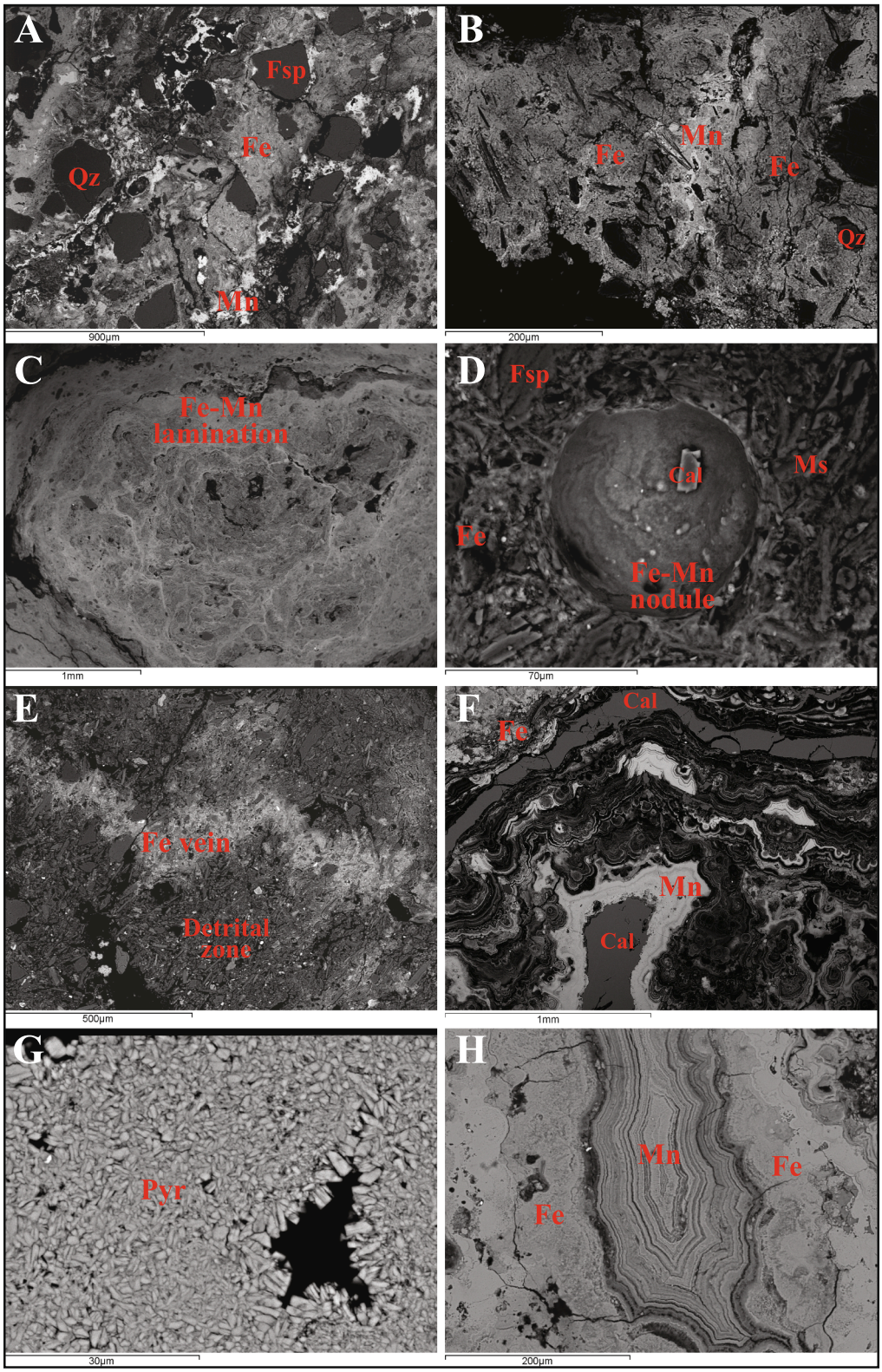

Fig. 2. Mineralogy and internal microtextures of the bog iron nodules and fragments (back-scattered electron images). (A) Quartz (Qz) and feldspar (Fsp) grains surrounded by Fe and Mn matrix in K-HG 1 nodule. (B) Differentiation between Fe (outer parts) and Mn oxides (inner part) in K-HG 1 nodule. (C) Cross-section of bog iron nodule from Peteranec-Ciglene showing concentric lamination of Fe (dark-grayish) and Mn (light-grayish) oxides. (D) Fe-Mn nodule surrounded by the Fe matrix and detrital zone including muscovite (Ms) in KI-LP 1 fragment. (E) Soil minerals zone with Fe oxides in the form of vein (light gray) in the central part of one KI-LP 1 fragments. (F) Highly Mn laminated zone with post-depositional calcite veins (Cal) in Novigrad Podravski NP-MB 16 fragment sample. (G) Mineralization of Mn oxides in the form of pyrolusite (Pyr) in the bog iron fragments from Novigrad Podravski location. (H) Differentiation of highly laminated Mn zone, surrounded by microcrystalline iron (Fe) zone in NP-MB 18 fragment.

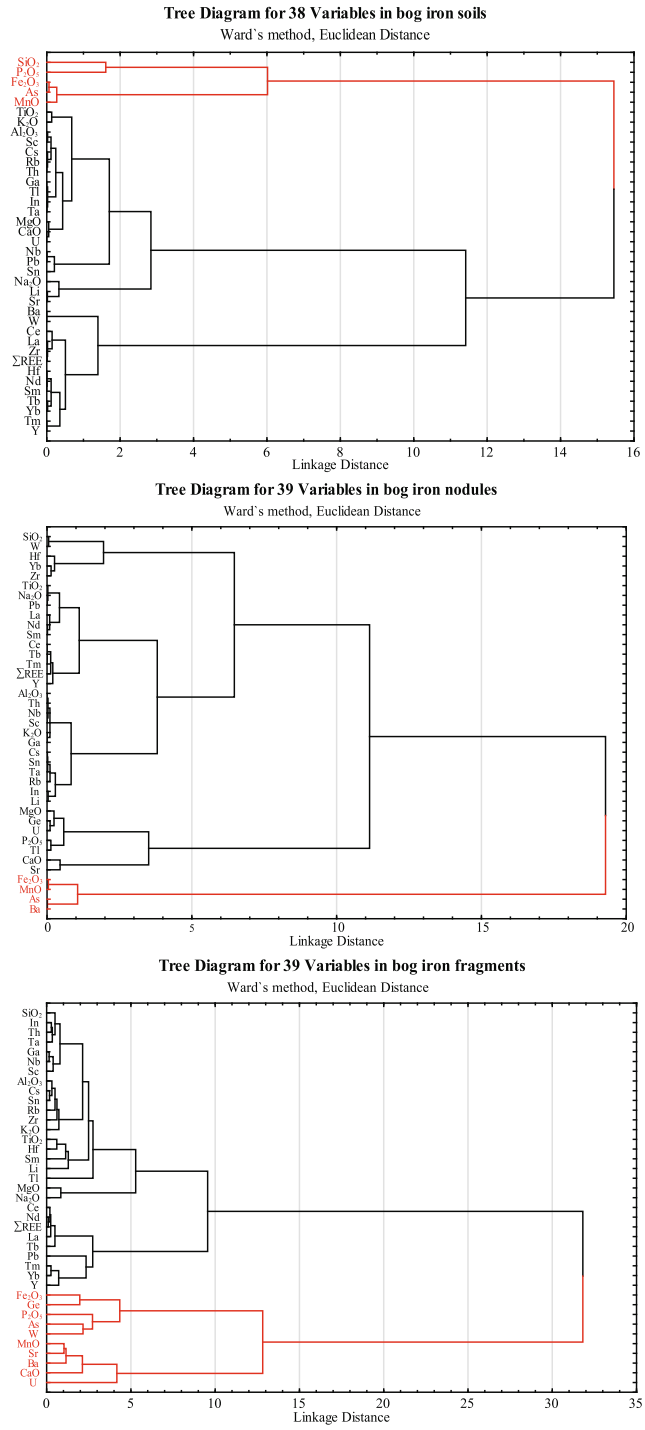

Fig. 3. Hierarchical cluster analysis of a) bog iron soils, b) bog iron nodules and c) bog iron fragments.

concentrations of Fe_2O_3 of all the investigated sites with values varying between 8.44 and 45.57 mass. % ($\chi = 23.19$, n = 5). Only Al_2O_3 (max. 14.62 mass. %), MnO (max. 5.49 mass. %) and P_2O_5 (max. 2.68 mass. %) are present in significant amounts in the samples, while other major oxides are present in variable low or trace amounts. LOI values vary between 2.39 and 11.60 mass. % ($\chi = 5.99$ mass. %). The TIC ($\chi = 0.08$ mass. %, n = 9) and TOC ($\chi = 0.36$ mass. %, n = 9) values in roasted iron ores show lower values than in the bog iron ores.

The geochemical composition of major oxides and microelements (Appendix B) in roasted iron ores were classified using hierarchical clustering as with the bog iron ores. Similar clustering behaviour as in the bog iron ores was recognized, with the formation of two main clusters (Fig. 5). One cluster consists of Fe_2O_3, As and Ge, while the other cluster consists of SiO_2, Al_2O_3 and other major oxides and microelements, including REE. A similar observation of the elevated linkage distance between the two main clusters in roasted iron ores suggests a significant geochemical difference between them.

4.3. Rare earth and microelemental distribution in bog iron ores and roasted iron ores

The ∑REE ranges from 114.31 to 200.09 ppm in bog iron soils, from 174.44 to 354.87 ppm in bog iron nodules, and from 52.62 to 209.97 ppm in the bog iron fragments (Appendix A). In addition, the ∑LREE/∑HREE ratio ranges from 12.17 to 17.86 in all the bog iron samples. In roasted iron ores, the ∑REE values range from 29.97 up to 455.67 ppm (Appendix B). The ∑LREE/∑HREE ratio is similar to that of the bog iron ores, with values ranging from 11.95 to 17.54.

As shown in Fig. 6A, the REE patterns of bog iron soils show LREE enrichment, with a distinct negative europium (Eu) anomaly. Experimentally roasted bog iron soil (K-HG 2R) exhibits almost identical geochemical pattern. The bog iron nodules show a slight discrepancy between samples, with sample P-C showing higher REE contents than the K-HG 1 and D-BG samples. Even so, all samples show the same trend as bog iron soils, with pronounced enrichment in LREE and a distinctive negative Eu anomaly (Fig. 6B). Bog iron fragments have the largest discrepancies in REE contents when observing different locations (Fig. 6C). Apart from the Novigrad Podravski site, the other samples have patterns similar to the first two bog iron ore types, with LREE enrichment and a negative Eu anomaly. All three bog iron fragments from the Novigrad Podravski–Milakov Berek site have different patterns with regard to the middle REEs with sample NP-MB 16 having positive Sm and Eu anomaly, sample NP-MB 17 slight positive Sm anomaly and sample NP-MB 18 negative Eu anomaly. The experimentally roasted sample NP-MB 16 has the same REE pattern as the original sample, although with a lower Sm and Eu anomaly. Similarly, the experimentally roasted sample NP-MB 18 shows an REE pattern that is almost identical to the original sample. Roasted iron ores show the same behaviour of REEs as the bog iron ores, with enrichment in LREE and a negative trend towards HREE (Fig. 6D). Samples from Hlebine–Dedanovice have the same REE patterns, while samples from other locations show slight variability in the REE contents.

Microelements and REE normalized to Upper Continental Crust show similar behaviour in all three bog iron types and in roasted iron ores (Fig. 7). Significant anomalies noticeable on all diagrams include a negative Rb and Ti, with a positive P anomaly. Several samples indicate positive Ba anomaly, noticeable in almost all fragment samples and in roasted samples from different sites. Soil and nodule samples have normalized ratios between 0.1 and 10, while fragments and roasted samples tend to have ratios between 0.1 and 0.01.

5. Discussion

5.1. Characteristics of the bog iron ores in the study area

Bog iron ores from the study area originate from archaeological excavations where samples were found in a clear context of bloomery iron production (V-S 1) or within settlement features related to iron production sites (V-VB 1–3, KI-LP), and from geological investigations. In the archaeological context, only bog iron ore fragments were found, while during geological investigations all three bog iron types were collected. As seen in Fig. 1, sites with bog iron occurrences are located on the Drava River alluvial terrace, which is in line with previously described findings of bog iron ores in similar study areas (Kaczorek and Sommer, 2003; Banning, 2008; Thelemann et al., 2017). During this study, the outer margins of the Drava River floodplain were not covered by the field investigations, so the question of bog iron ore occurrence in

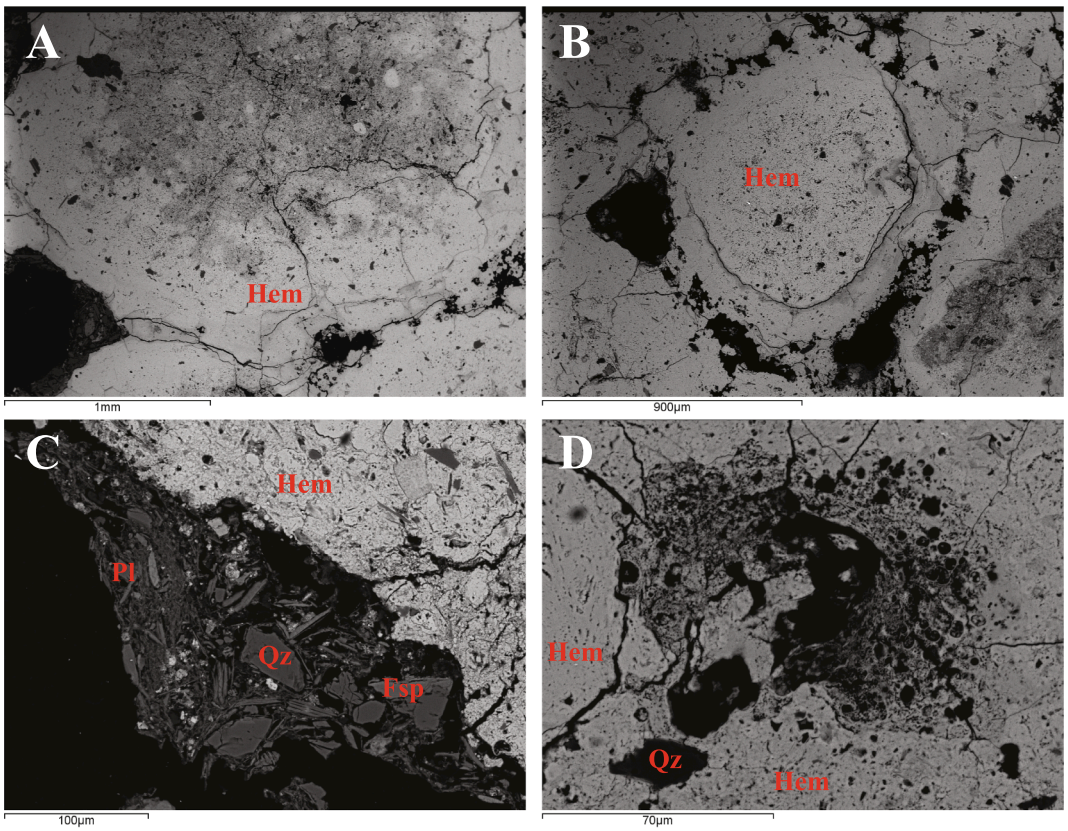

Fig. 4. SEM-EDS microphotographs of roasted iron ores from the Hlebine–Dedanovice location. (A) Homogenous masses of Fe oxides, presumably hematite (Hem). (B) Porous hematite (Hem) microtexture formed during roasting of iron ore. (C) Detrital accumulation of quartz (Qz), feldspar (Fsp) and plagioclase (Pl) in roasted ore sample, similar to bog iron samples. (D) Detrital quartz (Qz) grain surrounded with hematite (Hem); visible increased porosity.

these areas remains open.

As all bog iron samples were found at or near the surface, where oxidizing conditions prevail, the absence of Fe^{2+} minerals, such as vivianite and siderite, is to be expected (Stoops, 1983; Landuydt, 1990), while goethite is the main Fe mineral (Stoops, 1983; De Geyter et al., 1985; Landuydt, 1990; Ramanaidou and Wells, 2014). Due to bog iron soils representing soil material enriched with Fe matrix, the highest clay content is to be expected. As the cementation process and substitution of the Si matrix with an Fe-enriched matrix had only begun in the bog iron soils, it is certainly expected that this bog iron type has the lowest iron contents. On the other hand, bog iron nodules and bog iron fragments display lower clay contents than in soils due to a more advanced Fe mineralization substituting the total alumosilicate content. The geochemical composition of analysed bog iron ores points to a clear geochemical differentiation between the bog iron ore types. A difference in hardness between the soils and the nodules is attributed to the more advanced cementation processes in the nodules. Soil detrital material is fully cemented with Fe and Mn layers (as seen in Fig. 2C). This concentric internal structure is believed to be the result of alternating dry and wet periods, during which interchanges of oxidizing and reductive conditions took place (Palumbo et al., 2001; Gasparatos et al., 2005; Gasparatos et al., 2019). Spherical nodular shapes can be seen incorporated inside bog iron fragments, proving the theory that the fragments, as a final development phase, are formed by even further cementation with an Fe-enriched matrix, agglomerating smaller nodules into larger fragments (Fig. 2D). If the cementation process were to continue, the formation of a layered bog iron ore deposit is to be expected (Kaczorek and Zagórski, 2007). The diffraction reflexes of bog iron fragments often contain high background noises which probably indicate the enrichment in the amorphous iron phase (ferrihydrite), a mineral often associated with the bog iron ores (Kaczorek and Zagórski, 2007) that can be found in the soil groundmass. Extremely high concentrations of Mn were detected in the fragments from the Novigrad Podravski–Milakov Berek site. Based on similar results from other studies (Török and Kovács, 2010; Török et al., 2015), increased MnO contents result from localised changes in the redox conditions in the wider Drava River basin. Although displaying similar behaviour and origin, the precipitation of Mn occurs at higher Eh-pH conditions than the Fe precipitation (Atta et al., 1996). As these higher Mn precipitation conditions are rarely reached in the soils of the Podravina region (Brenko et al., 2020), the appearance of Mn is only to be expected at sites with higher Eh-pH conditions. Micro-morphological and textural differences in the samples from Novigrad Podravski points to different groundwater source and bog iron evolution than in the rest of the study area.

Calcite mineralization in sample NP-MB 16 occurs in the form of veinlets, cutting through and/or following Fe mineralization (Fig. 2F). Calcite probably formed around plant material due to localised changes in pH and an abundance of nitrates. Plant root that rapidly absorbs nitrate will take up more anions than cations, releasing carbonate anions into the soil to maintain balance and thus increasing the pH. The resulting increase in pH is sufficient to start $CaCO_3$ precipitation (Lambers et al., 2009).

Pleiner (2000) established an empirical boundary value for bloomery iron smelting of 79–86 mass. % Fe_2O_3, which is well beyond the iron contents in the bog iron ores found. However, experimental direct iron smelting in the last decades has shown that bog iron ores with much lower iron contents of up to 49 mass. % Fe_2O_3 or even lower in combination with higher graded ores could have been used for bloomery iron production (Crew and Charlton 2007; Thiele 2010; Crew et al. 2011). This would imply that all unroasted ore found on archaeological sites as well as samples of ore fragments found in the geological

Table 4
Geochemical contents of major oxides in roasted iron ores from archaeological sites in from Podravina region. All values given in mass. %.

Sample	Location	SiO_2	TiO_2	Al_2O_3	Fe_2O_3	MgO	MnO	CaO	K_2O	Na_2O	P_2O_5	BaO	SrO	LOI	TIC	TOC	Total
H-D 1	Hlebine–Dedanovice	4.17	0.01	0.59	84.94	0.11	0.33	0.63	0.09	0.01	0.38	0.01	<0.01	3.19	0.13	0.13	94.46
H-D 2		5.64	0.02	1.20	84.97	0.10	0.37	0.33	0.18	0.01	0.36	0.01	<0.01	2.83	0.15	0.12	96.02
H-D 3		6.75	0.02	1.28	83.17	0.13	0.77	0.43	0.22	0.09	0.69	0.05	<0.01	4.55	0.16	0.12	98.15
H-D 4		5.63	0.03	1.15	82.93	0.15	0.63	0.49	0.18	0.01	0.44	0.02	<0.01	3.13	0.03	0.3	94.79
H-VH 1	Hlebine–Velike Hlebine	16.74	0.13	3.08	73.20	0.26	0.06	0.47	0.58	0.29	0.65	0.01	<0.01	2.39	*	*	97.86
H-VH 2		6.54	0.03	1.19	76.16	0.08	0.02	0.30	0.23	0.11	0.44	<0.01	<0.01	11.60	0.06	1.3	96.70
H-VH 3		23.08	0.25	4.44	61.56	0.39	0.10	0.53	0.76	0.41	0.40	0.02	<0.01	6.98	*	*	98.92
V-S 2	Virje–Sušine	49.18	0.91	11.65	20.78	0.50	3.87	0.84	1.79	0.44	2.48	0.17	0.02	7.99	*	*	100.62
V-S 3		46.87	0.88	9.86	21.51	0.33	5.49	0.35	1.38	0.34	1.59	0.42	0.01	6.51	<0.02	0.22	95.54
V-S 4		62.67	0.89	14.62	8.44	1.25	0.15	1.13	2.29	1.25	1.74	0.07	0.02	5.70	0.03	0.3	100.22
V-S 5		49.36	0.92	11.29	19.65	0.74	4.80	1.37	2.09	0.46	2.68	0.15	0.02	6.82	0.08	0.49	100.35
V-S 6		29.88	0.45	7.28	45.57	0.45	0.36	0.87	1.10	0.34	0.91	0.04	<0.01	9.79	*	*	97.04
KI-LP 2	Koprivnički Ivanec–Log Parag	50.85	1.05	15.27	16.92	0.76	3.42	0.66	2.50	0.62	2.33	0.10	0.01	6.36	<0.02	0.28	100.85

* Sample volume too small to conduct all analyses.

investigation could have been used for bloomery iron production, although these cannot be considered high quality ores as the majority of samples have a low iron content between 37 and 49 mass. % Fe_2O_3 and rarely 68–70 mass. % Fe_2O_3. For the same reason, the quality of the final product and whether low-grade ores were utilized remains questionable.

5.2. Roasted iron ores characteristics in the study area

Samples of roasted bog iron ore originate from several excavated archaeological sites in the region (Hlebine–Dedanovice, Hlebine–Velike Hlebine, Virje–Sušine and Koprivnički Ivanec–Log Parag). These iron ores are considered to have been subjected to heat treatment (roasting) as a part of the preparation process for bloomery smelting. At the Hlebine–Velike Hlebine site, several shallow circular pits with a burnt bottom layer were identified and could be interpreted as roasting hearths. Experimental reconstruction of roasting hearths and roasting procedures from the site showed that the maximum range of temperatures reached was between 299 and 1038 °C, with an average temperature between 500 and 650 °C during six hours of roasting (Karavidović, 2020). During this kind of iron ore heat treatment, new Fe oxides form as primary by-products of Fe-oxyhydroxide roasting. Low TIC and TOC values are characteristic of roasted iron ores, where organic matter is mostly combusted when exposed to high temperatures (Rzepa et al., 2016). Hematite is the most common Fe phase, directly transforming from goethite (Cudennec and Lecerf, 2005). Magnetite can also be found in bog iron ores as a product of bacterial mineralization (Fassbinder et al., 1990), but is also considered to have been formed by roasting the iron ores with a lower air supply (Manasse and Mellini, 2002). Maghemite forms either through oxidation of magnetite, or by heating (300–425 °C) of other Fe oxides in the presence of organic compounds (Scheinost, 2005). Cudennec and Lecerf (2005) concluded that maghemite formed upon heating lepidocrocite (γ-FeOOH) at temperatures between 200 and 270 °C. At higher temperatures (above 600 °C), maghemite is known to transform to hematite (Fang et al., 2003). Quartz (or modification of quartz) is also present in the roasted iron ores, since it decomposes at temperatures above 1500 °C, while clay minerals are present in lower concentrations, due to roasting decomposition and preprocessing (washing) of the ore.

As is the case with unroasted bog iron ore, iron and silicon are the main components in roasted ores. Strong local and temporal differentiation is noticeable when regarding the Fe_2O_3 contents. Increased manganese contents occurring in roasted iron ores from Virje–Sušine site point to localised bog iron ore exploitation from the Virje–Sušine and nearby Novigrad Podravski–Milakov Berek sites. In both sites, samples tend to have increased Mn contents, indicating a possible local geochemical variation of bog ores with an elevated Mn content and mutual connection between the samples and sites. As bog iron ores tends to be enriched with Mn and P, the same enrichment is to be expected in the roasted ores (Thelemann et al., 2017).

The process of iron ore roasting is conducted for two main reasons; the mineral transformation of oxyhydroxides and non-oxide ores into oxides, which increases the Fe content, and to make the roasted ores more porous, and thus more supple for smelting (Pleiner, 2000). Samples from both Hlebine sites have Fe concentrations that exceed those of all the bog iron ore samples. On the other hand, the majority of samples from Virje–Sušine and the sample from Koprivnički Ivanec–Log Parag have extremely low Fe contents (from 8 to 21 mass. % Fe_2O_3), which poses the question of the quality and usefulness of these roasted ore samples. Samples of unroasted (V–S 1) and roasted ores from Virje–Sušine (V–S 5, 6) were found in the same archaeological context, in a layer of iron production waste (SU 314) in what can be interpreted as a waste discarding area. On the one hand, there is a possibility that these ores were not meant to be smelted and were discarded together with the smelting waste, which could be implied by the context and a noticeable difference in visual appearance of the samples (darker tonnes, lower density). On the other hand, an unroasted sample from the same

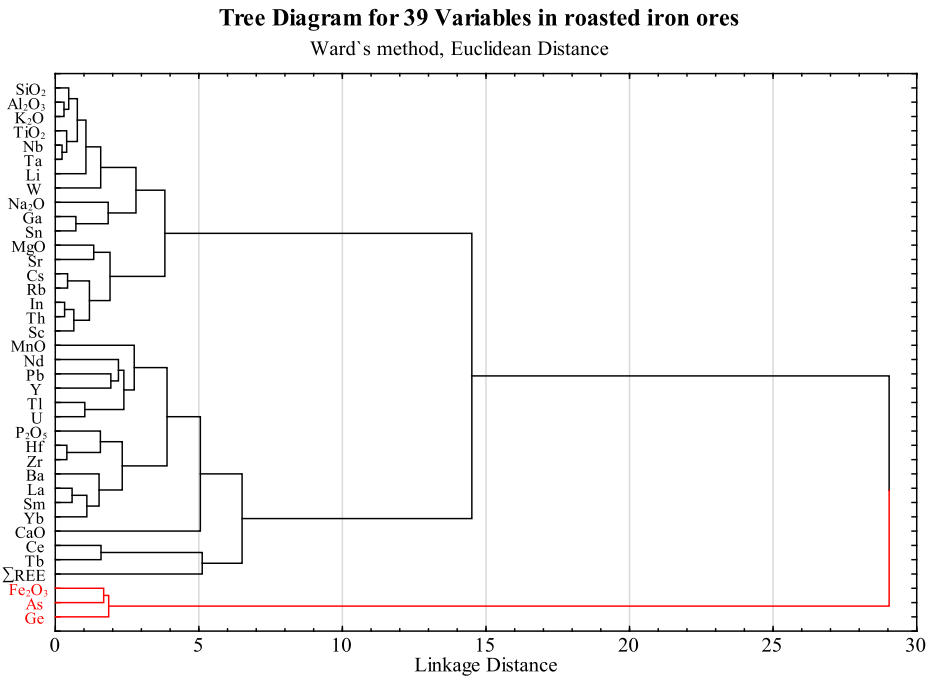

Fig. 5. Hierarchical cluster analysis in roasted iron ores.

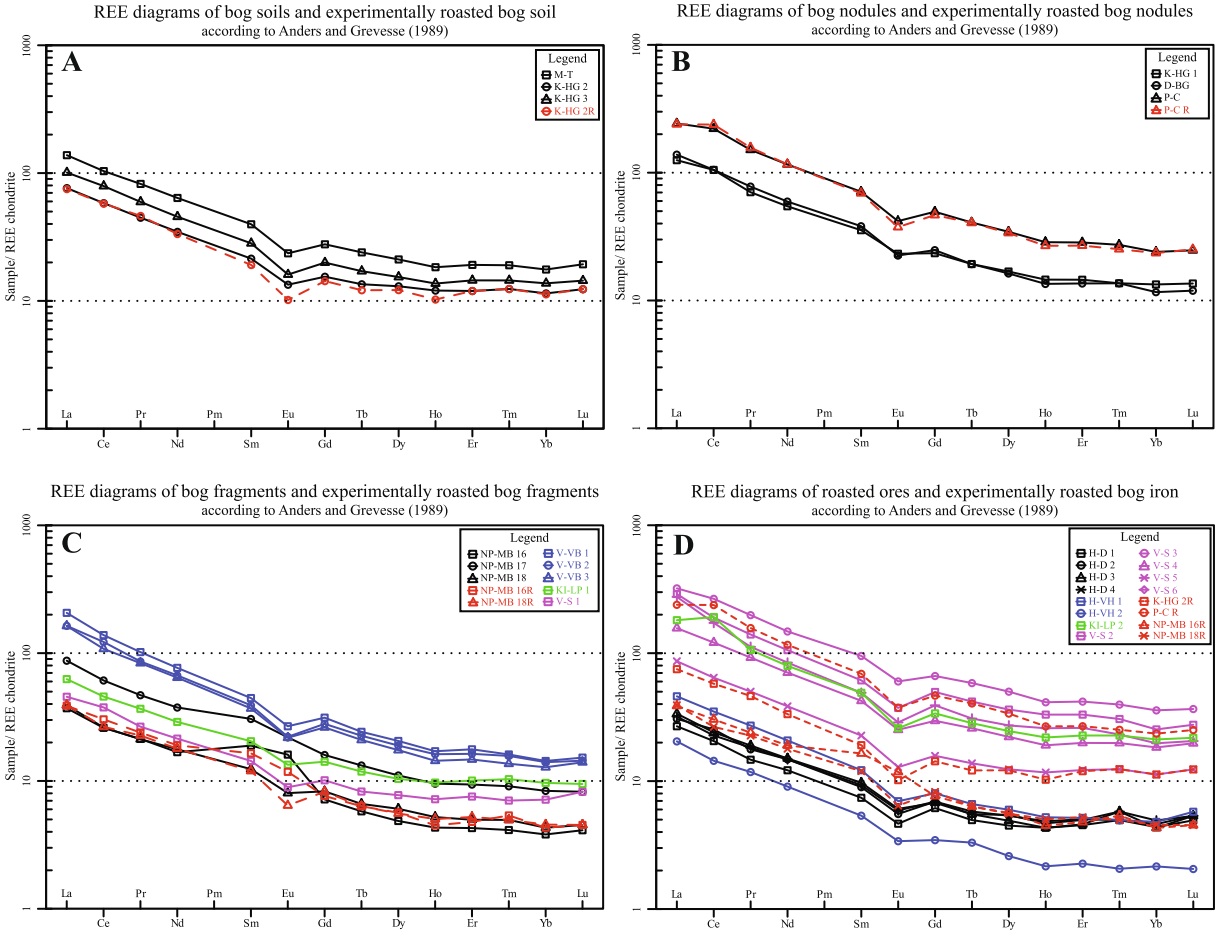

Fig. 6. Chondrite-normalized REE patterns of a) bog iron soils, b) bog iron nodules, c) bog iron fragments and d) roasted iron ores. The red line in each diagram represents experimentally roasted bog iron ores pattern. (For interpretation of the references to colour in this figure legend, the reader is referred to the web version of this article.)

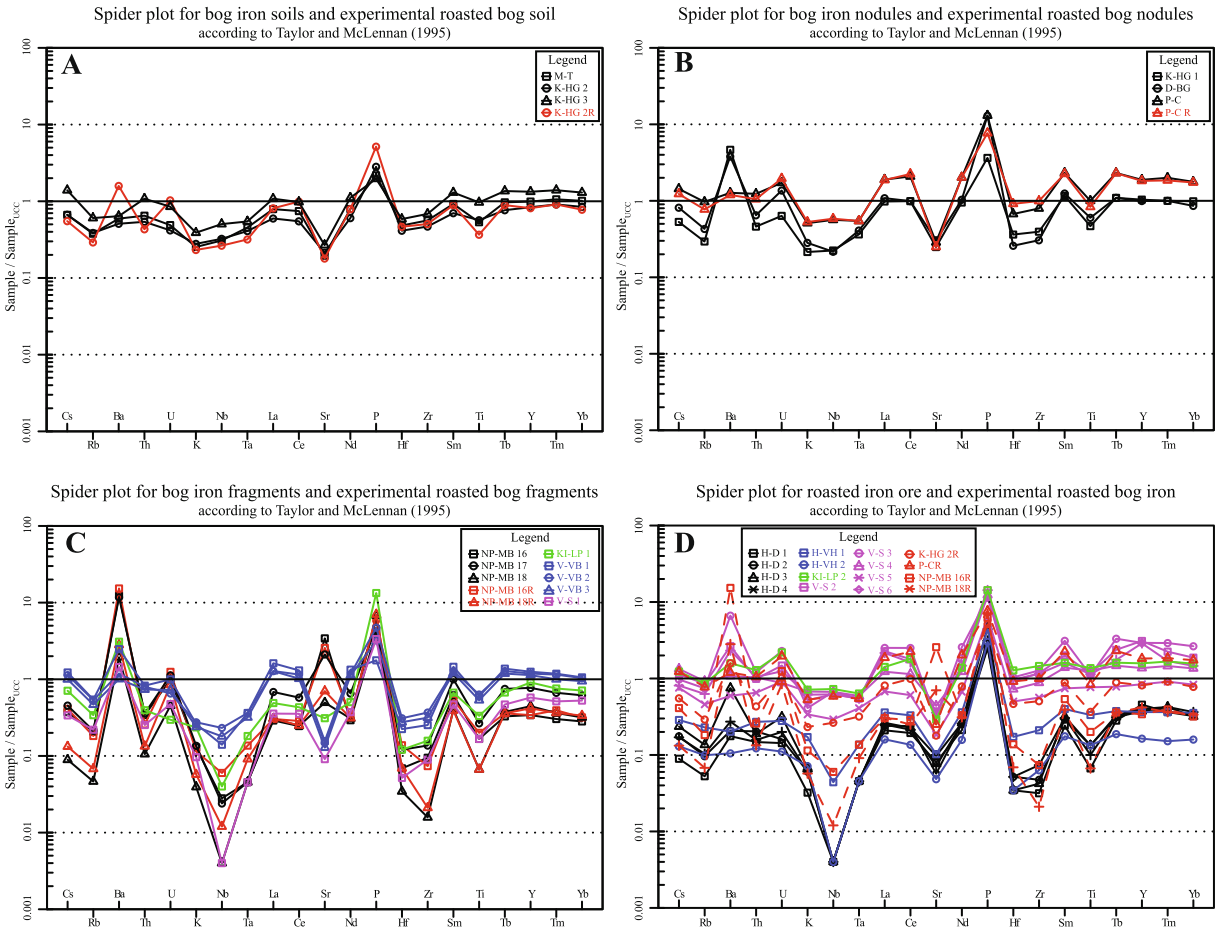

Fig. 7. Upper Continental Crust-normalized REE and microelemental patterns of a) bog iron soils, b) bog iron nodules, c) bog iron fragments and d) roasted iron ores. The red line in each diagram represents experimentally roasted bog iron ores pattern. (For interpretation of the references to colour in this figure legend, the reader is referred to the web version of this article.)

archaeological context has a high iron concentration and, generally, all the samples (unroasted and roasted) from the Virje sites have more variable and lower iron contents than the rest of the analysed samples. Also, it is to be expected that discrimination (if carried out) of ores was done prior to roasting. Ores with a lower iron concentration could have been used in combination with higher quality ore in the same smelting process as has been tested experimentally (Crew et al. 2011).

5.3. Correlation between the bog ores and roasted ores in the Podravina region

Macro-, micro-, and REEs behaviour in bog iron ores and roasted iron ore was analysed to establish the geochemical and genetic connection between them. The data set compiled during this study still falls short on two key requirements. The first major issue is the lack of bog iron ore findings from all the archaeological sites where roasted iron ores were discovered. This is due to the previously mentioned climate and anthropological changes in the environment (Thelemann et al., 2017; Brenko et al., 2020). Secondly, an insufficient number of samples was analysed to provide completely statistically reliable data sets. Nonetheless, an attempt was made to correlate the bog iron ores and the roasted iron ores of the Podravina region.

Determining the source material for iron production in the Podravina region was based on the following two main approaches: hierarchical clustering analysis and plotting of REEs and microelements. Hierarchical clustering was carried out to observe the correlation between the iron component of bog and roasted iron ores with other major oxides, micro- and REEs. According to Laveuf and Cornu (2009), secondary minerals found in soil, such as Fe- and Mn- oxyhydroxides, clay minerals, and resistant and relict rock-forming minerals are the main sinks of REEs.

The constructed dendrograms show that Fe and Mn were transported into the system as secondary phases, as they show distant clustering and correlation to other elements. Based on bog iron formation theory (Banning et al., 2013; Ramanaidou and Wells, 2014; Thelemann et al., 2017), where iron and other accompanying redox-sensitive elements are transported via groundwater close to the surface, where a higher oxygen concentration enables their oxidation and precipitation, such clustering of geochemical data is to be expected. Based on data clustering, the REE contents in bog iron ores were inherited from soils and clay minerals in the soil in which the ores were formed, giving a geographical signature of the ores that can be traced into the roasted ores.

The normalized REE patterns between different bog iron ore types are generally identical in their shape, implying a similar genetic origin. Some variation in REE behaviour can be seen in bog iron fragments, notably in sample NP-MB 16, which shows a positive Eu anomaly. This positive anomaly is due to the incorporation of Eu^{3+} into calcite, a mineral found in veins throughout the sample. Several studies (Lakshtanov and Stipp, 2004; Hellebrandt et al., 2017) suggest that Eu^{2+} and Eu^{3+} can be incorporated into a calcite structure, both as structural substitution of Ca^{2+} or by forming inner -sphere sorption species. Experimentally roasted bog iron ores show similar trends when compared to non-treated bog iron samples, with slight changes in some elements, mostly Eu, probably due to the nature of the element. As Eu^{2+} and Eu^{3+} have different charges and ionic radii, they partition differently between phases (e.g., minerals, melts and vapours), so that the ratio of Eu concentrations relative to the neighbouring REE (Sm and Gd)

depends on the redox conditions during the fractionation process.

Good quality roasted iron ores (with higher Fe content) from both Hlebine sites tend to have a lower REE content, which can stem from the ore pre-processing. Before roasting, bog iron ores could have been washed in local streams to remove gangue material such as clay, thus enriching the ore (Pleiner, 2000). As clay matter contains the majority of the REE signature, washing the ore would have removed a significant proportion of the REE.

To confirm geochemical connection between the bog iron ores and roasted iron ores, diagrams with normalization to Upper Continental Crust (Taylor and McLennan, 1995) were constructed. This normalization uses both microelements and REE. As included microelements tend to have higher mobility than REEs in soils, certain degree of differences is to be expected among the samples. However, normalized patterns of microelements and REEs are similar in shape, with certain key elements having characteristic positive and negative distribution anomalies. This includes positive P and Sm anomalies, with negative Rb and Ti anomalies, giving characteristic shape on the diagrams.

Another characteristic element useful for tracing geochemical origin of bog iron ores is Ba. Based on SEM-EDS analysis, Ba is closely related to Mn phase. As seen in Fig. 7, Ba is ranging from no enrichment to medium enrichment in bog iron fragments, and from depletion up to slight enrichment in roasted ores. This element could be used in further studies when observing iron slags from the study areas to give a more precise information on the locations of bog iron ore exploitation. As determined by archaeological surveys, bog iron was mined locally, with bog iron ore having slightly different characteristics based on the Eh/pH conditions during formation. Therefore, it is to be expected that Mn enriched bog iron ore will carry its geochemical signature (enriched Ba) through roasted ores and eventually into iron slags.

6. Conclusion

In the study area of the Podravina region, different types of bog iron ores and roasted iron ores were discovered in archaeological and geological investigations. Detected bog iron ores occur in the large area of the Drava River alluvial floodplain. Three different types of bog iron ores were recognized: bog iron soils, bog iron nodules and bog iron fragments. Each type is characterized by goethite as the main Fe mineral and a varying iron-silicon ratio, increasing from the soils to the fragments, indicating different types in the bog iron ore formation phases. Based on the ratios, the Fe content and availability, it is believed that only the bog iron fragments were used for iron production. Ore fragments from the Novigrad Podravski–Milakov Berek site imply locally different Eh-pH conditions that led to the Mn enrichments found in the samples from that site. The dendrogram indicates that Fe, Mn, and other redox-sensitive elements were transported into the soil system via groundwater and have no control on the primary REE and microelemental geochemical signature.

The analysed roasted iron ores contain several Fe minerals, commonly hematite, magnetite and maghemite, pointing to roasting temperatures between 300 and 1000 °C, and possibly different preprocessing at different sites. Variable contents of Fe and other elements in the roasted iron ores points to local and temporal variability in the used bog iron ores. Roasted ores from the Virje–Sušine site, where samples with Mn enrichment were found, point to a local exploration of bog iron ores because samples of bog iron ores from the nearby Novigrad Podravski–Milakov Berek site also have high enrichment of Mn. The hierarchical clustering analysis of roasted iron ores revealed similar clustering compared to the bog iron ores, where Fe shows distant correlation to the REEs.

Normalization and plotting of diagrams revealed similar patterns in both bog iron ores and roasted iron ores, indicating that samples are of the same regional origin. This proves that bog iron ores found on archaeological sites related to bloomery iron production, dated to late Antiquity and the early Middle Ages were locally exploited as source material for iron production in the Podravina region.

Declaration of Competing Interest

The authors declare that they have no known competing financial interests or personal relationships that could have appeared to influence the work reported in this paper.

Acknowledgment

This work has been fully supported by the Croatian Science Foundation under the project TransFER - Iron production along the Drava River in the Roman period and the Middle Ages: Creation and transfer of knowledge, technologies and goods (Grant No. 5047). We would like to thank our project partners from The Institute of Archaeology and City Museum of Koprivnica, whose continuous fieldwork led to archaeological discoveries of iron production culture in the Podravina region. We would also like to thank Kristina Šarić and Aleksandar Pačevski (University of Belgrade), who supported the SEM-EDS analyses.

Appendix A. Supplementary data

Supplementary data to this article can be found online at https://doi.org/10.1016/j.catena.2021.105353.

References

Anders, E., Grevesse, N., 1989. Abundances of the elements: meteoric and solar. Geochim. Cosmochim. Acta 53, 197–214. https://doi.org/10.1016/0016-7037(89)90286-X.

Atta, S.K., Mohammed, S.A., Van Cleemput, O., Zayed, A., 1996. Transformations of iron and manganese under controlled Eh, Eh-pH conditions and addition of organic matter. Soil Technol. 9, 223–237. https://doi.org/10.1016/S0933-3630(96)00013-X.

Banning, A., 2008. Bog iron ores and their potential role in arsenic dynamics: an overview and a „Paleo Example".Eng. Life Sci. 8, 641–649. https://doi.org/10.1002/elsc.200800014.

Banning, A., Rude, T.R., Dolling, B., 2013. Crossing redox boundaries – aquifer redox history and effects on iron mineralogy and arsenic availability. J. Hazard. Mater. 15, 905–914. https://doi.org/10.1016/j.jhazmat.2012.12.015.

Bašić, F., 2013. The Soils of Croatia. World Soils Book Series. Springer Science+Business Media, Dordrecht, p. 179p.

Blakelock, E., Martinón-Torres, M., Veldhuijzen, H.A., Young, T., 2009. Slag inclusions in iron objects and the quest for provenance: an experiment and a case study. J. Archaeol. Sci. 36, 1745–1757. https://doi.org/10.1016/j.jas.2009.03.032.

Brenko, T., Borojević Šoštarić, S., Ružičić, S., Sekelj Ivančan, T., 2020. Evidence for the formation of bog iron ores in the soils of the Podravina region, NE Croatia: geochemical and mineralogical study. Quat. Int. 536, 13–29. https://doi.org/10.1016/j.quaint.2019.11.033.

Bricker, O.P., Newell, W.L., Simon, N.S., 2003. Bog iron formation in the Nassawango watershed, Maryland. Gordon Conf. Catchment Sci.: Interact. Hydrol., Biol. Geochem. 7, 13–23. https://doi.org/10.2495/GEO040021.

Brkić, Ž., Briški, M., 2018. Hydrogeology of the western part of the Drava Basin in Croatia. J. Maps 14, 173–177. https://doi.org/10.1080/17445647.2018.1445043.

Brkić, Ž., Larva, O., Urumović, K., 2010. The quantitative status of the groundwater in alluvial aquifers in northern Croatia. Geol. Croat. 63, 283–298. https://doi.org/10.4154/GC.2010.23.

Charlton, M.F., Blakelock, E., Martinón-Torres, M., Young, T., 2012. Investigating the production provenance of iron artifacts with multivariate methods. J. Archaeol. Sci. 39, 2280–2293. https://doi.org/10.1016/j.jas.2012.02.037.

Crew, P., Charlton, M., 2007. The anatomy of a furnace... and some of its ramifications. In: La Niece, S., Hook, D., Craddock, P. (Eds.), Metals and Mines: Studies in Archaeometallurgy. Archetype Publications/British Museum, London, pp. 219–225.

Crew, P., Charlton, M., Dillmann, P., Fluzin, P., Salter, C., Truffaut, E. 2011. Cast iron from a bloomery furnace. In: Hošek, J., Cleere, H., Mihok, L. (Eds.), The Archaeometallurgy of Iron - Recent Developments in Archaeological and Scientific Research. Prague, pp. 237–262.

Cudennec, Y., Lecerf, A., 2005. Topotactic transformations of goethite and lepidocrocite into hematite and maghemite. Solid State Sci. 7, 520–529. https://doi.org/10.1016/j.solidstatesciences.2005.02.002.

De Geyter, G., Vandengerghe, R.E., Verdonck, L., Stoops, G., 1985. Mineralogy of holocene bog-iron ore in northern Belgium. Neues Jahrb. für Mineral. Abh. 153, 1–17. http://geoprodig.cnrs.fr/items/show/179216.

Devos, W., Senn-Luder, M., Moor, C., Salter, C., 2000. Laser ablation inductively coupled plasma mass spectrometry (LA-ICP-MS) for spatially resolved trace analysis of early-medieval archaeological iron finds. Int. J. Anal. Chem. 366, 873–880. https://doi.org/10.1007/s002160051588.

Fang, J., Kumbhar, A., Zhou, W.L., Stokes, K.L., 2003. Nanoneedles of maghemite iron oxide prepared from a wet chemical route. Mater. Res. Bull. 38, 461–467. https://doi.org/10.1016/S0025-5408(02)01066-8.
Fassbinder, J., Stanjekt, H., Vali, H., 1990. Occurrence of magnetic bacteria in soil. Nature 343, 161–163. https://doi.org/10.1038/343161a0.
Gasparatos, D., Tarenidis, D., Haidouti, C., Oikonomou, G., 2005. Microscopic structure of soil Fe-Mn nodules: environmental implications. Environ. Chem. Lett. 2, 175–178. https://doi.org/10.1007/s10311-004-0092-5.
Gasparatos, D., Massas, I., Godelitsas, A., 2019. Fe-Mn concretions and nodules formation in redoximorphic soils and their role on soil phosphorous dynamics: Current knowledge and gaps. Catena 182, 104106. https://doi.org/10.1016/j.catena.2019.104106.
Head, M.J., 2019. Formal subdivision of the quaternary system/period: present status and future directions. Quat. Int. 500, 32–51. https://doi.org/10.1016/j.quaint.2019.05.018.
Hellebrandt, S.E., Hofmann, S., Jordan, N., Barkleit, A., Schmidt, M., 2017. Incorporation of Eu(III) into calcite under recrystallization conditions. Sci. Rep. 6, 33137. https://doi.org/10.1038/srep33137.
Janoušek, V., Farrow, C.M., Erban, V., 2006. Interpretation of whole-rock geochemical data in igneous geochemistry: introducing Geochemical Data Toolkit (GCDkit). J. Petrol. 47 (6), 1255–1259. https://doi.org/10.1093/petrology/egl013.
Kaczorek, D., Sommer, M., 2003. Micromorphology, chemistry and mineralogy of bog iron ores from Poland. Catena 54, 393–402. https://doi.org/10.1016/S0341-8162(03)00133-4.
Kaczorek, D., Zagórski, Z., 2007. Micromorphological characteristics of the bsm horizon in soils with bog iron ore. Polish J. Soil Sci. 40, 81–87.
Karavidović, T. 2020. Rekonstrukcija postupka prženja rude: eksperimentalni pristup (Reconstruction of the ore roasting process: experimental approach). In: Vitezović, S., Antonović, D., Šarić, K. (Eds), Aktuelna interdisciplinarna istraživanja tehnologije u arheologiji Jugoistočne Europe, Zbornik radova prvog skupa sekcije za arheometriju, arheotehnologiju i eksperimentalnu arheologiju Srpskog arheološkog društva, Beograd, pp. 130–137.
Kopić, J., Loborec, J., Nakić, Z., 2016. Hydrogeological and hydrogeochemical characteristics of a wider are of the regional well field Eastern Slavonia – Sikirevci. Rud. Geolosko Naft. Zb. 31, 47–66. https://doi.org/10.17794/rgn.2016.3.4.
Lakshtanov, L.Z., Stipp, S.L.S., 2004. Experimental study of europium (III) coprecipitation with calcite. Geochim. Cosmochim. Acta 68, 819–827. https://doi.org/10.1016/j.gca.2003.07.010.
Lambers, H., Mougel, C., Jaillard, B., Hinsinger, P., 2009. Plant-microbe-soil interactions in the rhizosphere: an evolutionary perspective. Plant Soil 321, 83–115. https://doi.org/10.1007/s11104-009-0042-x.
Landuydt, C.J., 1990. Micromorphology of iron minerals from bog ores of the Belgian Campine area. Dev. Soil Sci. 19, 289–294. https://doi.org/10.1016/S0166-2481(08)70340-4.
Laveuf, C., Cornu, S., 2009. A review on the potentiality of Rare Earth Elements to trace pedogenetic processes. Geoderma 154, 1–12. https://doi.org/10.1016/j.geoderma.2009.10.002.
Leroy, S., Cohen, S.X., Verna, C., Gratuze, B., Téreygeol, Fluzin, P., Bertrand, L., Dillmann, P., 2012. The medieval iron market in Ariège (France). Multidisciplinary analytical approach and multivariate analyses. J. Archaeol. Sci. 39, 1080–1093. https://doi.org/10.1016/j.jas.2011.11.025.
Lóczy, D., Dezső, J., Czigány, S., Gyenizse, P., Pirkhoffer, E., Halász, A. 2014. Rehabilitation potential of the Drava River floodplain in Hungary. In: Conference Paper. doi: 10.13140/2.1.4324.4802.
Manasse, A., Mellini, M., 2002. Chemical and textural characterization of medieval slags from the Massa Marittima smelting sites (Tuscany, Italy). J. Cult. Herit. 3, 187–198. https://doi.org/10.1016/S1296-2074(02)01176-7.
Migaszewski, Z.M., Gałuszka, A., Dołęgowska, S., 2016. Rare earth and trace element signatures for assessing an impact of rock mining and processing on the environment: Wiśniówka case study, south-central Poland. Environ. Sci. Pollut. Res. 23, 24943–24959. https://doi.org/10.1007/s11356-016-7713-y.
Mihajlović, J., Bauriegel, A., Stärk, H.-J., Roßkopf, N., Zeitz, J., Milbert, G., Rinklebe, J., 2019. Rare earth elements in soil profiles of various ecosystems across Germany. App. Geochem. 102, 197–217. https://doi.org/10.1016/j.apgeochem.2019.02.002.
Palumbo, B., Bellanca, A., Neri, R., Roe, M.J., 2001. Trace metal partitioning in Fe-Mn nodules from Sicilian soils. Italy. Chem. Geol. 173, 257–269. https://doi.org/10.1016/S0009-2541(00)00284-9.
Pleiner, R. 2000. Iron in archaeology. The European Bloomery Smelters. Archeologický ústav AV CR, Prague.
Ramanaidou, E., Wells, M.A., 2014. 13.13 - Sedimentary hosted iron ores. In: Holland, H. D., Turekian, K.K. (Eds.), Treatise on Geochemistry, 2nd ed. Elsevier, Oxford, pp. 313–355. https://doi.org/10.1016/B978-0-08-095975-7.01115-3.
Rzepa, G., Bajda, T., Gaweł, A., Debiec, K., Drewniak, L., 2016. Mineral transformations and textural evolution during roasting of bog iron ores. J. Therm. Anal. Calorim. 123, 615–630. https://doi.org/10.1007/s10973-015-4925-1.
Scheinost, A.C., 2005. Metal oxides. In: Hillel, D. (Ed.), Encyclopedia of Soils in the Environment. Elsevier, Oxford, pp. 425–438. https://doi.org/10.1016/B0-12-348530-4/00194-6.
Schwab, R., Heger, D., Höppner, B., Pernicka, E., 2006. The provenance of iron artefacts from Manching: a multi-technique approach. Archaeometry 48, 433–452. https://doi.org/10.1111/j.1475-4754.2006.00265.x.
Sekelj Ivančan, T., 2014. Četvrta sezona arheoloških istraživanja nalazišta Virje – Volarski breg/Sušine. Annales Instituti Archaeologici 10, 99–103.
Sekelj Ivančan, T., 2017b. Ranosrednjovjekovni objekt na Sušinama u Virju. Cris, Časopis Povijesnog društva Križevci 19, 115–128.
Sekelj Ivančan, T., 2019. Arheološka istraživanja lokaliteta Hlebine-Dedanovice. Annales Instituti Archaeologici 15, 129–135.
Sekelj Ivančan, T., Marković, T. 2017. The primary processing of iron in the Drava River basin during the late Antiquity and the early Middle Ages – the source of raw materials. In: Archaeological Studies: Raw Material Exploitation from Prehistory to the Middle Ages, pp. 143–161.
Sekelj Ivančan, T., Valent, I. 2020, Similarities and differences between 7th and 8th century pottery as shown by archaeological sites in the vicinity of Hlebine, Book of abstracts from the Conference Avars and Slavs, Two sides of a belt strap end: Avars on the north and the south of the Khaganate, Vinkovci 6.-8. 2. 2020, pp. 10.
Sekelj Ivančan, T., Tkalčec, T., 2018. Settlement Continuity at Sušine Site near Virje (North Croatia) throughout the Middle Ages. Konštatínove listy 11, 35–66.
Sekelj Ivančan, T., Valent, I., 2017. Ostaci talioničke radionice na lokalitetu Hlebine-Velike Hlebine. Annales Instituti Archaeologici 13, 73–76.
Sekelj Ivančan, T. 2017, Ranosrednjovjekovno naselje na Volarskom bregu u Virju. In: Sekelj Ivančan, T., Tkalčec, T., Krznar, S., Belaj, J. (Eds.), Zbornik Instituta za arheologiju, vol. 6. Zagreb 2017, pp. 111–129.
StatSoft, Inc. 2012. Electronic Statistics Textbook. Tulsa, OK: StatSoft. Available form: <http://www.statsoft.com/textbook/>.
Stoops, G., 1983. SEM and light microscopic observations of minerals in bog-ores of the Belgian Campine. Geoderma 30, 179–186. https://doi.org/10.1016/0016-7061(83)90065-4.
Taylor, S.R., McLennan, S.M., 1995. The geochemical evolution of the continental crust. Rev. Geophys. 33, 241–265. https://doi.org/10.1029/95RG00262.
Thelemann, M., Bebermeier, W., Hoelzmann, P., Lehnhardt, E., 2017. Bog iron ore as a resource for prehistoric iron production in Central Europe – A case study of the Widawa catchment area in eastern Silesia, Poland. Catena 149, 474–490. https://doi.org/10.1016/j.catena.2016.04.002.
Thiele, A., 2010. Smelting experiments in the early medieval fajszi-type bloomery and the metallurgy of iron bloom. Period. Polytech. Mech. Eng. 54, 99–104. https://doi.org/10.3311/pp.me.2010-2.07.
Török, B., Kovács, Á. Gallina, Zs. 2015. Ironmetallurgy of the Pannonian Avars of the 7–9th century based on excavations and material examinations. Der Anscnhitt 26, 229–237.
Török, B., Kovács, Á., 2010. Crystallization of Iron Slags Found in Early Medieval Bloomery Furnaces. Mater. Sci. Forum 649, 455–460. https://doi.org/10.4028/www.scientific.net/MSF.649.455.
Valent, I., Zvijerac, I., Sekelj Ivančan, T. 2017. Topografija arheoloških lokaliteta s talioničkom djelatnošću na prostoru Podravine (eng. Topography of Archaeological localities with smelting plants in the area of Podravina). Podravina 16/32, 5–25 (in Croatian).

Paper 3: Brenko, T., Karavidović, T., Borojević Šoštarić, S. & Sekelj Ivančan, T. (2022) The contribution of geochemical and mineralogical characterization of iron slags in provenance studies in the Podravina region, NE Croatia. Geologia Croatica, 75/1.

Geologia Croatica
Journal of the Croatian Geological Survey and the Croatian Geological Society
2022 | 75/1 | – | 4 Figs. | 2 Tabs. | www.geologia-croatica.hr

The contribution of geochemical and mineralogical characterization of iron slags in provenance studies in the Podravina region, NE Croatia

Tomislav Brenko[1,*], Tena Karavidović[2], Sibila Borojević Šoštarić[1] and Tajana Sekelj Ivančan[2]

[1] University of Zagreb, Faculty of Mining, Geology and Petroleum Engineering, Department of Mineralogy, Petrology and Mineral Resources, Pierottijeva 6, 10 000 Zagreb, Croatia; (*corresponding author: tomislav.brenko@rgn.unizg.hr)
[2] The Institute of Archaeology, Jurjevska ulica 15, 10 000 Zagreb, Croatia

doi: 10.4154/gc.2022.11

Article history:
Manuscript received November 15, 2021
Revised manuscript accepted January 05, 2022
Available online January 31, 2022

Keywords: iron production, XRD, ICP-MS/AES, trace elements, NRC ratios, PCA, bog iron ore

Abstract

Archaeological excavations in the Podravina region led to discovery of sites with traces of bloomery iron production during Late Antiquity and the Early Middle Ages. Mineralogical analysis of the slags recognized fayalite as the main mineral phase, while geochemical analysis confirmed high Fe contents, typical for bloomery iron smelting. Based on the previously established occurrences of bog iron ores in the study area, provenance studies were carried out using trace and rare earth elements to create a geochemical signature. Similar shapes and patterns of bog iron ores and iron slag signatures imply a genetic connection between the ore and the slag, as well as variation related to the temporal and spatial context of both slags and ores.

1. INTRODUCTION

In ancient times, iron was one of the most valuable materials, and whole cultures relied upon iron production that was utilised to create an array of different objects. The main method for production of iron in pre-industrial times was the smelting of iron ores via a direct reduction process, in order to obtain an iron bloom. The metallurgical principle in this method relies on the chemical reduction of iron oxide(s) and oxyhydroxide(s) present in the iron ore by carbon or gases formed during smelting (PLEINER, 2000). During the smelting process, carbon monoxide (CO) from charcoal reacts with iron oxide(s)/oxyhydroxide(s) from the ore, forming iron particles and carbon dioxide (CO_2) (CHARLTON et al., 2010). Air could have been blown into a furnace through blowing holes/tuyeres incorporated in the furnace walls to elevate the temperature and improve the bloom formation. Additional material in the form of fluxes could have been added during the process to enhance iron gain and to lower melting temperatures (CHARLTON et al., 2012). Compounds such as silica, aluminium and unreduced iron partition from the iron as a liquid phase solidifying at the bottom of the furnace, forming furnace bottom slag (FBS) or they are discharged from the furnace, forming tap slag (TS) (PORTILLO-BLANCO et al., 2020). Textural characteristics of slag are depended on the cooling conditions, while the mineralogical and geochemical composition of smelting slags depends on the raw material used (ore, charcoal, furnace walls), potential use of flux materials (carbonates) and the way the process was carried out (air input, ratio of ore:charcoal etc.).

In the study area of the Podravina region, several sites with traces of iron production and processing were excavated (SEKELJ IVANČAN & KARAVIDOVIĆ, 2021) while over 150 potential sites were identified through field surveys (VALENT, 2021). Bog iron ores were also detected on some sites within an archaeological context and during surface field surveys (BRENKO et al., 2021), implying that they were potentially utilised for iron production. Iron ores, and especially bog iron ores (KACZOREK & SOMMER, 2003), are never formed purely from iron oxides/oxyhydroxides (RAMANAIDOU & WELLS, 2014), but rather as a combination of iron oxides/oxyhydroxides and aluminosilicate soil phases. The combination of heterogenous iron ore, with the possible addition of flux materials, charcoal and furnace lining during smelting, significantly complicates provenance studies. However, recent studies regarding the usage of major and trace elements (including rare earth elements) indicate the potential for following the geochemical signature from the iron ore to the iron slag (HORST-MADSEN & BUCHWALD, 1999, CREW, 2000; COUSTURES et al., 2003; SCHWAB et al., 2006; DESAULTY et al., 2009). Major element analysis is used as a first discriminator of the smelting process using Non-Reduced Compounds (NRC) ratios (DILLMAN & L'HÉRITIER, 2007). By comparing major element ratios in iron slags, it is possible to distinguish different ore sources. However, NRC ratios are only useful in limited cases when there are some significant differences among the ore deposit sites.

Therefore, special attention must be given to the differentiation of elements between the solid and liquid phases during smelting, especially the trace elements. Trace elements that prefer to remain in the solid phase (bloom) are termed compatible, while trace elements that go into the liquid phase (slag) are termed incompatible, as they are incompatible in the crystal structure and will try to partition at the first available opportunity, i.e. during smelting when high temperatures are introduced into the system (ROLLINSON, 1993). According to studies undertaken by COUSTURES et al. (2003) and DESAULTY et al. (2009), it can be deduced that the majority of incompatible elements will pass into the slag during the smelting process. DESAULTY et al. (2009) concluded that the enrichment factor of incompatible elements is close to their modal factor, meaning that their ratios should remain constant from the ore to the slag. A similar observation was previously made by COUSTURES et al. (2003) where plotting pairs of incompatible elements that have the same number of electrons and an equivalent ionic radius revealed that the incompatible pairs should retain the same ratios between the ore and the slag. Despite the fact that the slag can contain traces of iron particles from the bloom, due to their small size and low

quantities it can be considered that their effect on the overall trace element content in the slag is negligible.

Considering these aspects, this paper has two main aims: (i) defining the mineralogical and geochemical characteristics that can lead to determining temporal and spatial variation in tap and furnace bottom slags from three sites dated to the Late Antiquity and Early Middle Ages and (ii) constructing the geochemical signature of iron slags to compare it to the local bog iron ores. In order to do that, two different slag sample types were analysed using geochemical and mineralogical methods. To establish the provenance of the studied iron slags, the geochemical signature using 26 selected trace elements and rare earth elements (REEs) was established for all slag samples. Geochemical signatures of slags are compared to the geochemical signatures of previously analysed bog iron ores found in the study area (BRENKO et al., 2021).

2. GEOLOGICAL AND ARCHAEOLOGICAL SETTINGS

The archaeological sites related to iron production from which the slag and ore samples originate are dated to the Late Antiquity

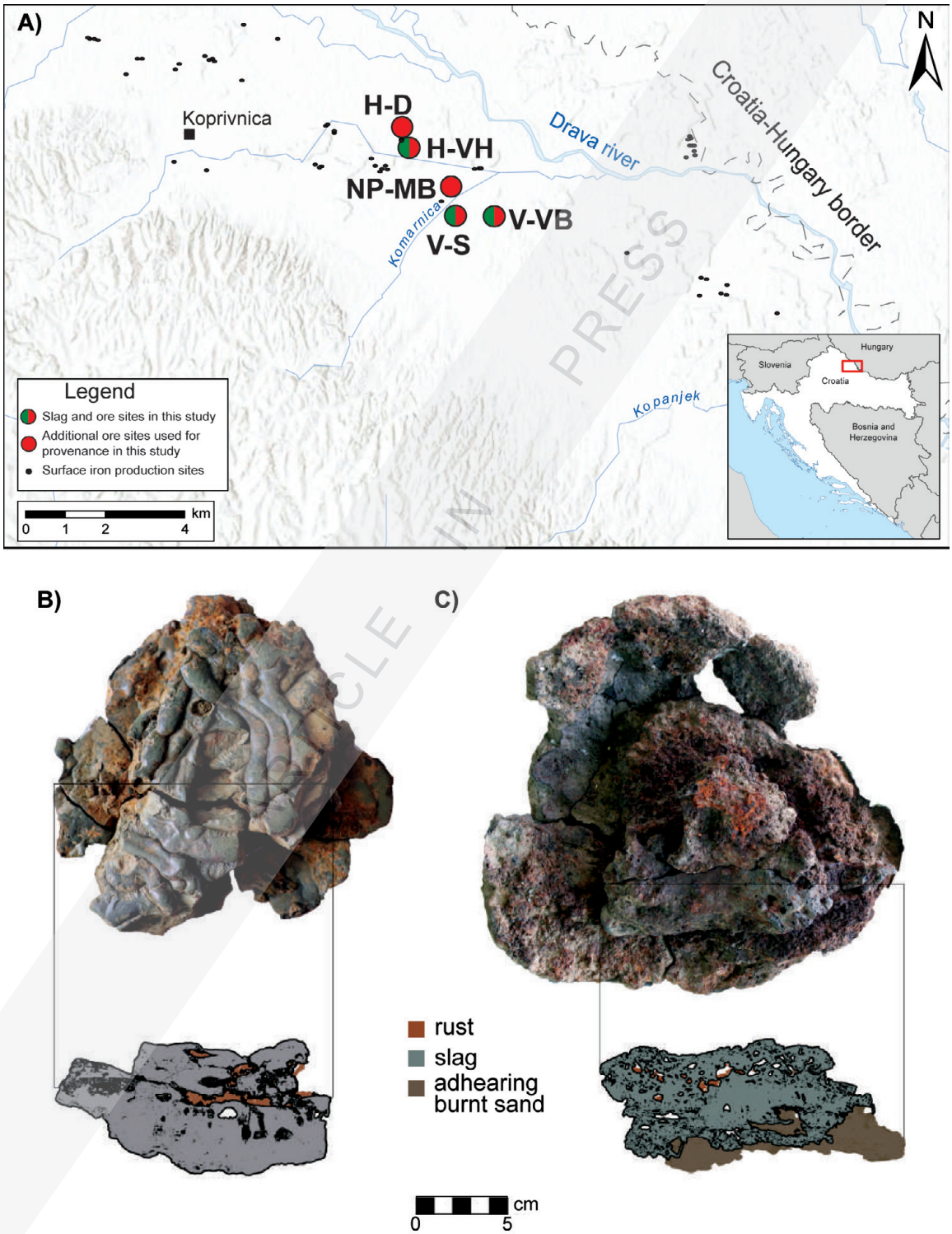

Figure 1. A) Map of the study area with locations of iron slags and iron ores used in this study. Typical morphology of B) tap slags and C) furnace bottom slags in the study area.

and Early Middle Ages, from the 4/5th (Virje-Sušine), 5/6th century (Virje-Volarski breg), as well as to the end of the 6th and mid-7th century (Virje-Sušine, Hlebine-Velike Hlebine) and to the end of the 8th and the beginning of the 9th centuries (Virje-Volarski Breg). Individual sites Virje-Volarski Breg and Virje-Sušine have several positions, where archaeological trenches were set on the basis of prior geophysical research, through which the area saturated with iron production debris was presumed. On all of the excavated positions traces of bloomery iron production workshops (SEKELJ IVANČAN & KARAVIDOVIĆ, 2021) were discovered. The basic technological solution, in terms of the type of furnace used, was similar on all sites. The furnaces were free-standing, with a shallow hearth from which the slag was tapped out during the smelting procedure. The shaft was built entirely of clay, saturated with sand to some degree. The sites are all located in the central part of the lowland Podravina region (Croatia), on a linear distance between 0.7–7 km (Fig. 1). The most prominent geographical feature in the area is the meandering Drava River. Surrounding the river is the low-lying terrain of three alluvial river terraces. The river valley formed during the last Holocene climatic warming period (HEAD, 2019), where constant floods resulted in the deposition of a variety of flood sediments, including gravels, sands and silts (LÓCZY et al., 2014). Hydrological (BRKIĆ et al., 2010; BRKIĆ & BRIŠKI, 2018) and hydrochemical (KOPIĆ et al., 2016) studies discovered that the groundwater table is close to the surface, with the aquifer system often showing elevated contents of iron and manganese. The majority of soils in the study area are determined as Fluvisols and Gleysols (BAŠIĆ, 2013). The combination of shallow groundwater enriched with iron results in the formation of bog iron ore in the study area (BRENKO et al., 2021), a sedimentary accumulation of iron and accompanying elements formed in soils due to the precipitation of iron in intervals with higher oxygen concentration (RAMANAIDOU & WELLS, 2014).

3. MATERIALS AND METHODS

In this study, 33 iron slag samples (Table 1) were selected and analysed. Samples can be categorized in two main slag groups: furnace bottom slags (FBS) and tap slags (TS). From each site,

Table 1. Mineral composition of selected tap slags and furnace bottom slags in the Podravina region. Mineral abbreviations: Ank – ankerite; Dol – dolomite; Fay – fayalite; Gth – goethite; Hem – hematite; Lct – leucite; Mag – magnetite; Pl – plagioclase; Px – pyroxene; Spl – spinel; Wus – wüstite; 10Å/14Å clay – phyllosilicates with 001 peaks at 10 or 14Å.

Sample	Trench / SU / Sample nr.	Site	Age	Fay	Qz	Gth	Hem	Mag	Wüs	Other minerals
H-VH TS 1	1/38B/133	Hlebine – Velike Hlebine	6–7th century	+++	–	–	–	+	+	Spl
H-VH TS 2	1/37A/1/137			+++	?	–	–	–	+	Spl, Dol (?)
H-VH TS 3	1/37A/1/140			+++	?	–	–	–	–	Spl, Dol (?)
H-VH TS 4	2/113/266			+++	+	+	–	–	?	Pl, Stishovite (?)
H-VH TS 5	2/113/270			+++	+	–	–	–	–	Px (?)
H-VH TS 6	2/109-110/251			+++	?	–	–	–	–	Spl
H-VH TS 7	2/109-110/251			+++	?	–	–	–	–	Spl (?)
H-VH TS 8	2/97/98/			+++	+	–	–	–	?	/
H-VH TS 9	2/65/169			+++	–	–	–	–	+	Spl
H-VH FBS 1	1/38A/135			+++	?	?	–	–	+	Spl, Px (?)
H-VH FBS 2	1/37A/144			+++	+	–	–	–	++	/
H-VH FBS 3	1/37A/1/137			+++	+	–	–	–	–	Px, 10Å clay (?)
H-VH FBS 4	1/001/25/36			+++	+	–	–	–	+	Px (?)
V-S TS 1	7/327/432	Virje – Sušine	4–5th century	+++	+	–	–	–	+	Spl
V-S TS 2	7/327/427-1			+++	+	–	–	–	++	Px
V-S TS 3	7/314/295-1			+++	?	–	–	–	++	/
V-S TS 4	7/317/305/			+++	+	–	–	–	++	Px (?)
V-S TS 5	7/314/295-7			+++	?	–	–	–	–	/
V-S TS 6	7/314/295-14			+++	+	–	–	–	+	Spl (?)
V-S FBS 1	5/237/126			++	+	?	–	–	++	Lct
V-S TS 7	5/270/125		6–7th century	+++	+	–	–	–	–	Spl (?), Pl
V-S TS 8	5/217/124			+++	+	?	+	–	–	Pl, Px (?)
V-S TS 9	5/240/115			++	+	–	–	–	–	Px, 10Å clay (?)
V-VB TS 1	3/191/55	Virje – Volarski Breg	5/6–7th century	+++	?	–	–	–	–	Spl (?)
V-VB TS 2	2a/138/140			+++	+	?	–	–	+	Spl
V-VB TS 3	2a/138/140			+++	?	–	–	–	++	Spl
V-VB FBS 1	3/201/74			+++	+	–	–	–	++	Spl, Px (?)
V-VB FBS 2	3/201/80			+++	+	+	–	–	++	Spl, Px (?)
V-VB FBS 3	3/187/54			+++	+	–	–	–	+	Spl, Lct
V-VB FBS 4	3/001/180/56a			+++	?	–	–	–	–	Spl, Lct
V-VB FBS 5	3/001/180/56b			+++	+	+	–	–	++	Px (?)
V-VB FBS 6	2a/173/51			++	?	++	+	–	++	Ank
V-VB FBS 7	1/38/95		8–9th century	++	++	+	–	–	+	Pl, 10Å / 14Å

+ – relative abundance of minerals based on X-ray diffraction (no quantitative value assigned to +); +++ major component, ++ minor component; + traces; ? – not enough diffraction peaks to fully confirm

both slag types were selected and analysed (Fig. 1B and C). The main objective of sample selection was to take into consideration samples from temporally and spatially different sites, as well as samples of different types of slag generated through the bloomery smelting process in order to compare their composition to local bog iron ores from archaeological and/or geological contexts.

In order to acquire a reliable mineralogical and geochemical dataset, a slate from the cross section of each sample was cut using a circular saw. By doing so, homogenization was ensured, and potential sampling of rusted or adhering clayey or sandy materials was avoided. Each slate was air-dried at room temperature for several days, removing excess moisture and then homogenized to powder fraction using a vibratory mill for several minutes in a steel grinding set. The mineralogical composition was determined by X-ray powder diffraction (XRD) using a Phillips vertical X-ray goniometer (type X'Pert) equipped with Cu tube and graphite crystal monochromator. Scan settings were 3–70° 2θ, 0.02° step size, 1 second count time per step while generator settings were 40 kV and 35 mA. Semi-quantitative mineral identification was conducted using PANalytical X'Pert HighScore software with standardised Powder Diffraction Files (PDF) of the International Centre for Diffraction Data (ICDD) (Newton Square, PA, USA) and by comparing peak shapes and heights with internal standards for quartz, feldspars and clay minerals, while fayalite, wüstite and other Fe mineral contents were estimated based on geochemical data. The geochemical composition, including the main oxides, major-, micro- and REEs was determined in MSALabs (Langley, Canada). Multielement contents of trace and REEs were analysed using inductively coupled plasma-mass spectrometry (ICP-MS), while 4-acid digestion including hydrochloric, nitric, perchloric and hydrofluoric acids was used for near total digestion. Only the most highly resistant minerals could possibly remain not fully dissolved. Based on two internal standards, several blanks and duplicates, instrumental precision was between 3–5% and the detection limits for most analysed elements were in the part per million (ppm) or lower bracket. Major oxide contents were determined using inductively coupled plasma-atomic emission spectrometry (ICP-AES) with lithium borate fusion. Loss on ignition (LOI) was determined by weight difference after ignition at 1000 °C.

This approach using trace elements and REEs was undertaken in the provenance studies of iron slags in the Podravina region. Based on the behaviour of the 26 selected elements, it is believed that the geochemical signature of the discovered iron slags could be traced back to ore used for archaeological iron production in the region. To supress the Oddo-Harkins effect and to

Table 2. Chemical composition of selected iron slags in the Podravina region. All values for major oxides and LOI given in mass. %.

Sample	Location	SiO_2	TiO_2	Al_2O_3	Fe_2O_3	MgO	MnO	CaO	K_2O	Na_2O	P_2O_5	LOI
H-VH TS 1	Hlebine - Velike Hlebine	22.52	0.24	4.51	65.36	0.53	0.79	1.09	0.59	0.29	0.67	-5.09
H-VH TS 2		25.16	0.23	4.85	63.15	0.57	0.79	1.63	0.77	0.28	0.59	-5.05
H-VH TS 3		26.51	0.27	5.49	66.40	0.65	0.96	2.24	0.92	0.45	0.66	-5.97
H-VH TS 4		29.84	0.27	5.21	61.13	0.78	2.00	1.99	0.81	0.36	0.83	-1.77
H-VH TS 5		26.30	0.22	4.18	66.46	0.81	1.97	1.84	0.67	0.28	0.81	-4.93
H-VH TS 6		27.36	0.30	6.01	60.45	0.67	1.00	1.45	0.97	0.39	0.77	-5.69
H-VH TS 7		32.57	0.35	6.81	58.85	0.88	1.22	2.51	1.67	0.47	0.68	-4.88
H-VH TS 8		27.63	0.28	5.89	59.60	0.60	1.56	2.49	0.99	0.41	0.78	-5.69
H-VH TS 9		26.80	0.25	5.36	65.15	0.81	1.82	2.32	0.83	0.38	0.96	-6.07
H-VH FBS 1		25.58	0.22	4.61	65.35	0.64	0.85	1.75	0.74	0.28	0.61	-4.96
H-VH FBS 2		22.33	0.21	4.99	62.63	0.53	0.73	2.20	0.97	0.30	0.69	-6.31
H-VH FBS 3		32.57	0.34	6.13	55.47	0.72	0.76	2.00	1.12	0.47	0.62	-3.72
H-VH FBS 4		26.64	0.36	5.10	62.68	0.67	0.45	1.66	1.15	0.51	0.74	-3.14
V-S TS 1	Virje - Sušine	25.20	0.19	4.59	54.43	0.52	0.99	1.25	0.82	0.36	0.88	-6.13
V-S TS 2		29.19	0.29	5.66	63.12	0.72	1.02	3.03	1.07	0.42	0.94	-5.26
V-S TS 3		20.88	0.14	3.74	61.02	0.54	0.64	1.99	0.67	0.29	0.99	-6.35
V-S TS 4		25.91	0.19	4.44	61.29	0.70	0.81	3.05	0.97	0.30	0.78	-5.92
V-S TS 5		35.41	0.38	7.23	58.03	0.72	1.00	1.87	1.28	0.56	0.52	-5.27
V-S TS 6		28.92	0.29	5.72	64.26	0.50	1.09	1.16	0.83	0.47	0.52	-5.77
V-S TS 7		37.28	0.38	7.01	55.98	0.70	1.04	1.47	1.08	0.60	0.58	-4.69
V-S TS 8		34.05	0.38	6.74	56.91	0.93	1.18	3.08	1.08	0.56	0.51	-3.87
V-S TS 9		27.96	0.26	5.45	61.11	0.62	0.92	1.68	0.83	0.44	0.49	-4.28
V-S FBS 1		25.72	0.27	4.59	54.87	0.99	0.53	3.63	2.84	0.34	1.15	-2.08
V-VB TS 1	Virje - Volarski Breg	28.57	0.33	7.89	55.80	0.97	1.52	1.86	1.13	0.41	0.66	-5.12
V-VB TS 2		25.90	0.25	7.26	53.46	0.79	1.09	1.90	1.12	0.34	0.93	-4.32
V-VB TS 3		25.67	0.24	6.68	57.60	0.75	1.26	1.98	1.19	0.36	1.03	-5.36
V-VB FBS 1		21.19	0.22	5.95	55.57	0.86	1.06	2.64	0.77	0.27	1.11	-3.35
V-VB FBS 2		18.55	0.16	4.91	53.23	0.54	0.51	1.58	0.68	0.28	0.87	-2.39
V-VB FBS 3		25.20	0.33	8.03	52.30	1.17	1.36	1.90	0.86	0.38	1.24	-0.52
V-VB FBS 4		23.76	0.30	7.89	54.49	1.11	0.59	2.26	1.16	0.32	0.92	-3.03
V-VB FBS 5		14.56	0.12	4.10	61.34	0.51	0.37	1.53	0.61	0.22	0.65	-2.33
V-VB FBS 6		11.69	0.11	4.34	60.06	0.47	0.31	0.76	0.45	0.10	0.59	4.02
V-VB FBS 7		27.96	0.27	5.03	56.49	0.69	1.06	1.77	1.09	0.43	0.73	-1.34

avoid artificial peaks in the geochemical signature of iron slags, the REEs and trace elements were normalized to Upper Continental Crust (RUDNICK & GAO, 2003) and then plotted on the appropriate diagrams for each archaeological site. Geochemical signatures of bog iron ores are derived from the dataset in BRENKO et al. (2021), where both unroasted and roasted iron ores were analysed. The analysed ores were found in the same archaeological context as iron slags or on temporally and spatially related sites as well as in their natural geological setting, during an archaeological field survey of the wider area around archaeological sites under study (samples from Novigrad Podravski).

4. RESULTS

4.1. Mineralogical and geochemical characteristics of iron slags

Tap slags (TS) tend to be dark grey in colour with high lustre, and occasional signs of porosity. Their upper surface usually contains signs of flow texture due to their previously melted state. Furnace bottom slags (FBS) are also greyish in colour, with parts of samples being red. They tend to be slightly concave in shape due to their position at the bottom of the furnace and usually have higher porosity than TS.

Mineralogically, both TS and FBS samples contain fayalite (Fe_2SiO_4) as the main mineral phase. Besides fayalite, all samples contain quartz in traces to moderate amounts, while wüstite (FeO) also occurs in the majority of samples as either a major or trace component. Other minerals, including iron minerals (magnetite, haematite and goethite) as well as pyroxene, spinel (hercynite) and leucite occur in trace amounts (Table 1). Additionally, slightly elevated background levels, especially noted in the Virje-Volarski breg site, point to the possible occurrence of amorphous matter, such as the glassy slag matrix.

Major oxides composition in the slags mainly consists of Fe_2O_3 ranging from 52.30 - 66.46 mas. % (χ = 59.52 mas. %) and SiO_2 ranging from 11.69 to 37.28 mas. % (χ = 26.22 mas. %) (Table 2). TS and FBS from the Hlebine-Velike Hlebine site have the highest Fe_2O_3 contents, with values between 55.47 - 66.46 mas. % (χ = 62.95 mas. %, n = 13). This is followed by Fe_2O_3 contents in slags from the Virje-Sušine positions, where the contents range from 54.34 - 64.26 mas. % (χ = 59.10 mas. %, n = 10), while slags from the Virje-Volarski Breg positions have the lowest contents, with values between 52.30 - 61.34 mas. % (χ = 56.03 mas. %, n = 10) (Table 2). Only Al_2O_3 with values between 3.74 - 8.03 mas. % (χ = 5.65 mas. %, n = 33) is present in significant quantities at all archaeological sites. Contents of CaO (0.76 – 3.63 mas. %, χ = 1.99 mas. %), MnO (0.31 – 2.00 mas. %, χ = 1.01), K_2O (0.45 – 2.84 mas. %, χ = 0.99 mas. %), P_2O_5 (0.49 – 1.24 mas. %, χ = 0.77 mas. %), MgO (0.47 – 1.17 mas. %, χ = 0.72 mas. %), Na_2O (0.10 – 0.60 mas. %, χ = 0.37 mas. %) and TiO_2 (0.11 – 0.38 mas. %, χ = 0.26 mas. %) are mostly present as minor components (Table 2).

NRC ratios for several major oxides are presented in Fig. 2 and compared with geochemical data from several studies from Croatia and Europe. Biplot diagrams revealed a positive linear correlation in the case of the SiO_2/Al_2O_3 ratio with the Virje-Volarski Breg site standing out due to higher Al contents (Fig. 2A). SiO_2/Fe_2O_3 and Fe_2O_3/MnO ratios show a grouping of data for all sites (Fig. 2B and 2C). Principal component analysis of the major oxide composition in iron slags resulted in ten principal components (PCs). The first principal component accounts for 49.20 % of the total variance with the second PC accounting for 18.90 % and the third for 11.47 % of the total variance (Fig. 3B, 3C). According to the obtained values in principal components, PC 1 particularly represents SiO_2, TiO_2, Al_2O_3, MgO, K_2O and Na_2O, while strongly representing MnO and CaO. PC 2 particularly represents P_2O_5, while Fe_2O_3 is only strongly represented by both PC 2 and PC 3. The resulting scatterplot of PC 1 plotted against PC 2 shows relatively scattered cloud datasets for all study sites (Fig. 3A), although confidence ellipses show some grouping. Samples from Hlebine-Velike Hlebine are grouped together, as all the samples are in relative proximity to one another. Samples from the concurrent Virje-Sušine site are grouped and plotted close to the Hlebine-Velike Hlebine samples. Samples of Virje-Volarski Breg dated to the end of the 5th and into the 6th century are plotted distantly from the first two groups and are widely dispersed. The samples from Virje-Sušine 4-5th century are also widely dispersed and overlap all other datasets.

4.2. Geochemical signature of slags based on trace elements

In order to define the geochemical signature of the iron slags, 26 trace elements and REEs were selected and normalized to the Upper Continental Crust. Apart for several incompatible elements, slag samples from the Hlebine-Velike Hlebine site have an almost identical geochemical signature. Slight variability can be seen in the total trace and REE contents, however, same characteristic peaks are appearing through all samples. These slag samples are compared with roasted ore samples (BRENKO et al., 2021) from the same site i.e. the same archaeological context interpreted as an iron production workshop and from a nearby and contemporary Hlebine-Dedanovice site. For the majority of the ore samples the patterns have similar shapes and peak heights. Some differentiation in ore geochemistry is noticeable, mostly the trace element contents (Cs-K) (Fig. 4A).

Samples from the Virje-Sušine site are divided in two groups, based on the ^{14}C age determined for charcoal samples from two spatially separate positions (BOTIĆ, 2021; Trench 5 and 7), both of which can be interpreted as iron production workshops, dated to the end of 4th and into the 5th century (Trench 7) and to the end of the 6th and into the ½ 7th century (Fig. 4B). These slag samples are compared with samples of natural and roasted bog iron ore found within the archaeological context (Trench 7) and geological samples of bog iron ore from a near-by location of Novigrad Podravski-Milakov Berek (linear distance 200-300 metres). Differentiation can be noted for the same trace elements (Cs-K), however the general shape of the signature is similar, with same peaks appearing as in the case of Hlebine-Velike Hlebine (Fig. 4B). When comparing these archaeological samples with bog iron ores from Novigrad Podravski major differences are seen in both the trace and REEs of the ores, such as Eu and Sm positive anomalies and a strong enrichment of Ba (Fig. 4B).

The Virje-Volarski Breg site is also divided into two groups based on two positions (Trench 2a and 3, Trench 1) where traces of differently dated iron production workshops were found (5/6thcentury and 8th/9th century). The ores used for provenance were discovered in an archaeological context within settlement features (Trench 2b) that can be dated relatively to 8/9th centuries and are spatially connected to both positions (linear distance 45–251 metres). Geochemical signatures of the ores and slags showed a great resemblance. Very small differentiation is present for Ba contents between the ore and slag, while other elements have the same peaks and peak heights (Fig. 4C).

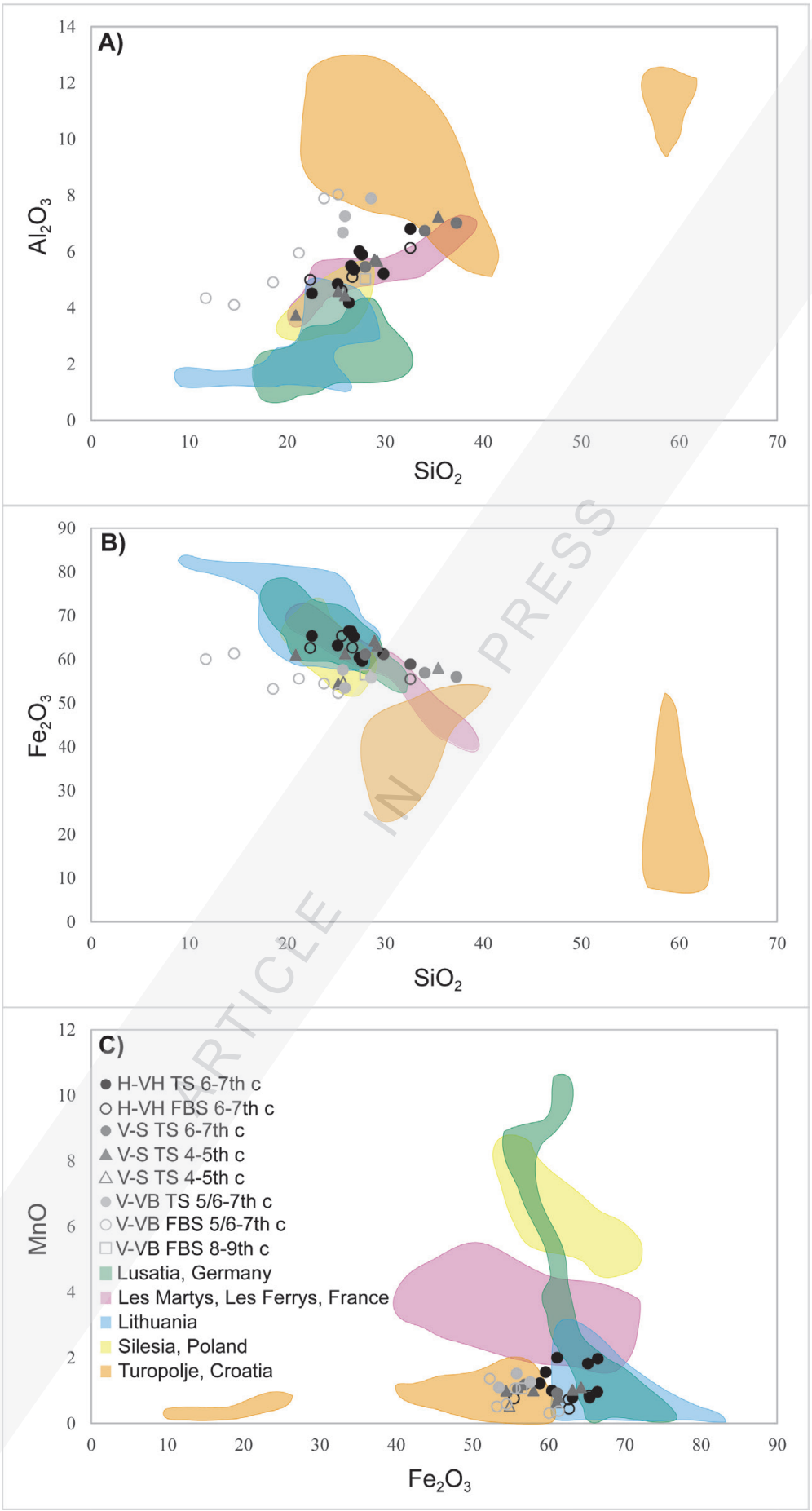

Figure 2. NRC ratios of slag for A) SiO_2/Al_2O_3, B) Fe_2O_3/SiO_2 and C) Fe_2O_3/MnO compared to other case studies in Croatia and Europe (according to HEIMANN et al., 2001; COUSTURES et al., 2003; SELSKIENE, 2007; THELEMANN et al., 2017 and NEMET et al., 2018).

A)

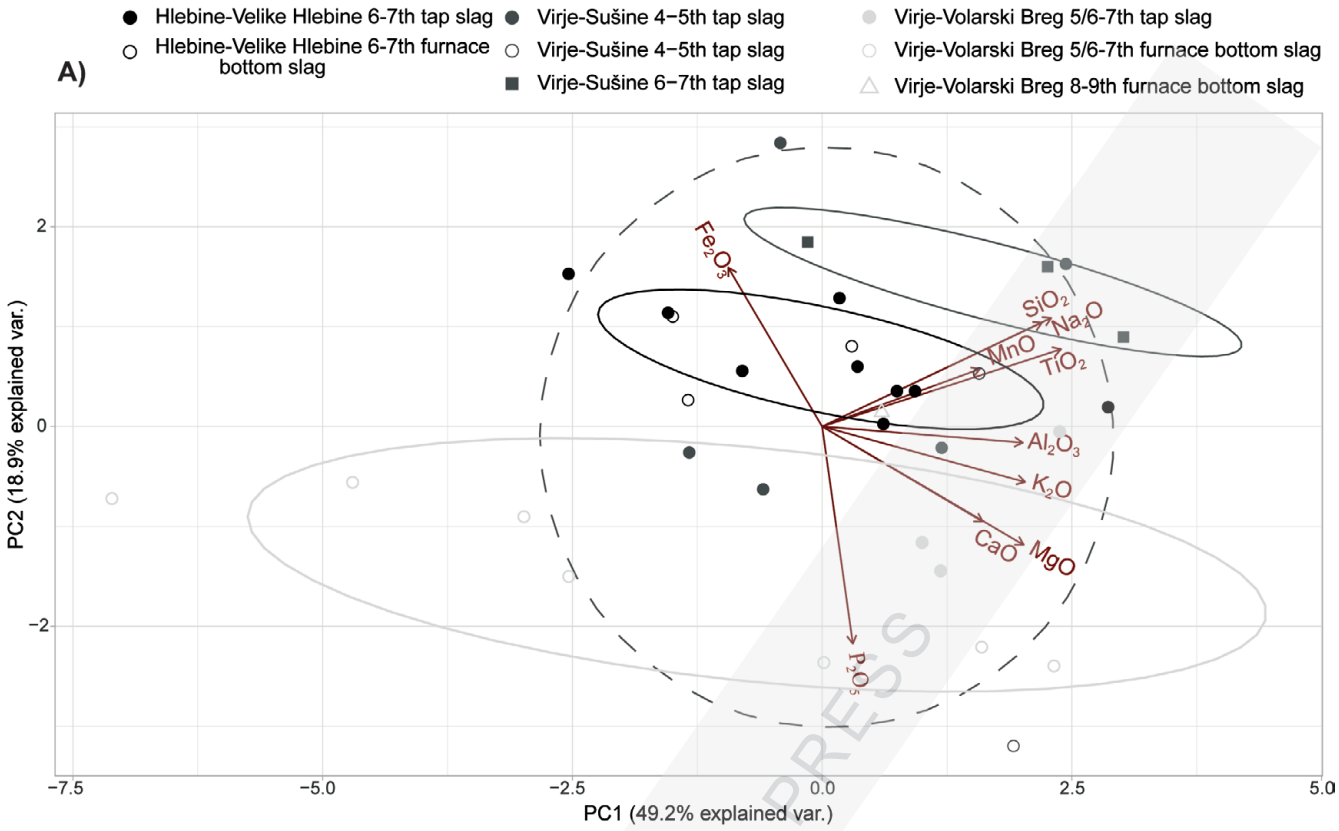

B)

Variable	Factor 1	Factor 2	Factor 3
SiO_2	0.87	-0.41	-0.10
TiO_2	0.91	-0.29	0.13
Al_2O_3	0.76	0.06	0.47
Fe_2O_3	-0.36	-0.60	-0.61
MgO	0.77	0.45	-0.05
MnO	0.60	-0.22	-0.39
CaO	0.61	0.36	-0.52
K_2O	0.77	0.21	0.01
Na_2O	0.84	-0.39	0.02
P_2O_5	0.12	0.83	-0.33

Principal component	Eigenvalue	% Total	Cumulative
1	4.92	49.25	49.25
2	1.89	18.90	68.15
3	1.15	11.47	79.62

C)

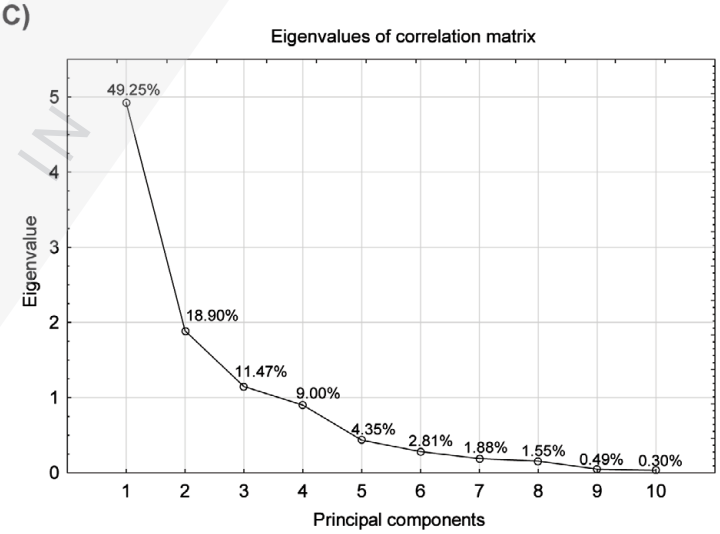

Figure 3. A) PCA scatterplot of PC 1 and PC 2 of the major oxide concentrations, B) Principal component loading and eigenvalues and C) Eigenvalues of covariance matrix plot.

5. DISCUSSION

5.1. Temporal and spatial differences in ore and slag characteristics

The mineralogical and geochemical composition of the ore, especially the gangue minerals associated with the iron minerals, has a predominant contribution to the mineralogical and geochemical composition of the resulting slags (PORTILLO-BLANCO et al., 2020). Fayalite in the slag was formed as the product of the thermal reaction between Fe minerals in the ore (goethite in bog iron ores, haematite in roasted bog iron ores) and quartz during the smelting process, forming the compound Fe_2SiO_4 that upon solidification formed olivine phase fayalite (CHARLTON et al., 2012). Studies suggest that the formation temperatures for this process were somewhere between 1100 and 1400 °C (POLLARD & HERON, 1996). Wüstite is a situationally occurring mineral in iron slags, mostly occurring in slags from the Virje sites. It is formed when iron oxide occurs in excess amounts (GORDON, 1997), with some studies suggesting that the crystallization starts to occur when the Fe/SiO_2 ratio exceeds 1.5 (KONGOLI & YAZAWA, 2001; KĄDZIOŁKA et al., 2020). Occurrence of magnetite in some tap slags indicates incomplete reduction during the process, or a secondary formation of magnetite due to the supply of excess air in the smelting system (MANASSE & MELLINI, 2002). Traces of goethite and haematite can be associated with oxidising conditions (MORTON & WINDGROOVE, 1969) to which the slags would be exposed af-

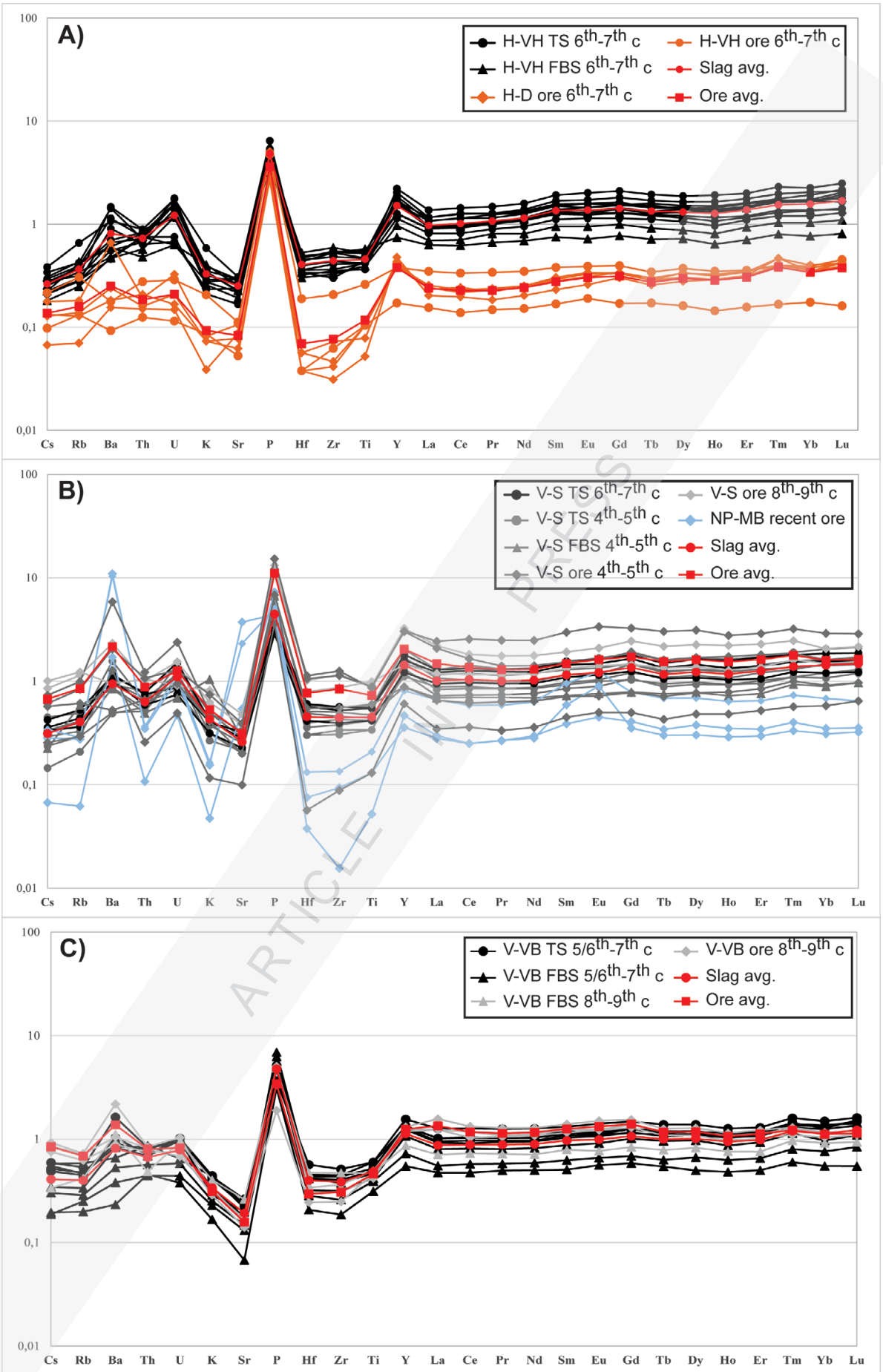

Figure 4. Geochemical signature of iron slags from A) Hlebine-Velike Hlebine, B) Virje-Sušine and C) Virje-Volarski Breg compared to discovered bog iron ores and roasted iron ores from same or nearby study sites.

ter being removed out of the furnace or through the post-depositional changes, influenced by oxidising conditions and humid soil layers. XRD analysis also revealed the occurrence of an Al-spinel phase (hercynite) in the smelting slags from all sites, with most occurrences from the Virje-Volarski Breg positions. The presence of hercynite indicates that the used ores had elevated contents of aluminium, possibly from Al-phases such as clay minerals and plagioclase. This is in line with previous studies of bog iron ores in the study area (BRENKO et al., 2021), where mineralogical analysis pointed to the occurrence of soil minerals such as clays and feldspars/plagioclase.

The sum of iron, silica and aluminium contents in all locations is mostly around 85 – 90 mass. %, clearly indicating that all samples are metallurgical slags produced during the bloomery iron-making process (BANI-HANI et al., 2012). The geochemical composition of the slag samples shows similarity to other available study cases from Europe (Fig. 2). It is worth noting that chemical data of iron slags in this study is similar to data obtained by NEMET et al. (2019) for slag samples from the neighbouring Turopolje region, especially in regard to MnO contents, indicating overall similar chemical conditions in the wider area. Upon closer inspection of the major oxide ratios, the regularity and behaviour of major oxides for each site can be detected. Studies (BLAKELOCK et al., 2009; CHARLTON et al., 2012) suggest that certain oxide ratios remain similar between the ore and the slag and could be used to distinguish the usage of different ores between different sites. Previous research regarding possible ore sources for iron production in the Podravina region (BRENKO et al., 2021) indicated higher aluminium contents in bog iron ores from sites within the Virje area (Sušine and Volarski Breg) when compared to the Hlebine area (Velike Hlebine and Dedanovice). Based on the geochemical data, it is highly likely that in each workshop locally available ore from different, probably nearby deposit(s) was used. Iron ore used in the Hlebine-Velike Hlebine site probably contained a lower quantity of gangue minerals (clay minerals and feldspars), therefore having lower Al contents. It is also possible that the ore was pre-processed by washing or that the ore was carefully chosen, while avoiding clayey ore lumps, as was proposed by BRENKO et al. (2021) based on the REE contents. On the other hand, some of the ore used at the Virje-Volarski Breg site, both from the workshop dated to 8/9th and to the 5/6th centuries, was probably slightly enriched with gangue minerals, which led to an increase of Al in some slags from these positions. Increase in Al content might be a micro-regional feature typical for the Virje area, although this is not entirely supported by the composition of all slag samples from the workshop dated to 4/5th centuries at the Virje-Sušine site. However, archaeological evidence strongly suggests that separation of the ore was carried out at this site as several samples of roasted bog iron ore were found in a waste discarding area (BRENKO et al., 2021) so it could be presumed that the ore was more thoroughly pre-processed and/or more carefully selected. Another option could be that the ores used for individual smelting procedures were not all of the same microregional origin as at the other positions in the Virje area.

This study revealed that the discovered iron ores from the Virje-Sušine and Virje-Volarski Breg sites tend to have increased Mn contents with values sometimes reaching over 20 mass. %. However, as shown in Table 2, analysed iron slags have low Mn contents, with values around 1 mass. %. Such low Mn contents imply that ore was processed for both manganese and for clay minerals. However, as some Mn can still be incorporated into the iron bloom (albeit on rare occasions) (NAVASITIS & SELSKIENĖ, 2007), further investigation into iron bloom geochemistry could reveal whether the ore was truly pre-processed for Mn as well. This could also mean that bog iron ores of different composition were used within a single workshop. The latter would be in line with general bog iron ore characteristics, that can be of very variable quality and overall composition, even if found within the same deposit, and more so in relation to different microenvironmental conditions under which they were formed i.e. different deposits within the same region. A sign of inconsistency of overall characteristics of used ore or the way that the ore was smelted can be seen in the wide dispersion of slag samples from the Late Antiquity, the Virje-Sušine workshop (4/5th centries) as well as from the workshop on the Virje-Volarski Breg site belonging to the end of 5/6th century (Fig. 3).

5.2. Provenance studies

Numerous studies have been carried out, in an attempt to establish the relationship between possible iron ore and iron slags (PLEINER, 1967; DEVOS et al., 2000; SCHWAB, 2006; BLAKELOCK et al., 2009), which is not always unbiased, due to numerous reasons. The ore used in iron smelting accounts for around 77–100 % of the chemical composition of slag, and therefore, slag derives the majority of its bulk composition from ore, with part of the composition depending on the furnace structural ceramics, fuel and flux material (CREW, 2000). This can be reflected in the frequency distribution charts of major element NRC ratios. COUSTURES et al. (2003) determined that although clay and charcoal alter the trace element composition of the slag, the variability is so insignificant that the correlation coefficient of the two is acceptable. Previous study (BRENKO et al., 2021) suggested that it is possible to determine the type of used ore by comparing the geochemical signature of rare earth and trace elements between samples of bog iron ore and archaeological samples of roasted bog iron ore. However, the method of clustering and correlation was used on archaeological samples that were exposed to an average temperature between 550 and 600 °C, with a maximum spike in temperature of 1038 °C (KARAVIDOVIĆ, 2020), where limited mobility was recognized between rare earth and trace elements. As iron slags are formed at temperatures much higher than roasted ores, some degree of mobility and fractionation in trace elements is to be expected, even in the case when considering immobile elements such as REEs or trace elements (LINTHEWAS & SETIAWAN, 2018). Slight differentiation of rare earth and trace element contents can be noticed in all sites when comparing the signature of tap slags and furnace bottom slags. Based on the diagrams in Fig. 4, it seems that tap slags have slightly higher contents of REEs and trace elements than furnace bottom slags which can be explained by the thermodynamic behaviour of the incompatible elements, as they are more likely to separate to a more liquid phase, such as the tap slag. Therefore, the type of analysed slag inevitably holds some degree of influence on the overall geochemical signature, at least content related.

The ideal case in determining the type of used ore in an archaeological context would be to compare the ore found in the same context as the slag itself, which is rarely possible due to the nature of the archaeological record where used raw materials are often not discovered. However, in the case of the Hlebine-Velike Hlebine, slags could be compared to two archaeological samples of roasted ore from the same site interpreted as an iron production workshop, and four samples of roasted ore from a close-by

concurrent Hlebine-Dedanovice site. The total contents of trace and REEs between the ore and slag samples differ in favour of the slag that can be attributed to iron depletion from the ore to the slag (DESAULTY et al., 2009). Analysed iron slags have lower Fe contents than the ore samples used for provenance (BRENKO et al., 2021). However, when the same elements are plotted on a multielemental diagram, they exhibit characteristic peaks that could indicate the provenance of the slag material. The first noticeable peak is the high positive enrichment of phosphorus in both ores and slags. Studies often indicate that bog iron ores contain significant contents of P_2O_5 (STOOPS, 1983; LANDUYDT, 1990; TÖRÖK & THIELE, 2013; THELEMANN et al., 2017). This is a strong indication in the usage of bog iron ores for iron production in the study area. Trace elements such as Cs, Rb, K and U are often observed in variable contents in the soils (MAES et al., 1999; GINGELE & DECKER, 2007; ZAUNBRECHER et al., 2015; FULLER et al., 2015). Such behaviour was also detected through soil profiles in the Podravina region (BRENKO et al., 2020). Therefore, some variability in the geochemical signatures of bog iron ores formed in such soils, and accompanying slags is to be expected, especially if the soils are subjected to constant redox changes such as in the Podravina region due to fluctuation of groundwater. The REEs (Y-Lu) part of the diagram is almost identical in shape and patterns in both ores and slags, indicating a similar genetic origin between them.

Bog iron ores from the archaeological context of the Virje-Sušine site and ores found in a geological context from a nearby Novigrad Podravski-Milakov Berek site are compared with the iron slags from Virje-Sušine. It can be seen that the geochemical signature of slag samples found in the context of the workshop dated between the end of 4th and the beginning of 5th century, and samples from another workshop dated between the end of the 6th and into 7th century show slight discrepancies to one another. This suggests variety in the ore used, most notably the clay minerals, that could be due to exploitation of different deposits or different ore-processing activities. Additionally, the geochemical signature of the compared ores belonging to the same archaeological context, the workshop at Virje-Sušine dated to 4/5th centuries, also shows pattern variability. A possible explanation for this is found within the archaeological context as all of the ore samples were found in layers of smelting debris, implying that these ores were possibly not meant to be used, due to their inadequate metallurgical characteristics as proposed by BRENKO et al. (2021). However, a distinctive positive phosphorus peak is again present in both ores and slag, indicating that bog ores were used as the primary ore source. Based on the mineralogy of the analysed bog iron ores from the study site and nearby Novigrad Podravski site, differentiation of the used ores can be achieved by observing their Ba and Sr contents. Previous study (BRENKO et al., 2021) suggests that Ba in the ore correlates well with the Mn amorphous phase, while an Eu anomaly occurs due to the substitution of Eu^{3+} with Ca^{2+} in the calcite structure (HELLEBRANDT et al., 2017), a mineral that was discovered occurring in the ore samples from that location. This implies that Mn-rich ores were most likely not used in the individual smelting episodes represented in selected samples. This anomaly also provides evidence to propose that the composition of bog iron ores from the same regional origin can vary significantly in relation to the location of the deposit and presumably the period when bog iron ore was formed.

The clearest situation in terms of provenance can be seen in the Virje-Volarski Breg site. The ore samples were found in features within a settlement context dated to the 8/9th centuries, that is spatially connected to the concurrent iron production workshop from which the analysed slag originates (Trench 1). This implies that the ore discovered at this location was used for iron smelting and production on the same site. All three ore samples have an almost identical geochemical signature to the signature of the slags, with all the characteristic peaks as indicated by the average ore and average slag lines on Fig. 4C. When compared to the slag samples from the workshop dated to the 5/6th centuries, a similar degree of overlapping geochemical signatures is seen. Here, some slag samples show depletion in overall contents while others are of almost identical signature. Some differentiation can be noticed in the Ba contents, but these can also be attributed to slight variations in the Mn contents of the bog iron ore, as previous study (BRENKO et al., 2021) showed correlation between Mn and Ba in bog iron ores.

6. CONCLUSION

In the study area of the Podravina region, iron was produced via the direct process i.e. bloomery smelting in the Late Antiquity and the Early Middle Ages, as excavated archaeological sites suggest. The analysed slag is divided into two groups based on macroscopic analysis: tap slag and furnace bottom slag. Both slag types are characterized by fayalite as the main Fe mineral phase. Occurrences of other Fe minerals, such as wüstite, haematite and magnetite imply some variability in the smelting processes. Overall, the major oxide composition of analysed slags suggests differentiation for some NRC ratios, such as slight Al_2O_3 differentiation at the Virje-Volarski Breg site. This is related to a higher clay content in the ores used within the Virje-Volarski Breg workshops but as samples of slag and ores originate from differently dated sites, these characteristics could be connected to the usage of iron ores that were formed under similar micro-environmental conditions, presumably in the surroundings of the Virje site.

An attempt was made to determine the provenance of iron slags in the Podravina region, through the analysis of trace and rare earth elements in both slags and locally discovered ores. Methods included normalization and plotting of selected elements, forming geochemical signatures for both ores and slags, that were then further compared and analysed. Specific peaks, such as the positive P peak implies the usage of locally discovered bog iron ore as the main raw material. In the case of the Virje-Volarski breg site, identical shapes and peak heights undeniably point to the usage of bog iron ore as the main raw material. Differentiation and inconsistency can be seen in signatures from Hlebine-Velike Hlebine and Virje-Sušine, most notably in the trace element contents. Such differentiation stems from trace elements that are incorporated into clay minerals, such as Cs, Rb and K, questioning their usability as such in the provenance studies. However, general shape of the signatures points toward bog iron ore usage on Hlebine-Velike Hlebine and Virje-Sušine sites.

Differentiation between the potential location of the deposits and/or time when the ores were formed can also be presumed from the ores signature, as the ore samples from the archaeological context of Virje-Sušine site and the geological context from the nearby Novigrad Podravski-Milakov Berek site exhibited a different geochemical signature, most notably in regard to Ba content. Therefore, study indicates the possibility of discrimination in the usage of ores based on their micro-locational or temporal provenance, by detailed mineralogical analysis followed by geochemical analysis.

ACKNOWLEDGMENT

This work has been fully supported by the Croatian Science Foundation under the project TransFER - Iron production along the Drava River in the Roman period and the Middle Ages: Creation and transfer of knowledge, technologies and goods (Grant No. 5047). We would like to thank our project partners from The Institute of Archaeology and City Museum of Koprivnica, whose continuous fieldwork led to archaeological discoveries of iron production culture in the Podravina region. We would also like to thank Stanko Ružičić, PhD, whose comments helped improve the quality of this manuscript.

Dataset statement

The data that supports the finding of this study is available from the corresponding author upon reasonable request.

REFERENCES

BANI-HANI, M., ABD-ALLAH, R. & EL-KHOURI, L. (2012): Archaeometallurgical finds from Barsinia, Northern Jordan: Microstructural characterization and conservation treatment.– J. Cult. Herit., 13, 314–325. doi: 10.1016/j.culher.2011.12.005

BAŠIĆ, F. (2013): The Soils of Croatia (1st ed.).– Springer Science+Business Media Dordrecht. doi: 10.1007/978-94-007-5815-5

BLAKELOCK, E., MARTINÓN-TORRES, M., VELDHUIJZEN, H.A. & YOUNG, T. (2009): Slag inclusions in iron objects and the quest for provenance: an experiment and a case study.– J. Archaeol. Scie., 36, 1745–1757. doi: 10.1016/j.jas.2009.03.032

BOTIĆ, K. (2021): Absolute dating of Virje and Hlebine sites.– In: SEKELJ IVANČAN, T. & KARAVIDOVIĆ, T. (eds.): Interdisciplinary Research into Iron Metallurgy along the Drava River in Croatia - The TransFER Project, Oxford: Archaeopress, 92–100. doi: 10.32028/9781803271026-5

BRENKO, T., BOROJEVIĆ ŠOŠTARIĆ, S., KARAVIDOVIĆ, T., RUŽIČIĆ, S. & SEKELJ IVANČAN, T. (2021): Geochemical and mineralogical correlations between the bog iron ores and roasted iron ores of the Podravina region, Croatia.– Catena, 204, 105353. doi: 10.1016/j.catena.2021.105353

BRENKO, T., BOROJEVIĆ ŠOŠTARIĆ, S., RUŽIČIĆ, S. & SEKELJ IVANČAN, T. (2020): Evidence for the formation of bog iron ores in the soils of the Podravina region, NE Croatia: Geochemical and mineralogical study.– Quatern. Int., 536, 13–29. doi: 10.1016/j.quaint.2019.11.033

BRKIĆ, Ž. & BRIŠKI, M. (2018): Hydrogeology of the western part of the Drava Basin in Croatia.– J. Maps., 14, 173–177. doi: 10.1080/17445647.2018.1445043

BRKIĆ, Ž., LARVA, O. & URUMOVIĆ, K. (2010): The quantitative status of the groundwater in alluvial aquifers in northern Croatia.– Geol. Croat., 63, 283–298. doi: 10.4154/GC.2010.23

CHARLTON, M.F., CREW, P., REHREN, TH. & SHENNAN, S.J. (2010): Explaining the evolution of ironmaking recipes–an example from northwest Wales.– J. Anthropol. Archaeol., 29, 352–367. doi: 10.1016/j.jaa.2010.05.001

CHARLTON, M.F., BLAKELOCK, E., MARTINÓN-TORRES, M. & YOUNG, T. (2012): Investigating the production provenance of iron artifacts with multivariate methods.– J. Archaeol. Sci., 39, 2280–2293. doi: 10.1016/j.jas.2012.02.037

COUSTURES, M.P., BÉZIAT, D. & TOLLON, F. (2003): The use of trace element analysis of entrapped slag inclusions to establish ore – bar iron links: examples from two Gallo-roman iron-making sites in France (Les Martys, Montagne Noire, and Les Ferrys, Loiret).– Archaeometry, 45, 599–613. doi: 10.1046/j.1475-4754.2003.00131.x

CREW, P. (2000): The influence of clay and charcoal ash on bloomery slags.– In TIZZONI, C.C. & TIZZONI M. (eds.): Iron in the Alps: Deposits, Mines and Metallurgy from Antiquity to the XVI Century, Bienno, p. 38–48.

DESAULTY, A-M., DILLMANN, P., L'HÉRITIERA, M., MARIET, C., GRATUZE, B., JORON, J-L. & FLUZIN, P. (2009): Does it come from the Pays de Bray? Examination of an origin hypothesis for the ferrous reinforcements used in French medieval churches using major and trace element analyses.– J. Archaeol. Sci., 36, 2445–2462. doi: 10.1016/j.jas.2009.07.002

DEVOS, W., SENN-LUDER, M., MOOR, C. & SALTER, C. (2000): Laser ablation inductively coupled plasma mass spectrometry (LA-ICP-MS) for spatially resolved trace analysis of early-medieval archaeological iron finds.– Int. J. Anal. Chem., 366, 873–880. doi: 10.1007/s002160051588

DILLMANN, P. & L'HÉRITIER, M. (2007): Slag inclusion analyses for studying ferrous alloys employed in French medieval buildings: supply of materials and diffusion of smelting processes.– J. Archaeol. Sci, 34/11, 1810–1823. doi: 10.1016/j.jas.2006.12.022

FULLER, A.J., SHAW, S., WARD, M.B., HAIGH, S.J., MOSSELMANS, F.W., PEACOCK, C.L. STACKHOUSE, S., DENT, A.J., TRIVEDI, D. & BURKE, I.T. (2015): Caesium incorporation and retention in illite interlayers.– Appl. Clay Sci., 108, 128–134. doi: 10.1016/j.clay.2015.02.008

GINGELE, F.X. & DE DECKKER, P. (2005): Clay mineral, geochemical and Sr-Nd isotopic fingerprinting of sediments in the Murray-Darling fluvial system, southeast Australia.– Aust. J. Earth Scie., 52, 965–974. doi: 10.1080/08120090500302301

GORDON, R.B. (1997): Process deduced from ironmaking wastes and artefacts.– J. Archaeol. Sci., 24, 9–18. doi: 10.1006/jasc.1995.0092

HEAD J. M. (2019). Formal subdivision of the Quaternary System/Period: Present status and future directions.– Quatern. Int., 500, 32–51. doi: 10.1016/j.quaint.2019.05.018

HEIMANN, R.B., KREHER, U., SPAZIER, I. & WETZEL G. (2001): Mineralogical and chemical investigations of bloomery slags from prehistoric (8th century BC to 4th century AD) iron production sites in Upper and Lower Lusatia, Germany.– Archaeometry, 43, 227–252. doi: 10.1111/1475-4754.00016

HELLEBRANDT, S.E., HOFMANN, S., JORDAN, N., BARKLEIT, A. & SCHMIDT, M. (2017): Incorporation of Eu(III) into Calcite under Recrystallization conditions.– Sci. Rep-UK., 6, 33137. doi: 10.1038/srep33137

HORST-MADSEN, L. & BUCHWALD, V.F. (1999): The characterisation and provenancing of ore, slag and iron from the Iron Age settlement in Snorup.– The Journal of the Historical Metallurgy Society, 33/2, 57–67.

KACZOREK, D. & SOMMER, M. (2003): Micromorphology, chemistry and mineralogy of bog iron ores from Poland.– Catena, 54, 393–402. doi: 10.1016/S0341-8162(03)00133-4

KĄDZIOŁKA, K., PIETRANIK, A., KIERCZAK, J., POTYSZ, A. & STOLARCZYK, T. (2020): Towards better reconstruction of smelting temperatures: Methodological review and the case of historical K-rich Cu-slags from the Old Copper Basin, Poland.– J. Archaeol. Sci., 118, 105142. doi: 10.1016/j.jas.2020.105142

KARAVIDOVIĆ, T. (2020): Rekonstrukcija postupka prženja rude: eksperimentalni pristup.– In: VITEZOVIĆ, S., ANTONOVIĆ, D. & ŠARIĆ, K. (eds.):*Aktuelna interdisciplinarna istraživanja tehnologije u arheologiji Jugoistočne Europe, Zbornik radova prvog skupa sekcije za arheometriju, arheotehnologiju i eksperimentalnu arheologiju Srpskog arheološkog društva*, [Current interdisciplinary technology in archaeology research of south-eastern Europe, Proceedings from first meeting of archaeometry, archaeotechnology and experimental archaeology of Serbian Archaeological Society], 130–137.

KONGOLI, F. & YAZAWA, A. (2001): Liquidus surface of $FeO-Fe_2O_3-SiO_2-CaO$ slag containing Al_2O_3, MgO, and Cu_2O at intermediate oxygen partial pressures.– Metall. Mater. Trans. B., 32, 583–592. doi: 10.1007/s11663-001-0114-7

KOPIĆ, J., LOBOREC, J. & NAKIĆ, Z. (2016): Hydrogeological and hydrogeochemical characteristics of a wider are of the regional well field Eastern Slavonia – Sikirevci.– The Mining-Geological-Petroleum Bulletin, 31, 47–66. doi: 10.17794/rgn.2016.3.4

LANDUYDT, C.J. (1990): Micromorphology of iron minerals from bog ores of the Belgian

Campine area.– Dev. Soil Sci., 19, 289–294. doi: 10.1016/S0166-2481(08)70340-4.

LINTJEWAS, L. & SETIAWAN, I. (2018): Mobility of rare earth element in hydrothermal process and weathering product: a review.– IOP Conf. Series: Earth and Environmental Science, 118. doi: 10.1088/1755-1315/118/1/012076

LÓCZY, D., DEZSŐ, J., CZIGÁNY, S., GYENIZSE, P., PIRKHOFFER, E. & HALÁSZ, A. (2014): Rehabilitation potential of the Drava River floodplain in Hungary.– In: 2nd International Water Resources and Wetlands. Conference Paper.

MANASSE, A. & MELLINI, M. (2002): Chemical and textural characterization of medieval slags from the Massa Marittima smelting sites (Tuscany, Italy).– J. Cult. Herit., 3, 187–198. doi: 10.1016/S1296-2074(02)01176-7

MAES, E., ISERENTANT, A., HERBAUTS, J. & DELVAUX, B. (1999): Influence of the nature of clay minerals on the fixation of radiocaesium traces in an acid brown earth-podzol weathering sequence.– Eur. J. Soil Sci., 50, 117–125. doi: 10.1046/j.1365-2389.1999.00224.x

MORTON, G. R., & WINGROVE, J. (1969): Constitution of bloomery slags, part 1: Roman.– J. Iron Steel I., 207, 1556–1564.

NAVASAITIS, J. & SELSKIENĖ, A. (2007): Metallographic Examination of Cast Iron Lump Produced in the Bloomery Iron Making Process.– Mat. Sci., 13/2, 167–173.

NAVASAITIS, J., SELSKIENĖ, A. & ŽALDARYS, G. (2010): The Study of Trace Elements in Bloomery Iron.– Mater. Sci.+, 16/2, 113–118.

NEMET, I., RONČEVIĆ, S., BUGAR, A., ZUBIN FERRI, T. & PITAREVIĆ, L. (2018): Classification analysis of archaeological findings from early-iron production (Turopolje region, NW Croatia) based on multi-analytical profiling.– J. Anal. Atom. Spectrom., 33, 2053–2061. doi: 10.1039/C8JA00202A

PLEINER, R. (1967): Die Technologie des Schmiedes in der Großmährischen Kultur.– Slovenská Archeológia, 15/1, 77–188.

PLEINER, R. (2000): Iron in Archaeology. The European Bloomery Smelters.– Archeologický ústav AV CR, Prague, 400 p.

POLLARD, M. & HERON, C. (1996): Archaeological Chemistry.– Royal Society of Chemistry, Cambridge, 456 p. doi: 10.1039/9781847550156

PORTILLO-BLANCO, H., CRUZ ZULUAGA, M., ANGEL ORTEGA, L., ALONSO-OLAZABAL, A., CEPEDA-OCAMPO, J.J. & MARTINEZ SALCEDO, A. (2020): Mineralogical Characterization of Slags from the Oiola Site (Biscay, Spain)

to Assess the Development in Bloomery Iron Smelting Technology from the Roman Period to the Middle Ages.− Minerals-Basel, 10, 321. doi: 10.3390/min10040321

RAMANAIDOU, E. AND WELLS, M.A. (2014): Sedimentary Hosted Iron Ores.− In: HOLLAND, H.D. & TUREKIAN, K.K. (eds.): Treatise on Geochemistry 2nd ed., 313–355. Elsevier, Oxford. doi: 10.1016/B978-0-08-095975-7.01115-3

ROLLINS, H. (1993): Using geochemical data (1st ed.).− London, United Kingdom, 384 p.

RUDNICK, R.L. & GAO, S. (2003): Composition of the continental crust.− Treatise on Geochemistry, 3, 1–64. doi: 10.1016/B0-08-043751-6/03016-4

SCHWAB, R., HEGER, D., HÖPPNER, B. & PERNICKA, E. (2006): The provenance of iron artefacts from Manching: a multi-technique approach.− Archaeometry, 48, 433–452. doi: 10.1111/j.1475–4754.2006.00265.x

SEKELJ IVANČAN, T. & TKALČEC, T. (2018): Settlement Continuity at Sušine Site near Virje (North Croatia) throughout the Middle Ages.− Konštatínove listy 11, 35–66. doi: 10.17846/CL.2018.11.2.35-66

SEKELJ IVANČAN, T. & KARAVIDOVIĆ, T. (2021): Archaeological Record of Iron Metallurgy Along the Drava River.− In: SEKELJ IVANČAN, T. & KARAVIDOVIĆ, T. (eds.): Interdisciplinary Research into Iron Metallurgy along the Drava River in Croatia - The TransFER Project, Oxford: Archaeopress, 43−91. doi: 10.32028/9781803271026-4

SELSKIENĖ, A. (2007): Examination of smelting and smithing slags formed in bloomery iron-making process.− Chemija, 18, 22–28.

STOOPS, G. (1983): SEM and light microscopic observations of minerals in bog-ores of the Belgian Campine.− Geoderma, 30, 179–186. doi: 10.1016/0016-7061(83)90065-4.

THELEMANN, M., BEBERMEIER, W., HOELZMANN, P. & LEHNHARDT, E. (2017): Bog iron ore as a resource for prehistoric iron production in Central Europe – A case study of the Widawa catchment area in eastern Silesia, Poland.− Catena, 149, 474–490. doi: 10.1016/j.catena.2016.04.002

TÖRÖK, B. & THIELE, A. (2013): Extracting phosphoric iron under laboratorial conditions smelting bog iron ores.− In: IOP Conference Series: Materials Science and Engineering, Volume 47, 2nd International Conference on Competitive Materials and Technological Processes (IC-CMTP2) 8–12 October 2012, Miskolc-Lillafüred, Hungary, 012034. doi: 10.1088/1757-899X/47/1/012034

VALENT, I. (2021): Archaeological Finds of Metallurgical Activities on the Territory of the River Drava Basin During Iron Age and Antiquity.− In SEKELJ IVANČAN, T., KARAVIDOVIĆ, T., TKALČEC, T., KRZNAR, S. & BELAJ, J. (eds.), Secrets of iron - from raw material to an iron object, Proceedings of the 7th International Scientific Conference on Mediaeval Archaeology of the Institute of Archaeology, Serta Instituti Archaeologici, Zagreb: Institut za arheologiju.

ZAUNBRECHER, L.K., CRAWFORD ELLIOTT, W., WAMPLER, J.M., PERDRIAL, N. & KAPLAN, D.I. (2015): Enrichment of Cesium and Rubidium in Weathered Micaceous Materials at the Savannah River Site, South Carolina.− Environ. Sci. Technol., 49, 4226–4234. doi: 10.1021/es5054682

3. DISCUSSION

3.1. Bog iron ore formation mechanism and characteristics in the Podravina region

The dominant feature in the Podravina region is the meandering Drava River, which holds an influence on the geological, pedological and hydrogeological characteristics of the study area. Due to the river flow and occasional flooding in the area (**Lóczy, 2013**), constant sediment flux is present in the river valley, forming several kilometres wide area that has the characteristics of a typical floodplain, with alluvial sediments, such as silty deposits, being the most prominent feature (**Lóczy et al., 2014**). Archaeological studies on the left bank of the Drava River, in the Inner Somogy region (Hungary), discovered traces of iron archaeology connected with bog iron ore (**Gömöri, 2006; Török et al., 2015**), while in the Podravina region archaeological investigation led to discoveries of iron slags and roasted ore (**Sekelj Ivančan and Karavidović, 2021**), without discovering ore material. Based on the similar geological, pedological and hydrogeological characteristics between Podravina region and Inner Somogy region, occurrence of bog iron ore was assumed in the Podravina region, which led to soil profiling campaign in the region (**Brenko et al., 2020**).

In analysed soil profiles, bottom parts were usually greyish in colour, indicating seasonally swampy soils with a developed gley horizon (**Husnjak, 2014**), while upper parts were light to dark brown, and were showing signs of iron (Fe) accumulation, mostly as precipitations on the soil particles in the form of soft masses or pore linings. This affected colour of the interval, showing orange and red patches where Fe was present in significant concentrations (**Schwertmann and Fitzpatrick, 1992**). Based on geochemistry of trace and rare earth elements (**Brenko et al., 2020**), it can be established that investigated soils can be traced to the same parent material, established as the flooding material from the eastern Alps and transported by the Drava River (**Halamić et al., 2003**). However, six analysed soil profiles showed different thickness and quantities of Fe-enriched material in upper intervals, that can be connected to variable microregional geographical, geological and hydrogeological characteristics in the region. Previous studies (**Kaczorek and Sommer, 2004; Stanton et al, 2007; Banning, 2008**) established that groundwater is the main carrier of Fe (and other redox-sensitive elements) which enables the precipitation of bog iron ore in the soils. By comparing hydrogeological regime in the Podravina region (**Brkić and Briški, 2018**) with geographical data of the analysed soil profiles, different influence of groundwater was detected, which is reflected in the quantity of precipitated Fe in soil profiles. High groundwater levels at the

Imbriovec-Berek soil profile are usually near or occasionally over the top-most interval of the profile, which was evident during the fieldwork. Due to longer exposure to groundwater and wet conditions, the availability and circulation of atmospheric oxygen is impaired within the profile, which leads to the formation of reductive conditions through the profile. Under reductive conditions, Fe is more mobile than under oxidising conditions (**Mansfeldt et al., 2012**) and is not precipitating within the soil profile, as indicated by low Fe contents throughout this profile. On the other hand, by comparing hydrogeological regimes in profiles Koprivnički Ivanec-Log Parag, Virje-Sušine, Peteranec-Gorice and Hlebine-Dedanovice, it can be established that groundwater very rarely or never reaches zones with available atmospheric oxygen (shallower parts of the profile). This again leads to smaller quantities of Fe precipitation in these profiles as indicated by the mineralogical and geochemical data (**Brenko et al., 2020**). However, these contents are still higher that the Clark's values for Upper Continental Crust (**Rudnick and Gao, 2003**), indicating Fe anomaly in the general study area. The Kalinovac-Hrastova Greda soil profile contains the highest contents of Fe as well as As and P. The average groundwater level depth at the Kalinovac-Hrastova Greda soil profile is around 100 cm, with groundwater reaching a maximum depth of 10 cm below the surface during high-water periods (**Brkić and Briški, 2018**). This means that most of the time, the upper 100 cm of the profile is well aerated, with high quantity of available oxygen. During wet season, when the groundwater table reaches upper parts of the profile, the Fe^{2+} from the groundwater encounters available oxygen, triggering the oxidation to Fe^{3+} and precipitation in the form of iron mottles and linings, mostly in the 60–100 cm interval. Continuous precipitation leads to the formation of goethite enriched layer as seen by the mineralogical analysis (**Brenko et al., 2020**). Very slight enrichment of Mn was discovered within the same profile, although in slightly upper part of the profile when compared to the Fe enrichment. This differentiation in the precipitation depths of Fe and Mn arises from different behaviour of the two observed elements in interchanging redox conditions. Both elements are often occurring together, with Mn usually present in lower contents (**Nádaská et al., 2012**). **Hem** (**1963**) concluded that in the systems where the oxides are the most dominant phases, such as in this case, where Fe_2O_3 and SiO_2 are the most abundant phases, Mn precipitation and mobility is highly affected by the changes in the Eh/pH conditions. Manganese starts to precipitate at higher Eh than Fe, making it more mobile of the two in the lower parts of the profile where Eh is lower (**Atta et al., 1996**). This difference in the Eh/pH behaviour and precipitation explains why Fe enrichment is often found in the lower parts of the profile, while Mn enrichment is overlaying it at shallower depth. Based on the observed soil

mineralogical and geochemical characteristics, formation mechanism of bog iron ore in the Podravina region can be established (**Figure 3-1**). Bog iron ore forms seasonally, during high groundwater periods (rainy season, snow melting), when groundwater enriched with Fe, Mn and As (**Habuda-Stanić et al., 2013; Kopić et al., 2016**) starts to rise and fluctuate between 10 and 100 cm depth. There, Fe oxidises and precipitates as goethite (possibly at first as amorphous Fe and/or ferrihydrite/lepidocrocite). The accumulation of Fe starts at the depth where the oxidation firstly occurs (around 100 cm), with majority of Fe being accumulated at the 60–100 cm interval, as evident from the Kalinovac profile. Continuous period of precipitation over several decades or hundreds of years could lead to development of fully formed bog iron ore deposit. However, under present conditions with regards to agricultural activities and melioration in the Podravina region, it is highly unlikely that bog iron ore deposit could be fully formed, with occurrence such as Kalinovac-Hrastova Greda representing the initial formation phase.

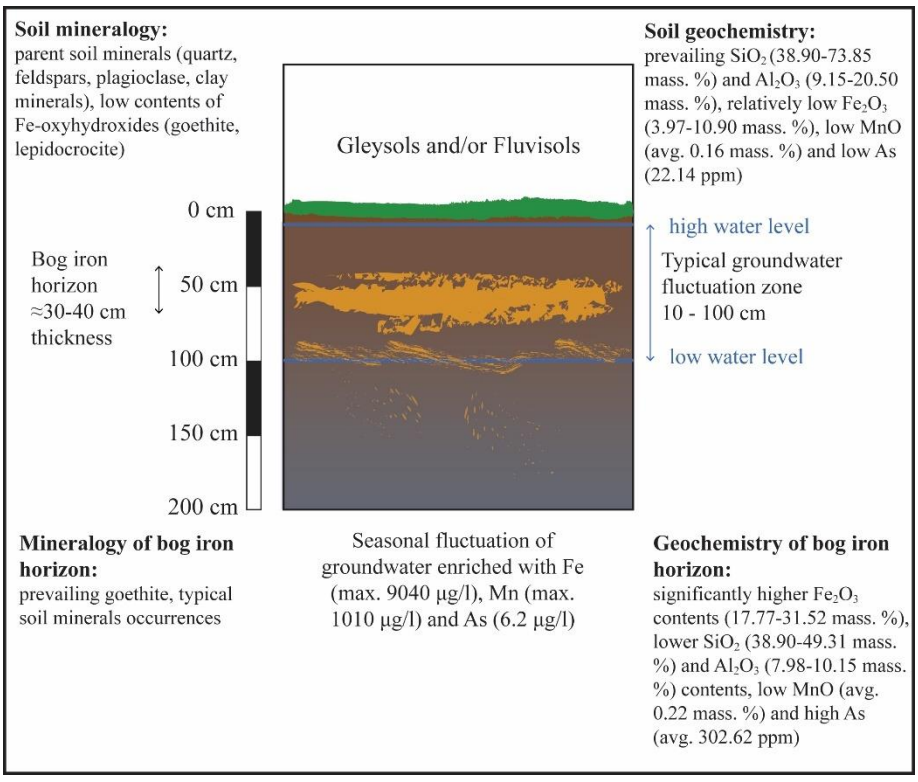

Figure 3-1. Bog iron ore formation mechanism in the Podravina region

Established formation mechanism is well in line with the discovered bog iron ore types discovered in the study area. The three types correspond to the three bog iron ore formation phases (**Thelemann et al., 2017**) exhibiting both macromorphological, mineralogical and geochemical differences (**Figure 3-2**).

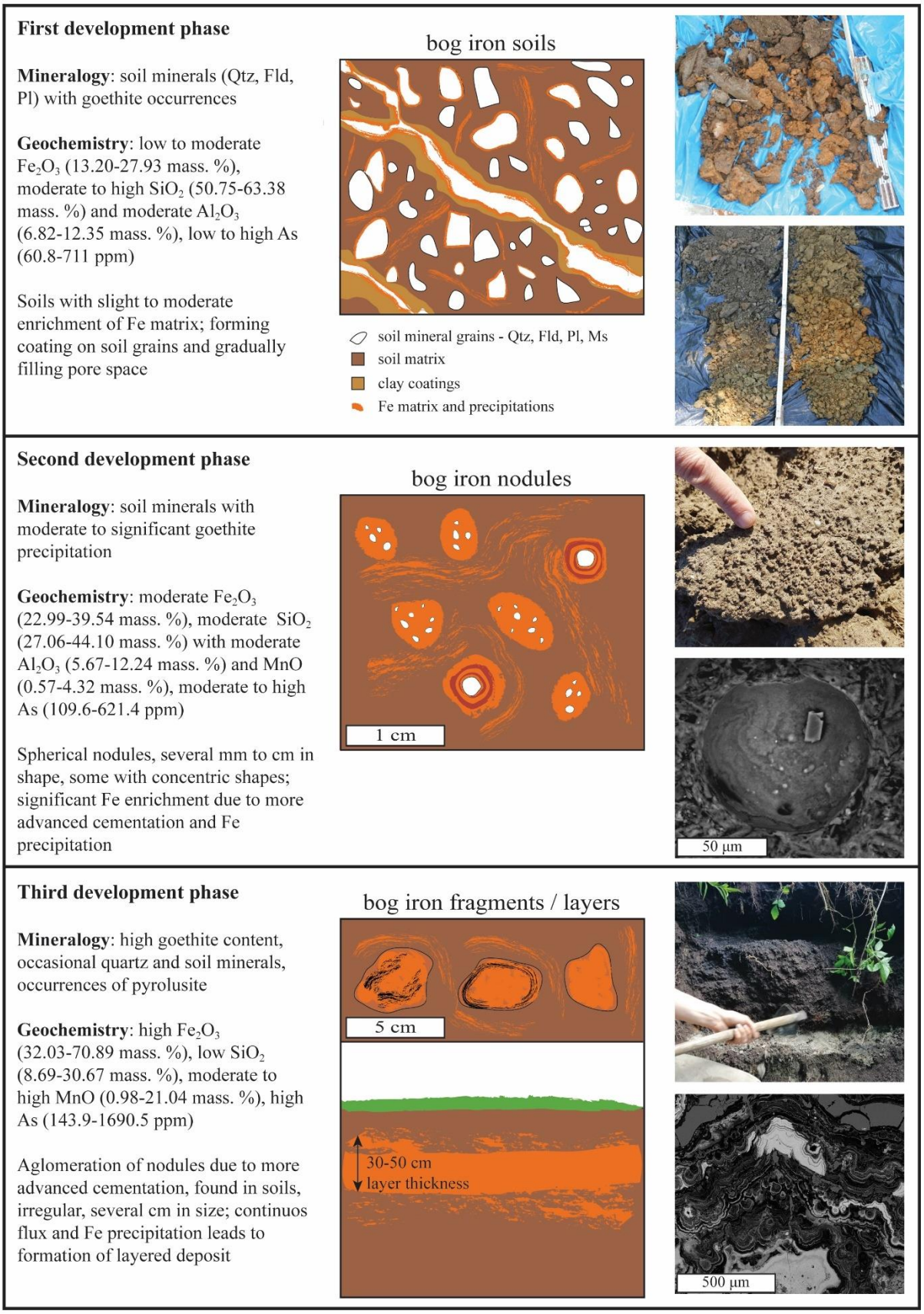

Figure 3-2. Illustrative sketches of the three bog iron ore formation phases from the study area with mineralogical and geochemical characteristics and examples for each phase (soil photos taken by Tajana Sekelj Ivančan, fragment photo taken by Tena Karavidović)

All three types differ from the surrounding soil due to a visible discoloration, typical for Fe-enriched materials (**Schwertmann and Fitzpatrick, 1992; Scheinhost and Schwertmann, 1999**). Bog iron soil has the lowest content of goethite and the highest contents of quartz and clay minerals as they represent soil material enriched with Fe matrix, where the Fe precipitation process has only begun, or is occurring in inhibited conditions. Precipitation of Fe^{3+} in the form of amorphous or low crystalline Fe oxyhydroxides, such as ferrihydrite, and later goethite, is starting to form coatings on individual soil grains, and gradually filling the pore space of the parent soil material, slowly repressing and replacing the soil matrix (**Kaczorek et al., 2004; Banning, 2008**). Soil matrix is originally occupied by typical soil and floodplain minerals, such as quartz, feldspars and clay minerals (**Sokolova et al., 2013; Długosz et al., 2018**). As the cementation process and the substitution of soil matrix with an Fe-enriched matrix had only begun in the bog iron soils, it is expected that this bog iron phase has the lowest Fe_2O_3 contents. Continuation of Fe cementation leads to the formation of bog iron nodules with equal quantities of goethite and quartz. Nodules are usually rounded in shape, several millimetres to centimetre in size. A difference in hardness between the soils and the nodules is attributed to the more advanced Fe cementation processes in the nodules. Lastly, bog iron fragments are formed as a result of further cementation and agglomeration of bog iron nodules. Both bog iron nodules and bog iron fragments display variable, but lower clay contents than bog iron soils which can also be attributed to the more advanced Fe cementation, substituting the total alumosilicate content.

Based on SEM-EDS analysis of two nodule samples (K-HG 1, P-C) and three fragment samples (NP-MB 16, NP-MB 18 and KI-LP 1), further conclusions towards bog iron ore formation and geochemical distribution of selected trace elements could be established. These samples were selected based on their iron archaeometallurgical potential and due to extremely high Mn contents in the case of NP-MB 16 sample (**Brenko et al., 2021a**). In both nodules and fragments, detrital grains are mainly composed of quartz and feldspars that are often dispersed in micro-crystalline matrix. Based on the back-scattered images, micro-crystalline matrix has three main components: zones with Fe-enrichment (grey to dark grey reflection), Mn-enrichment (light grey to white) and phyllosilicates (soil matrix) (darker grey). Alternating Fe and Mn lamination are in line with the proposition of periodical precipitation of Fe and Mn due to seasonal fluctuation of groundwater enriched with Fe and/or Mn (**Ramanaidou and Wells, 2014**) and variable Eh/pH conditions (**Atta et al., 1996**). Detrital grains of soil minerals are used as nucleation places, around which the precipitation is occurring, as suggested by the 70 μm Fe-Mn nodule embedded in the Fe-

enriched matrix, which was found in a bog iron fragment from Koprivnički Ivanec-Log Parag location (**Figure 3-2**). Two morphologically different Mn phases were also recognized; well laminated amorphous phase, with varying lamina sizes but no recognizable mineral grains and well-developed, tabular crystals, several μm in size. EDS analysis revealed differences in the chemical composition of the two Mn phases, where amorphous phase contains elevated barium contents, which is almost absent in the well crystalized phase. Bog iron fragments from Novigrad Podravski-Milakov Berek location stand out from other bog iron types with regards to MnO contents, which varies from moderate amount in the NP-MB 18 samples, up to extremely high contents (14.85 and 21.04 mass. %) in two NP-MB 16 and NP-MB 17 samples. High MnO contents were also detected by **Török and Kovács** (**2010**) and **Török et al.** (**2015**) in Southern Somogy (northern Drava alluvial plain). Although both Fe and Mn are present in groundwater, conditions where Mn precipitation at such high quantities is possible points to localised differentiation with regards to Eh/pH at some sites. Therefore, it is proposed that samples from Novigrad Podravski have a different groundwater source and that they underwent different bog iron evolution and formation than the rest of observed samples in the study area.

Pleiner (**2000**) established an empirical boundary value of 79–86 mass. % Fe_2O_3 in iron ore necessary for successful bloomery iron smelting, which is well beyond the average iron contents found in the bog iron ore of the Podravina region. Therefore, the discovered bog iron ore archaeometallurgical potential and its utilization seems low. However, certain studies in the previous decades (**Crew and Charlton, 2007; Thiele, 2010; Crew et al., 2011**), in which experimental smelting was conducted, revealed that bog iron ore with 49 mass. % Fe_2O_3 could be utilized to produce iron bloom. This implies that some bog iron fragments found during geological and archaeological surveys could have been used as the primary ore material for bloomery iron production. However, as the Fe_2O_3 contents in these fragments are below empirical boundary, the quality of the final iron product remains dubious.

3.2. Geochemical and mineralogical characterization of roasted iron ore and iron slags in the Podravina region

Two thermally threated types of archaeological samples were analysed, roasted iron ore and iron slags. Samples of roasted ore were discovered at four archaeological sites: Hlebine-Dedanovice, Hlebine-Velike Hlebine, Koprivnički Ivanec-Log Parag and Virje-Sušine. They are differentiated from the bog iron ore due to their visual appearance as they are mostly reddish in colour, often with porous morphology as a result of gaseous phases evaporating and

new Fe oxides forming during exposure to localised high temperatures, such as those in the roasting pits (**Figure 3-3**). The process of iron ore roasting is conducted for two main reasons: the mineral transformation of oxyhydroxides and non-oxide iron ores into oxides, increasing the total Fe content and making the roasted ore more porous, thus making them more pliable for smelting (**Pleiner, 2000**). Reddish colour is attributed to the mineral hematite, the main mineralogical constituent of roasted iron ore, that formed due to the mineral transformation of goethite (**Cudennec and Lecerf, 2005**), with first transformation occurring at temperatures above 170 °C (**Rzepa et al., 2016**), although usually transforming around 300 °C and above. Other Fe minerals include magnetite ($FeFe_2O_4$) and maghemite (γ-Fe_2O_3) (**Manasse and Mellini, 2002; Scheinost, 2005**) formed at temperatures in 350–400 °C range.

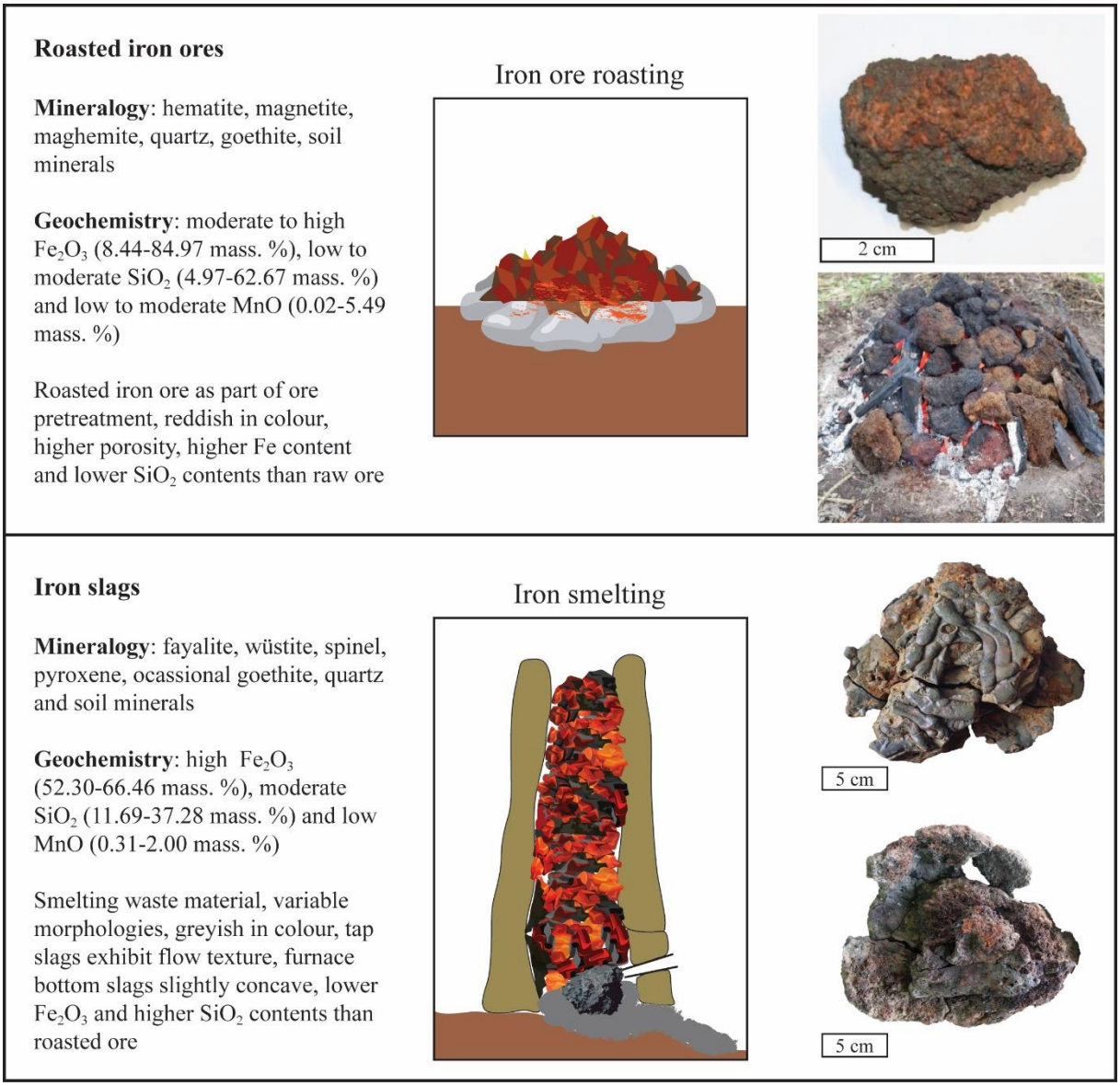

Figure 3-3. Schematic drawings of iron ore roasting and smelting with examples and characteristics from the study area (ore roasting and slag photos taken by Tena Karavidović)

Temporal and spatial differentiation regarding Fe_2O_3 contents can be noted between the sample sites, with samples from Hlebine-Dedanovice having the highest average Fe_2O_3 contents. Samples from Hlebine-Velike Hlebine have medium Fe_2O_3 contents, while samples from Virje-Sušine have the lowest average Fe_2O_3 contents and the highest variability. High Fe_2O_3 contents in roasted iron ore from Hlebine-Dedanovice site are above the empirical boundary established by **Pleiner** (**2000**), implying that good quality of iron products could be expected, when considering Fe_2O_3 contents alone. On the other hand, low Fe_2O_3 contents in samples from Virje-Sušine and Koprivnički Ivanec-Log Parag exhibit low iron production potential, implying doubtful usefulness and overall quality, indicating that this ore was possibly not meant to be used in iron production. These conclusions are in line with archaeological context, as the Virje-Sušine samples were found in the same iron production waste discarding layer, indicating that this ore was separated from quality ore and discarded. However, unroasted ore sample with high Fe_2O_3 content was discovered inside the same archaeological context, implying significant bog iron ore variability all throughout the study area. Roasted ore from Virje-Sušine also stand out due to significantly higher Al_2O_3 contents (7.28–14.62 mass. %), which is in line with their low quality and higher contents of gangue minerals (clays).

Three slag types were analysed in the study area, furnace bottom slags (FBS), tap slags (TS) and bloom refining slags (BRS), discovered in archaeological sites Hlebine-Velike Hlebine, Virje-Sušine, and Virje-Volarski breg (**Sekelj Ivančan and Karavidović, 2021**). During iron production, tap slags and furnace bottom slags are formed in the smelting process, while bloom refining slags are formed during later stages, in the primary and secondary bloom forming and smiting process. Mobility and differentiation of trace and rare earth elements was detected between different slag types (**Brenko et al., 2021b**), with FS and TS having similar contents, while BRS having lower contents, indicating some elements were mobilised during smithing processes. Therefore, attention is only given to FBS and TS, as explained in the following provenance subchapter.

Based on their position during smelting, both slag types exhibit different morphologies. Tap slags are released (taped) from the furnace during the smelting process, which is reflected in their upper surface, where visible flow texture is recognizable (**Figure 3-3**). Furnace bottom slags, as the name refers, are found in the bottom part of the furnace, below the iron bloom. Due to that, they tend to be concave in shape (**Figure 3-3**). Both slag types mostly consist of fayalite mineral phase (Fe_2SiO_4), as a thermal by-product of a reaction between Fe-oxyhydroxide/oxide with quartz during the smelting process in the furnace (**Charlton et al.,**

2012). Occurrences of hematite and magnetite imply that oxygen was present in the furnace system, changing redox conditions from reductive to oxidative. Sporadically occurring mineral wüstite, which is mostly occurring in slags from the Virje sites, points to excess in iron oxide contents, as studies suggest that the crystallization starts to occur when the Fe_2O_3/SiO_2 ratio exceeds 1.5 (**Kongoli and Yazawa, 2001; Kądziołka et al., 2020**). XRD analysis also revealed presence of spinel phase (hercynite, $FeAl_2O_4$) in the smelting slags from all sites, with most occurrences from Virje-Volarski breg positions. The presence of hercynite indicates that the ore used at that location had increased contents of aluminium, possibly from Al-phases such as clay minerals and plagioclase, implying spatial differentiation between the bog iron ore deposits of the Podravina region. Geochemical contents of major oxides are in line with mineralogical composition as slags are mostly comprised of Fe_2O_3 (52.30–66.46 mass. %, avg. = 59.52 mass. %), SiO_2 (11.69–37.28 mass. %, avg. = 26.22 mass. %) and Al_2O_3 (3.74–8.03 mass. %, avg. = 5.65 mass. %). These contents are in line with other similar studies of iron slags in Croatia and Central Europe (**Brenko et al., 2022 and references therein**).

3.3. Provenance studies of roasted iron ore and iron slags

Contrary to the provenance studies of archaeological artefacts made from marble (**Moens et al., 1992**), clay or obsidian (**Pollard and Heron, 1996**), tracking roasted and smelted metals back to their raw materials, i.e. iron ore, by directly comparing geochemical contents of major, trace or rare earth elements is generally considered to be extremely difficult, and in some cases, impossible. Major obstacle to successfully tracing selected elements from raw material to roasted and smelted material lies in carefully selecting and predicting thermal behaviour of observed elements. In this study, provenance analysis was conducted in two steps, firstly by establishing geochemical and genetic link between raw bog iron ore and roasted iron ore, and then establishing the connection towards iron slags.

Several groups of secondary minerals, such as Fe- and Mn-oxides/oxyhydroxides, clay minerals, resistant and relict rock-forming minerals can incorporate trace and REEs. To determine which mineral phase controls the distribution of trace and REEs, a correlation analysis between major oxides and selected trace and REEs inside bog iron ore and roasted iron ore was conducted. Geochemical correlation and connection of major oxides with selected trace and rare earth elements for all three bog iron types was analysed using hierarchical clustering analysis (HCA). This statistical classification of samples and geochemical variables is based on visual observation of constructed dendrograms (**Brenko et**

al., 2021a). For all three bog iron types, a clear differentiation into two geochemically different clusters was observed. One cluster consists of Fe and selected redox-sensitive elements (Mn, As and P), while other cluster consists of remaining major oxides, trace and rare earth elements. The constructed dendrograms have twofold meaning. Firstly, this distribution confirms that Fe and other redox-sensitive elements were transported into soil-bog ore system, as stated in the bog iron ore formation theory (**Banning et al., 2013; Ramanaidou and Wells, 2014, Thelemann et al., 2017**). Secondly, based on the data clustering, it can be observed that trace and rare earth element contents in bog iron ore were inherited from soil and clay minerals found in soil. Therefore, trace and rare earth elements could be used to create a geographical and geochemical signature of proposed ore material that could be used towards determining provenance of archaeological samples of roasted iron ore and iron slags.

Experimental reconstruction of roasting processes in the study area (**Karavidović, 2020**) points to average temperatures in the 500–650 °C interval, with the maximum temperature of 1038 °C. Therefore, to determine mobility of selected trace and rare earth elements with regards to roasting temperatures, experimental roasting of three bog iron ore types was conducted. Experimentally roasted samples were also mineralogically and geochemically analysed and plotted on appropriate diagrams. The normalized trace and REE patterns between different bog iron ore types, experimentally roasted samples and samples of archaeological roasted iron ore are generally identical in their shape, implying a similar genetic origin. Similar positions and heights of several characteristic peaks, such as the positive P and Sm anomalies and the negative Rb and Ti anomalies, points to their mutual link, i.e., that the archaeological samples of roasted iron ore were formed due to the roasting of bog iron ore from the study area. Smaller differentiation in trace and REE patterns is noticeable for bog iron fragments from Novigrad Podravski-Milakov Berek location. They exhibit positive Eu anomaly, as opposed to negative Eu anomaly visible on patterns of bog iron soils, nodules and other fragments, and they also have significantly higher positive Ba anomaly. Positive Eu anomaly is in correlation with calcite mineral in the samples as some studies suggest that Eu^{2+} and Eu^{3+} can be incorporated into calcite structure (**Lakshtanov and Stipp, 2004; Hellebrandt et al., 2017**). On the other hand, according to SEM-EDS analysis, Ba contents are proportionally related to Mn contents in the bog iron ore. As determined previously, bog iron ore at Novigrad Podravski site were under different Eh/pH conditions than other sites, which resulted in higher Mn, and consequently higher Ba contents. This

implies that bog iron ore fragments discovered at Novigrad Podravski site were most likely not used for roasting and iron production in the study area.

Similar provenance methodology was proposed for iron slag provenance. However, as iron slags are formed at significantly much higher temperatures (1200 °C compared to 600 °C), under variable conditions inside the furnace and as a result of a different smelting and smiting processes, some degree of mobility and geochemical differentiation is to be expected, especially when considering incompatible elements that can be mobilised under high temperatures (**Rollins, 1993**). Therefore, pairs of selected incompatible trace elements were plotted on biplot diagrams (**Brenko et al., 2021b**) (**Figure 3-4**). Visual observation of element pairs points to differentiation according to slag types, with furnace bottom slags and tap slags having higher contents of selected trace and REEs than bloom refining slags. This geochemical differentiation is well in line with expected behaviour of incompatible elements during smelting and smiting processes. Incompatible elements are one of the first groups of elements that will be incorporated into the liquid phase. During smelting, tap slag has the lowest viscosity, and will more readily incorporate incompatible elements, while furnace bottom slag, as a moderately viscous phase, will incorporate moderate contents of incompatible elements. Bloom refining slag is formed during primary and secondary smiting process while refining iron bloom. Iron bloom incorporates compatible elements, such as siderophile elements Cr, V and Ni, thus reducing available positions for incompatible elements (**Navasaitis et al., 2010; Brenko et al., 2021b**).

Based on this geochemical differentiation, only tap slags and furnace bottom slags were further considered in the provenance study. In the ideal case, slags would be compared to ore samples from the same location, age and context. This is rarely possible as the primary raw materials are often not found during archaeological excavations. However, in the case of Hlebine-Velike Hlebine, geochemical signature of slag samples could be compared to signatures of two roasted ore samples from the same context (H-VH 1 and H-VH 2) and four concurrent roasted ore samples from nearby Hlebine-Dedanovice site. Slag samples from Virje-Sušine site were compared to the bog iron ore found during archaeological survey and to bog iron ores from Novigrad Podravski-Milakov Berek. Virje-Sušine slags were also compared to roasted iron ore samples found in features within a settlement context dated to 8/9th centuries, that is spatially connected to the concurrent iron production workshop from which the analysed slag originates.

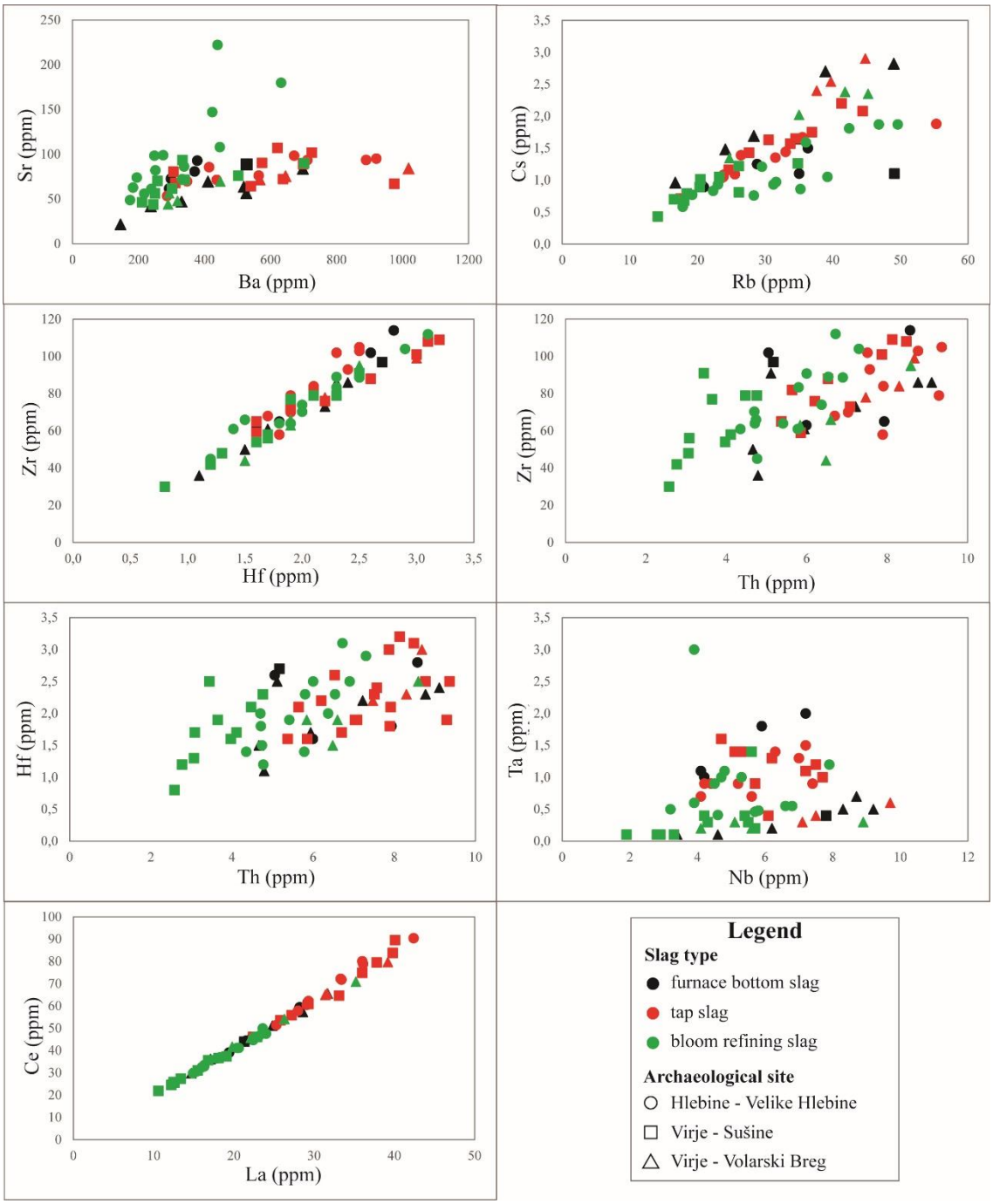

Figure 3-4. Trace and REE pairs diagrams for iron slags in the Podravina region (modified according to **Brenko et al., 2021b**)

When comparing geochemical signatures from all three archaeological sites, similar peaks and shapes can be recognized. One such characteristic peak is the high positive phosphorus peak recognizable in both ores and slags. Phosphorus is often associated with bog iron ore, where it can be present in significant quantities (**Stoops, 1983; Landuydt, 1990; Török & Thiele, 2013; Thelemann et al., 2017**). This is a strong indication of bog iron ore usage for iron production in the study area. On the other hand, some variability is noticeable,

especially with regards to Cs, Rb, K and Ba. These elements are often found in variable contents in soils and in clay minerals (**Maes et al., 1999; Gingele & De Decker, 2007; Zaunbrecher et al., 2015; Fuller et al., 2015**), with similar behaviour detected in the soils of the Podravina region (**Brenko et al., 2020**). Therefore, some variability in geochemical signature is possible, and expected, especially when the soils in which the ore is forming are under the influence of groundwater fluctuation with constant redox changes. SEM-EDS confirmed that barium is associated with Mn phase, whose contents are variable under different Eh/pH conditions, therefore, variability in Ba contents is also expected. However, REE part of the plotted diagrams is equivalent between ores and slags, indicating genetic connection between the two sample types.

Therefore, it can be safely proposed that bog iron ore was the primary raw ore material used for iron production in the Podravina region during Late Antique and Early Middle Age periods.

4. CONCLUSION

In the Podravina region, previous archaeological surveys and excavations led to discoveries of various types of iron slags, roasted iron ore and furnace materials, indicating that iron was locally produced in the area. Based on the archaeological context, iron was produced via direct process, i.e. bloomery smelting during Late Antiquity and Early Middle Ages. Although previous geological surveys did not recognize occurrences of iron ore in the region, geological, hydrogeological and pedological characteristics in the region pointed to possible bog iron ore occurrences. Therefore, over 50 soil profiles were drilled and five Gleysols and one Fluvisol located on second Drava River terrace were chosen and analysed due to visual Fe accumulations through the profiles. All profiles are characterized with greyish bottom parts, indicating gley horizon, and light to dark brown upper parts with signs of Fe accumulation as precipitations on soil particles in the form of soft masses or pore linings. Mineral analysis revealed presence of goethite alongside typical soil minerals, such as quartz, feldspars, clay minerals and micas. Geochemical analysis confirmed elevated Fe_2O_3 contents in each analysed soil profile, with the middle part of Kalinovac-Hrastova Greda profile reaching 31.52 mass. % Fe_2O_3. Therefore, it is believed that Kalinovac profile represent currently forming bog iron ore deposit, where groundwater fluctuation between 10 and 100 cm enables Fe precipitation due to the reaction of Fe^{2+} with available oxygen.

Established formation mechanism is well in line with the bog iron ore types discovered in the study area. Bog iron soils, nodules and fragments correspond to the three bog iron ore formation phases, with bog iron soils being the first, and bog iron fragments being the final phase. All three types are characterized with goethite and quartz as the main minerals. Goethite quantities increase from the soil phase to the fragment phase, while vice-versa is detected for quartz. Geochemical composition revealed Fe_2O_3 and SiO_2 as the two main oxides, with varying iron-silicon ratios, increasing from the soils to the fragment samples, indicating different phases of the cementation process during formation. SEM-EDS analysis pointed out the presence of Fe and Mn laminas, confirming seasonal precipitation and cementation due to variable groundwater table formation mechanism. Analyses on the bog iron fragments from the Novigrad Podravski-Milakov Berek revealed presence of pyrolusite, an Mn-oxyhydroxide, and high MnO contents which implies that this site underwent a different bog iron ore formation due to the locally different Eh/pH conditions that led to variable Fe and Mn enrichments.

Mineral analysis of roasted iron ore from four archaeological sites confirmed abundance of several Fe minerals, with hematite being the most common, forming directly from goethite due to exposure to temperatures above 300 and below 1000 °C, with average temperature in the 500–650 °C interval. Geochemical analysis revealed variable contents of Fe_2O_3 and other major oxides at different sites, pointing to spatial and temporal variability in the used raw material. Roasted iron ore from Virje-Sušine site, which is several hundred meters away from the Novigrad Podravski site, points to local exploitation of available ore, as both bog iron ore from Novigrad Podravski and Virje-Sušine have increased Mn contents.

Two slag types from three archaeological sites were analysed: tap slag and furnace bottom slag, distinguished by their morphology, with tap slag having recognizable flow texture on their upper surface, and furnace bottom slag usually being concave in shape. Both slag types contain fayalite as the main mineral, formed in the thermal reaction between Fe-oxide/oxyhydroxide and silica from the iron ore. Occurrences of wüstite, hematite and magnetite point to some variability and redox changes during the smelting process. Contents of Fe_2O_3 and SiO_2 show similar contents between the sites, while elevated Al_2O_3 contents at Virje-Volarski Breg site indicates higher clay contents in the ore used at this site. However, as the compared ore and slag samples are dated to different periods, this Al differentiation could be connected to similar micro-enviromental conditions, presumably in the surroundings of the Virje-Volarski breg site, implying temporal variability in the used ore.

Provenance study was performed in two steps, firstly between bog iron ore and roasted iron ore, and then establishing iron slags provenance towards both bog iron and roasted iron ore. Hierarchical analysis of bog iron ore indicates that Fe, Mn and other redox sensitive elements were transported into the soil system by groundwater, and therefore have no control on the majority of the primary trace and REEs geochemical signatures. Normalization of trace and REEs contents in bog iron ore and roasted iron ore and their subsequent plotting on appropriate diagrams indicates similar geochemical signatures with characteristic shapes, such as positive P and Sm peaks, and negative Rb and Ti peaks. Based on plotting of pairs of selected trace elements, similar methodology was undertaken for iron slags provenance. Selected 26 trace and REEs were used to construct geochemical signatures of slags from three archaeological sites. Similar peaks, such as high positive P peak, were recognized, implying bog iron ore usage, while similar shape of the REE part of the plotted diagrams confirmed geochemical and genetic connection to the study area. Therefore, it was confirmed that bog iron ore was used as the primary raw ore material for iron production during Late Antique and Early Middle Ages in the Podravina region.

5. LITERATURE

Anders, E. & Grevesse, N. (1989) Abundances of the elements: Meteoric and solar. Geochimica et Cosmochimica Acta, 53, 197–214.

Atta S.K., Mohammed, S.A., Van Cleemput, O. & Zayed, A. (1996) Transformations of iron and manganese under controlled Eh, Eh-pH conditions and addition of organic matter. Soil Technology, 9(4), 223–237.

Banning, A. (2008) Bog Iron Ores and their Potential Role in Arsenic Dynamics: An Overview and a „Paleo Example". Engineering in Life Science 8(6), 641-649.

Banning, A., Rüde, T.R. & Dölling, B. (2013) Crossing redox boundaries – aquifer redox history and effects on iron mineralogy and arsenic availability. Journal of Hazardous Materials, 15, 905–914.

Blakelock, E., Martinón-Torres, M., Veldhuijzen, H.A. & Young, T. (2009) Slag inclusions in iron objects and the quest for provenance: an experiment and a case study. Journal of Archaeological Science, 36, 1745–1757.

Brenko, T., Borojević Šoštarić, S., Ružičić, S. & Sekelj Ivančan, T. (2020) Evidence for the formation of bog iron ores in the soils of the Podravina region, NE Croatia: Geochemical and mineralogical study. Quaternary International, 536, 13–29.

Brenko, T., Borojević Šoštarić, S., Karavidović, T., Ružičić, S. & Sekelj Ivančan, T. (2021a) Geochemical and mineralogical correlations between the bog iron ores and roasted iron ores of the Podravina region, Croatia. Catena, 204, 105353.

Brenko, T., Borojević Šoštarić, S. & Ružičić, S. (2021b) Mineralogical and Geochemical Characterization of Selected Bog Iron Ores and Archaeological Samples of Roasted Iron Ores and Iron Slags Towards Their Provenance Studies in the Podravina Region. In: Sekelj Ivančan, T. & Karavidović, T. (eds.) Interdisciplinary Research into Iron Metallurgy along the Drava River in Croatia - The TransFER Project, Oxford: Archaeopress, 92–100.

Brenko, T., Karavidović, T., Borojević Šoštarić, S. & Sekelj Ivančan, T. (2022) Geochemical and mineralogical characterization of iron slags towards their provenance studies in the Podravina region, NE Croatia. Geologia Croatica, 75/1.

Breuning-Madsen, H., Rønsbo, J. & Holst, M.K. (2000) Comparison of the composition of iron pans in Danish burial mounds with bog iron and spodic material. Catena, 39, 1–9.

Bricker, O.P., Newell, W.L. & Simon, N.S. (2003) Bog iron formation in the Nassawango watershed, Maryland. Gordon Conference on Catchment Science: Interactions of Hydrology, Biology and Geochemistry, 7.

Brkić, Ž. & Briški, M. (2018) Hydrogeology of the western part of the Drava Basin in Croatia. Journal of Maps, 14(2), 173–177.

Buchwald, V.F. & Wivel, H. (1998) Slag Analysis as a Method for the Characterization and Provenancing of Ancient Iron Objects. Materials Characterization, 40/2, 73–96.

Buchwald, V.F., 2005. Iron and Steel in Ancient Times. The Royal Danish Academy of Sciences and Letters, Copenhagen.

Charlton, M.F., Crew, P., Rehren, T.H. & Shennan, S.J. (2010) Explaining the evolution of ironmaking recipes–an example from northwest Wales. Journal of Anthropological Archaeology, 29, 352–367.

Charlton, M.F., Blakelock, E., Martinón-Torres, M. & Young, T. (2012) Investigating the production provenance of iron artifacts with multivariate methods. Journal of Archaeological Science, 39, 2280–2293.

Charlton, M.F. (2015) The last frontier in “sourcing”: The hopes, constraints and future for iron provenance research. Journal of Archaeological Science, 56, 210–220.

Church, S.E., Kimball, B.A., Fey, D.L., Ferderer, D.A., Yager, T.J., & Vaughn, R.B. (1997) Source, transport, and partitioning of metals between water, colloids, and bed sediments of the Animas River, Colorado: U.S. Geological Survey Open-File Report 97–151, 135.

Coustures, M.P., Béziat, D. & Tollon, F. (2003) The use of trace element analysis of entrapped slag inclusions to establish ore – bar iron links: examples from two Gallo-roman iron-making sites in France (Les Martys, Montagne Noire, and Les Ferrys, Loiret). Archaeometry, 45, 599–613.

Coustures, M.P., Rico, C., Béziat, D., Djaoui, D., Long, L., Domergue, C. & Tollon, F. (2006) La provence des barres de fer Romaines des Saintes-Maries-De-La-Mer (Bouches-Du_Rhône). Gallia 63, 243–261.

Crerar, D.A., Knox, G.W. & Means, J.L. (1979) Biogeochemistry of bog iron of the New Jersey Pine barrens. Chemical Geology, 24, 111–135.

Crew, P. & Charlton, M. (2007) The anatomy of a furnace ... and some of its ramifications. In: La Niece, S., Hook, D., Craddock, P. (eds.) Metals and Mines: Studies in Archaeometallurgy. Archetype Publications/British Museum, 219–225.

Crew, P., Charlton, M., Dillmann, P., Fluzin, P., Salter, C. & Truffaut, E. (2011) Cast iron from a bloomery furnace. In: Hosek, J., Cleere, H. & Mihok, L. (eds.) The Archaeometallurgy of Iron. Institute of Archaeology of the ASCR, Prague, 239–262.

Crew, P. (2000) The influence of clay and charcoal ash on bloomery slags. In Tizzoni, C.C. & Tizzoni M. (eds.) Iron in the Alps: Deposits, Mines and Metallurgy from Antiquity to the XVI Century, Bienno, 38–48.

Cudennec, Y. & Lecerf, A. (2005) Topotactic transformations of goethite and lepidocrocite into hematite and maghemite. Solid State Science, 7, 520–529.
De Geyter, G., Vandengerghe, R.E., Verdonck, L. & Stoops, G. (1985) Mineralogy of holocene bog-iron ore in northern Belgium. Neues Jahrbuch fuer Mineralogie, 153, 1–17.

Desai, M. (2018) An Overview of Iron Provenance and Its Possible Extension to Crucible Steel Archaeometallurgy. Heritage: Journal of Multidisciplinary Studies in Archaeology, 6, 926–944.

Desaulty, A-M., Dillmann, P., L'Héritiera, M., Mariet, C., Gratuze, B., Joron, J-L. & Fluzin, P. (2009) Does it come from the Pays de Bray? Examination of an origin hypothesis for the ferrous reinforcements used in French medieval churches using major and trace element analyses. Journal of Archaeological Science, 36, 2445–2462.

Długosz, J., Kalisz, B. & Łachacz, A. (2018) Mineral matter composition of drained floodplain soils in north-eastern Poland. Soil Science Annual, 69(3), 184–193.

Fuller, A.J., Shaw, S., Ward, M.B., Haigh, S.J., Mosselmans, F.W., Peacock, C.L. Stackhouse, S., Dent, A.J., Trivedi, D. & Burke, I.T. (2015) Caesium incorporation and retention in illite interlayers. Applied Clay Science, 108, 128–134.

Gingele, F.X. & De Deckker, P. (2007) Clay mineral, geochemical and Sr-Nd isotopic fingerprinting of sediments in the Murray-Darling fluvial system, southeast Australia. Australija Journal of Earth Sciences, 52, 965–974.

Gömöri, J. (2006) The Bloomery Museum at Somogyfajsz (Hungary) and some Archaeometallurgical Sites in Pannonia from the Avar- and Early Hungarian Period. Journal of Metallurgy. Association of Metallurgical Engineers of Serbia, 183–196.

Gordon, R.B. & van der Merwe, N.J. (1984) Metallographic study of iron artefacts from the eastern Transvaal, South Africa. Archaeometry, 26, 108–127.

Habuda-Stanić, M., Santo, V., Sikora, M. & Benkotić, S. (2013) Microbiological quality of drinking water in public and municipal drinking water supply systems in Osijek-Baranja County, Croatia. Croatian Journal of Food Science and Technology, 5, 61–69.

Halamić, J., Galović, L., Šparica Miko, M. (2003) Heavy Metal (As, Cd, Cu, Hg, Pb and Zn) Distribution in Topsoil Developed on Alluvial Sediments of the Drava and Sava Rivers in NW Croatia. Geologia Croatica, 56(2), 215–232.

Haubner, R., Schatz, I., Schatz, F., Scheiblechner, W., Schubert, W.D. & Strobl, S. (2014) Archaeometallurgical Simulations of the Processes in Bloomery Furnaces from the Hallstatt and Medieval Period. Materials Science Forum, 782, 641–644.

Hedges, R.E.M. & Salter, C.J. (1979) Source determination of iron currency bars through analysis of the slag inclusions. Archaeometry, 22, 161–175.

Hellebrandt, S.E., Hofmann, S., Jordan, N., Barkleit, A. & Schmidt, M. (2017) Incorporation of Eu(III) into Calcite under Recrystallization conditions. Scientific Reports, 6, 33137.
Hem, J.D. (1963) Chemical equilibria affecting the behaviour of manganese in natural water. Hydrological Sciences Journal, 8(3), 30–37.

Humpris, J., Charlton, M., Keen, J., Sauder, L. & Alshishani, F. (2018) Iron Smelting in Sudan: Experimental Archaeology at The Royal City of Meroe. Journal of Field Archaeology, 43/5, 399–416

Husnja, S. (2014) Sistematika Tala Hrvatske (*eng.* Soil Systematics of Croatia) [*in Croatian*]. Hrvatska sveučilišna naklada, Zagreb, 373.

Kaczorek, D. & Sommer, M. (2003) Micromorphology, chemistry and mineralogy of bog iron ores from Poland. Catena, 54, 393–402.

Kaczorek, D. & Zagórski, Z. (2007) Micromorphological characteristics of the bsm horizon in soils with bog iron ore. Polish Journal of Soil Science, 40, 81–87.

Kaczorek, D., Sommer, M., Andruschkewitsch, I., Oktaba, L., Czerwinski, Z. & Stahr, K., (2004) A comparative micromorphological and chemical study of „Rasseneisenstein "(bog iron ore) and „Ortstein". Geoderma, 121, 83–94.

Kądziołka, K., Pietranik, A., Kierczak, J., Potysz, A. & Stolarczyk, T. (2020) Towards better reconstruction of smelting temperatures: Methodological review and the case of historical K-rich Cu-slags from the Old Copper Basin, Poland. Journal of Archaeological Science, 118, 105142.

Karavidović, T. (2020) Rekonstrukcija postupka prženja rude: eksperimentalni pristup [*in Croatian*]. In Vitezović, S., Antonović, D. & Šarić, K. (eds.) Aktuelna interdisciplinarna istraživanja tehnologije u arheologiji Jugoistočne Europe, Zbornik radova prvog skupa sekcije

za arheometriju, arheotehnologiju i eksperimentalnu arheologiju Srpskog arheološkog društva, 130–137.

Killick, D. (2004) Social constructionist approaches to the study of technology. World Archaeology, 36, 571–578.

Kongoli, F. & Yazawa, A. (2001) Liquidus surface of FeO-Fe_2O_3-SiO_2-CaO slag containing Al_2O_3, MgO, and Cu_2O at intermediate oxygen partial pressures. Metallurgical and Materials Transactions B, 32, 583–592.

Kopić, J., Loborec, J. & Nakić, Z. (2016) Hydrogeological and hydrogeochemical characteristics of a wider are of the regional well field Eastern Slavonia – Sikirevci. The Mining-Geology-Petroleum Engineering Bulletin, 31(3), 47–66.

Lakshtanov, L.Z. & Stipp, S.L.S. (2004) Experimental study of europium (III) coprecipitation with calcite. Geochimica et Cosmochimica Acta, 68, 819–827.

Landuydt, C.J. (1990) Micromorphology of iron minerals from bog ores of the Belgian Campine area. Developments in Soil Science, 19, 289–294.

Leroy, S., Cohen, S.X., Verna, C., Gratuze, B., Téreygeol, Fluzin, P., Bertrand, L. & Dillmann, P. (2012) The medieval iron market in Ariège (France). Multidisciplinary analytical approach and multivariate analyses. Journal of Archaeological Science, 39, 1080–1093.

Ling, J., Hjärthner-Holdar, E., Grandin, L., Billström, K. & Persson, P.O. (2013) Moving metals or indigenous mining? Provenancing Scandinavian Bronze Age artefacts by lead isotopes and trace elements. Journal of Archaeological Science, 40, 291–304.

Ling, J., Stos-Gale, Z. A., Grandin, L., Billström, K., Hjärthner-Holdar, E. & Persson, P.O. (2014) Moving metals II: Provenancing Scandinavian Bronze Age artefacts by lead isotope and elemental analyses. Journal of Archaeological Science, 41, 106–132.

Lóczy, D. (2013) Hydrogeomorphological-geoecological foundations of floodplain rehabilitation: Case study from Hungary. Lambrecht Academic Publishing, Saarbrücken. 382.

Lóczy, D., Dezső, J., Czigány, S., Gyenizse, P., Pirkhoffer, E. & Halász, A. (2014) Rehabilitation potential of the Drava River floodplain in Hungary. 2nd International Water Resources and Wetlands. Conference Paper.

Madera, P., Kik, D. & Suliga I. (2018) Slag-pit bloomery furnace of the Tarchalice type Reconstruction and experimental research. Archeologické rozhledy, 70, 435–449.

Maes, E., Iserentant, A., Herbauts, J. & Delvaux, B. (1999) Influence of the nature of clay minerals on the fixation of radiocaesium traces in an acid brown earth-podzol weathering sequence. European Journal of Soil Science, 50, 117–125.

Manasse, A. & Mellini, M. (2002) Chemical and textural characterization of medieval slags from the Massa Marittima smelting sites (Tuscany, Italy). Journal of Cultural Heritage, 3, 187–198.

Mansfeldt, T., Schuth, S., Häusler, W., Wagner, F.E. & Kaufold, S., 2012. Iron oxide mineralogy and stable iron isotope composition in a Gleysol with petrogleyic properties. Journal of Soils and Sediments, 12(1), 97–114.

Moens, L., Roos, P., De Paepe, P. & Scheurleer, R. L. (1992) Provenance determination of white marble sculptures from the Allard Pierson Museum in Amsterdam, based on chemical, microscopic and isotopic criteria. In: Waelkens, M., Herz, N. & Moens, L. (eds.) Ancient stones: Quarrying, trade and provenance, 269–276, Acta Archaeologica Lovaniensia Monographiae, Leuven University Press, Leuven

Mušić, B. & Horn, B. (2021) Results of Geophysical Investigations Related to the Excavated Remains of the Late Antique and Early Mediaeval Iron Production Sites in the Podravina Region, Croatia. In: Sekelj Ivančan, T. & Karavidović, T. (eds.): Interdisciplinary Research into Iron Metallurgy along the Drava River in Croatia - The TransFER Project, Oxford: Archaeopress, 18−42.

Nádaská, G., Lesnỳ, J. & Michalík, I. (2012) Environmental aspect of manganese chemistry. Hungarian Electronic Journal of Sciences. http://heja.szif.hu/ENV/ENV-100702-A/env100702a.pdf. Accessed 07.12.2021.

Navasaitis, J., Selskienė, A. & Žaldarys, G. (2010) The Study of Trace Elements in Bloomery Iron. Materials Science, 16(2), 113–118.

Paynter, S., 2006. Regional variations in bloomery smelting slag of the Iron Age and Romano-British periods. Archaeometry, 48, 271–292.

Pinney, N., Kubicki, J.D., Middlemiss, D.S., Grey, C.P. & Morgan, D. (2009) Density Functional Theory Study of Ferrihydrite and Related Fe-oxyhydroxides. Chemistry of Materials, 21(24), 5727–5742.

Pleiner, R. (2000) Iron in Archaeology. The European Bloomery Smelters. Archeologický ústav AV CR, Prague, 400.

Pollard, M. & Heron, C. (1996): Archaeological Chemistry. Royal Society of Chemistry, Cambridge, 456.

Postawa, A., Hayes, C., Criscuoli, A., Macedonio, F., Angelakis, A., Rose, J. & McAvoy, D. (2013) Best Practice Guide on the Control of Iron and Manganese in Water Supply (1st ed.). IWA Publishing, 96.

Ramanaidou, E. & Wells, M.A. (2014) 13.13 - Sedimentary Hosted Iron Ores In: Holland, H.D. & Turekian, K.K. (eds.) Treatise on Geochemistry, 2nd ed., Elsevier, Oxford, 313–355.

Ratajczak, T. & Rzepa, G. (2011) Lokalne Kopaliny Mineralne Mineralne A Możliwości Ich Wykorzystania W Ochronie Środowiska (Na Przykładzie Mazurskich Rud Darniowych) [*in Polish*]. Inżynieria Ekologiczna 27, 161–169.

Rehren, T., Charlton, M., Chirikure, S., Humphris, J., Ige, A. & Veldhuijzen, H.A. (2007) Decisions set in slag: the human factor in African iron smelting. In: La Niece, S., Hook, D.R.

& Craddock, P.T. (eds.) Metals and Mines – Studies in Archaeometallurgy. Archetype, British Museum, London, 211–218.

Rehren, T. (2001) Aspects of the production of cobalt-blue glass in Egypt. Archaeometry, 43, 483–489.

Robion-Brunner, C. (2020) What Is the Meaning of the Extreme Variability of Ancient Ironworking in West Africa?. Mobile Technologies in the Ancient Sahara and Beyond, Cambridge University Press, 290-314.

Rollins, H. (1993) Using geochemical data (1st ed.). London, United Kingdom, 384.

Rudnick, R.L. & Gao, S. (2003) Composition of the continental crust. Treatise on Geochemistry, 3, 1–64.

Rzepa, G., Bajda, T., Gaweł, A., Debiec, K. & Drewniak, L. (2016) Mineral transformations and textural evolution during roasting of bog iron ores. Journal of Thermal Analysis and Calorimetry, 123, 615–630.

Scheinhost, A.C. & Schwertmann, U. (1999) Color Identification of Iron Oxides and Hydroxysulfates. Soil Science Society of America Journal, 63(5), 1463–1471.

Scheinost, A.C. (2005) Metal oxides. In: Hillel, D. (ed.) Encyclopedia of Soils in the Environment, Elsevier, Oxford, 425–438.

Schwab, R., Heger, D., Höppner, B. & Pernicka, E. (2006) The provenance of iron artefacts from Manching: a multi-technique approach. Archaeometry, 48, 433–452.

Schwertmann, U. & Fitzpatrick, R.W. (1992) Iron Minerals in Surface Environments. Catena, 21, 7–30.

Sekelj Ivančan, T. & Karavidović, T. (2021) Archaeological Record of Iron Metallurgy Along the Drava River. In: Sekelj Ivančan, T. & Karavidović, T. (eds.): Interdisciplinary Research

into Iron Metallurgy along the Drava River in Croatia - The TransFER Project, Oxford: Archaeopress, 43−91.

Sekelj Ivančan, T. (2014) Četvrta sezona arheoloških istraživanja nalazišta Virje – Volarski breg/Sušine. Annales Instituti Archaeologici, 10, 99–103.

Sekelj Ivančan, T. (2015) Arheološki ostaci triju naselja na Sušinama u Virju. Annales Instituti Archaeologici, 11, 50–53.

Sekelj Ivančan, T. & Marković, T. (2017) The primary processing of iron in the Drava River basin during the late Antiquity and the early Middle Ages – the source of raw materials. In: Vitezović, S. & Antonović, D. (eds.) Archaeotechnology studies: Raw material exploitation from prehistory to the Middle Ages, 143–160.

Serneels, V. & Crew, P. (1997) Ore-slag relationship from experimentally smelted bog-iron ore. Abstracts: Early Ironworking in Europe, archaeology and experiment Plas Tan y Bwlch, 78–82.

Sokolova, T.A., Tolpeshta, I.I., Rusakova, E.S. & Maksimova, Y.G. (2013) Clay minerals in the Stream Floodplain Soils in the Undisturbed Landscapes of the Southern Taiga (with the Soil of the State Central Forest Nature and Biosphere Reserve as an example. Moscow University Soil Science Bulletin, 68(4), 154–163.

Stanton M.R., Yager, D.B., Fey, D.L. & Wright, W.G. (2007) Formation and Geochemical Significance of Iron Bog Deposits. In: Church, S.E., von Guerard, P. & Finger, S.E. (eds.) Integrated Investigations of Environmental Effects of Historical Mining in the Animas River Watershed, San Juan County, Colorado, 693–720.

Starley, D. (1999) Determining the technological origins of iron and steel. Journal of Archaeological Science, 26, 1127–1133.

Stoops, G. (1983) SEM and light microscopic observations of minerals in bog-ores of the Belgian Campine. Geoderma, 30, 179–186.

Stos-Gale, Z.A. & Gale, N.H. (2009) Metal provenancing using isotopes and the Oxford archaeological lead isotope database (OXALID). Archaeological and Anthropological Sciences, 1, 195–213.

Taylor, S.R. & McLennan, S.M. (1995) The Geochemical Evolution of the Continental Crust. Reviews of Geophysics, 33, 241–265.

Thelemann, M., Bebermeier, W., Hoelzmann, P. & Lehnhardt, E. (2017) Bog iron ore as a resource for prehistoric iron production in Central Europe – A case study of the Widawa catchment area in eastern Silesia, Poland. Catena, 149, 474–490.

Thiele, A. (2010) Smelting experiments in the early medieval fajszi-type bloomery and the metallurgy of iron bloom. Periodica Polytechnica Mechanical Engineering, 54, 99–104.

Török, B. & Kovács, Á. (2010) Crystallization of Iron Slags Found in Early Medieval Bloomery Furnaces. Materials Science Forum, 649, 455–460.

Török, B., Kovács, Á. & Gallina, Zs. (2015) Ironmetallurgy of the Pannonian Avars of the 7–9th century based on excavations and material examinations. Der Anscnhitt, 26, 229–237.

Valent, I., Zvijerac, I. & Sekelj Ivančan, T. (2017) Topografija arheoloških lokaliteta s talioničkom djelatnošću na prostoru Podravine [*in Croatian*]. Podravina, 16 (32), 5–25.

Valent, I. (2021): Archaeological Finds of Metallurgical Activities on the Territory of the River Drava Basin During Iron Age and Antiquity. In Sekelj Ivančan, T., Karavidović, T., Tkalčec, T., Krznar, S. & Belaj, J. (eds.) Secrets of iron - from raw material to an iron object, Proceedings of the 7th International Scientific Conference on Mediaeval Archaeology of the Institute of Archaeology, Serta Instituti Archaeologici, Zagreb: Institut za arheologiju.

Veldhuijzen, H.A. & Rehren, T. (2007) Slags and the city: early iron production at Tell Hammeh, Jordan, and Tel Beth-Shemesh, Israel. In: La Niece, S., Hook, D., Craddock, P. (eds) Metals and Mines: Studies in Archaeometallurgy. Archetype Publications, London, pp. 189–201.

Veldhuijzen, H.A. (2005). Technical ceramics in early iron smelting. The role of ceramics in the early first millennium BC iron production at Tell Hammeh (az-Zarqa), Jordan. In: Prudencio, I., Dias, I., Waerenborgh, J.C. (eds.) Understanding People Through Their Pottery: Proceedings of the Seventh European Meeting on Ancient Ceramics (EMAC '03). Instituto Portugue's de Arqueologia (IPA), Lisboa, 295–302.

Vodyanitskii, Y.N. (2010) Iron Minerals in Urban Soils. Eurasian Soil Science, 43(2), 1410–1417.

Wilson, L. & A.M. Pollard. (2001) The provenance hypothesis. In: Brothwell D.R. & Pollard A.M. (eds) Handbook of archaeological sciences, Chichester: John Wiley & Sons, Ltd, 507–517.

Young, T. (2010) Analysis of bog iron ore from Littleton Manor, Reigate, Surrey. GeoArch Report, 1–12.

Zaunbrecher, L.K., Crawford Elliott, W., Wampler, J.M., Perdrial, N. & Kaplan, D.I. (2015) Enrichment of Cesium and Rubidium in Weathered Micaceous Materials at the Savannah River Site, South Carolina. Environmental Science & Technology, 49, 4226–4234.

6. BIOGRAPHY OF THE AUTHOR

Tomislav Brenko was born on September 21, 1991 in Zagreb. After finishing elementary school, he attended 9. gymnasium in Zagreb. In 2010 he started the undergraduate studies of Geological Engineering at the Faculty of Mining, Geology and Petroleum Engineering, which he graduated in 2013. At the same Faculty, in 2015, he graduated with excellent results and highest honours - Summa cum laude - in Geology of Mineral Resources and Geophysical Exploration. He received the Rector's Award for a research paper on the paleolimnological reconstruction of Modro Jezero, and two Dean's Awards for academic achievements in the academic years 2013/14 and 2014/15. After graduation, he worked as an assistant at the Department of Mineralogy, Petrology and Mineral Resources and in 2016 he started postgraduate studies in Applied Geosciences, Mining and Petroleum Engineering.

As a teaching assistant at the Department of Mineralogy, Petrology and Mineral Resources, he holds exercises in Optical Mineralogy and Systematic Mineralogy. He assisted students in writing four master's theses and seven bachelor's theses. As an author, he published five papers indexed in Web of Science and Scopus databases and one chapter in a book. He has been a member of the Croatian Geological Society since 2016.
Since 2019 he has also been working on international research project "iTARG3T: Innovative targeting & processing of W-Sn-Ta-Li ores: towards EU's self-supply", financed by the European Institute of Innovation and Technology (EIT Raw Materials).

List of published papers and chapters:

- Brenko, T., Karavidović, T., Borojević Šoštarić, S. & Sekelj Ivančan, T. (2022) Geochemical and mineralogical characterization of iron slags towards their provenance studies in the Podravina region, NE Croatia. Geologia Croatica, 75/1.
- Brenko, T., Borojević Šoštarić, S. & Ružičić, S. (2021b) Mineralogical and Geochemical Characterization of Selected Bog Iron Ores and Archaeological Samples of Roasted Iron Ores and Iron Slags Towards Their Provenance Studies in the Podravina Region. In: Sekelj Ivančan, T. & Karavidović, T. (eds.) Interdisciplinary Research into Iron Metallurgy along the Drava River in Croatia - The TransFER Project, Oxford: Archaeopress, 92–100.
- Brenko, T., Borojević Šoštarić, S., Karavidović, T., Ružičić, S. & Sekelj Ivančan, T. (2021a) Geochemical and mineralogical correlations between the bog iron ores and

roasted iron ores of the Podravina region, Croatia. Catena, 105353.

- Brenko, T., Borojević Šoštarić, S., Ružičić, S. & Sekelj Ivančan, T. (2020) Evidence for the formation of bog iron ore in soils of the Podravina region, NE Croatia: Geochemical and mineralogical study. Quaternary International 536, 13–29.
- Bevandić, S., Brenko, T., Babajić, E. & Borojević Šoštarić, S. (2018) Formation mechanisms of Fe-Mn concretions in the Vijenac Quarry, Dinaric Ophiolite Zone. Rudarsko-geološko-naftni zbornik, 33, 63–74.
- Orlović-Leko, P., Omanović, D., Ciglenečki, I., Vidović, K. & Brenko, T. (2017) Application of electrochemical methods in the physicochemical characterization of atmospheric precipitation. Bulgarian Chemical Communications, 49, 211–217.